

Supporting Information

Discovery of a Chemical Probe Bisamide (CCT251236): An Orally Bioavailable Efficacious Pirin Ligand from a Heat Shock Transcription Factor 1 (HSF1) Phenotypic Screen

Matthew D. Cheeseman,¹ Nicola E. A. Chessum,¹ Carl S. Rye,¹ A. Elisa Pasqua,¹ Michael J. Tucker,¹ Birgit Wilding,¹ Lindsay E. Evans,¹ Susan Lepri,¹ Meirion Richards,¹ Swee Y. Sharp,¹ Salyha Ali,^{1,2} Martin Rowlands,¹ Lisa O'Fee,¹ Asadh Miah,¹ Angela Hayes,¹ Alan T. Henley,¹ Marissa Powers,¹ Robert te Poele,¹ Emmanuel De Billy,¹ Loredana Pellegrino,¹ Florence Raynaud,¹ Rosemary Burke,¹ Rob L. M. van Montfort,^{1,2} Suzanne A. Eccles,¹ Paul Workman,^{1,*} Keith Jones^{1,*}

¹ Cancer Research UK Cancer Therapeutics Unit at The Institute of Cancer Research, London SW7 3RP, United Kingdom.

² Division of Structural Biology at The Institute of Cancer Research, London SW7 3RP, United Kingdom.

Table of Contents

NMR Spectra of Final Compounds S2 to S23

CDK Inhibition Assay S24

Cancerxgene Cell Line Profiling S25 to S30

DiscoverX KinomeScan S31 to S36

HSP72 Cell-Based ELISA S37 to S39

Kinase Inhibition Assays S40 to S42

BRAF Inhibitors S43 to S45

Solubilizing Group Optimization S46 to S47

Mouse Pharmacokinetics S48 to S49

In Vivo Mouse Efficacy Studies S50 to S51

Cerep Diversity Screen S52 to S54

SILAC Target Identification S55 to S58

Pirin Surface Plasmon Resonance (SPR) S59 to S62

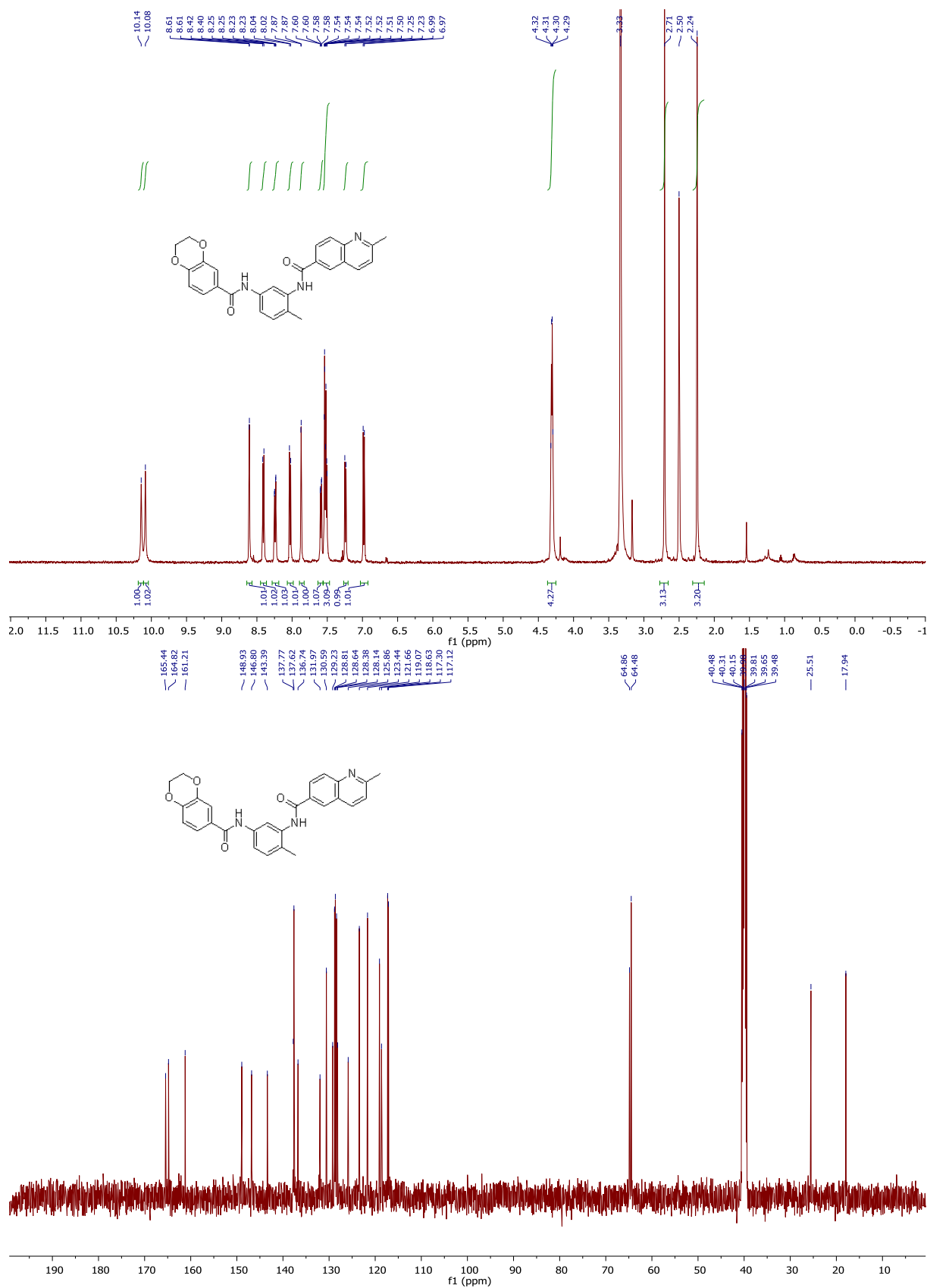
Pirin Crystallography S63 to S64

Full Experimental Procedures S65-S76

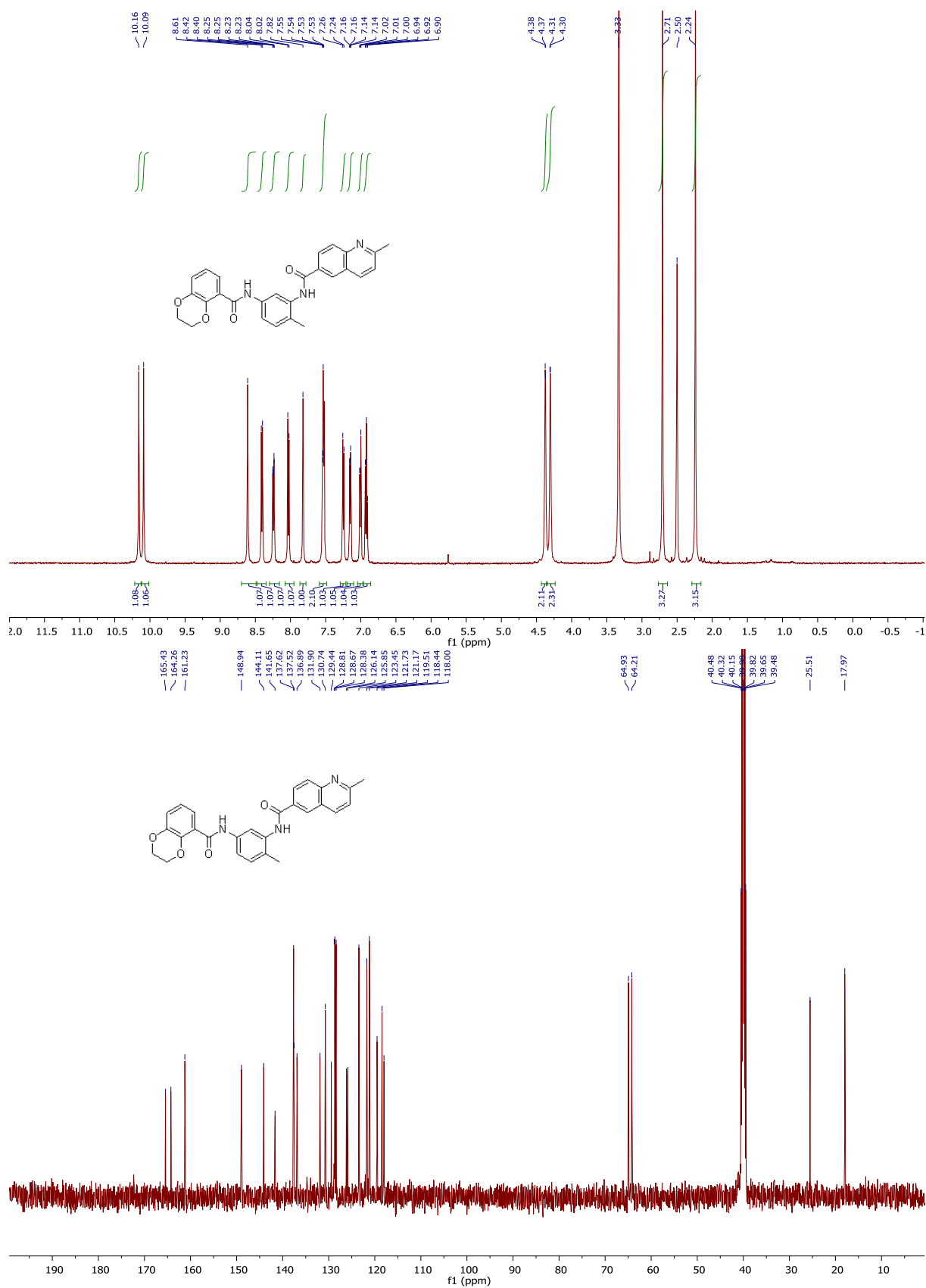
References S77

NMR Spectra of Final Compounds

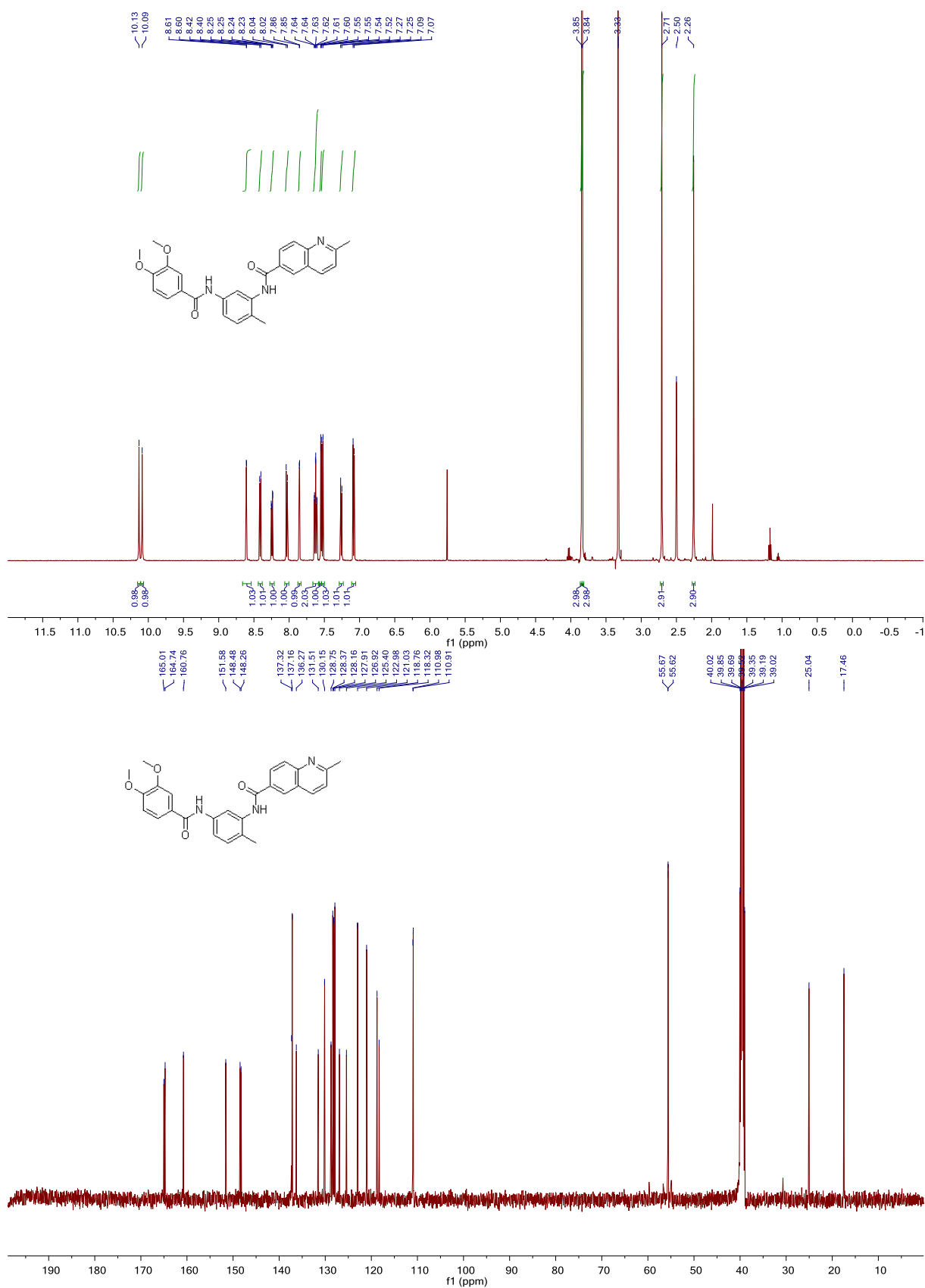
1 (CCT245232) ^1H NMR (DMSO- d_6 , 500 MHz) and ^{13}C NMR (DMSO- d_6 , 126 MHz)



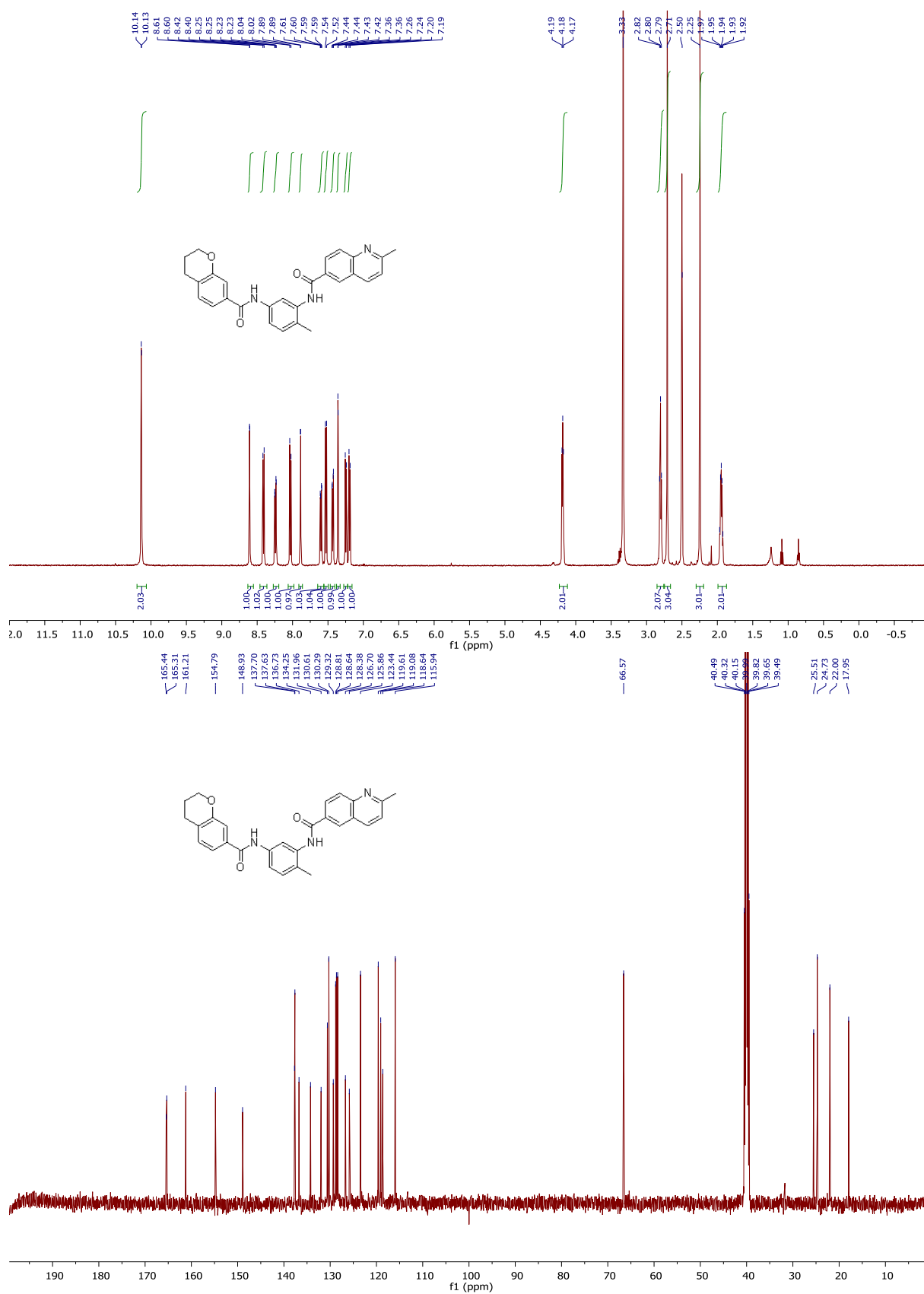
6 ^1H NMR (DMSO- d_6 , 500 MHz) and ^{13}C NMR (DMSO- d_6 , 126 MHz)



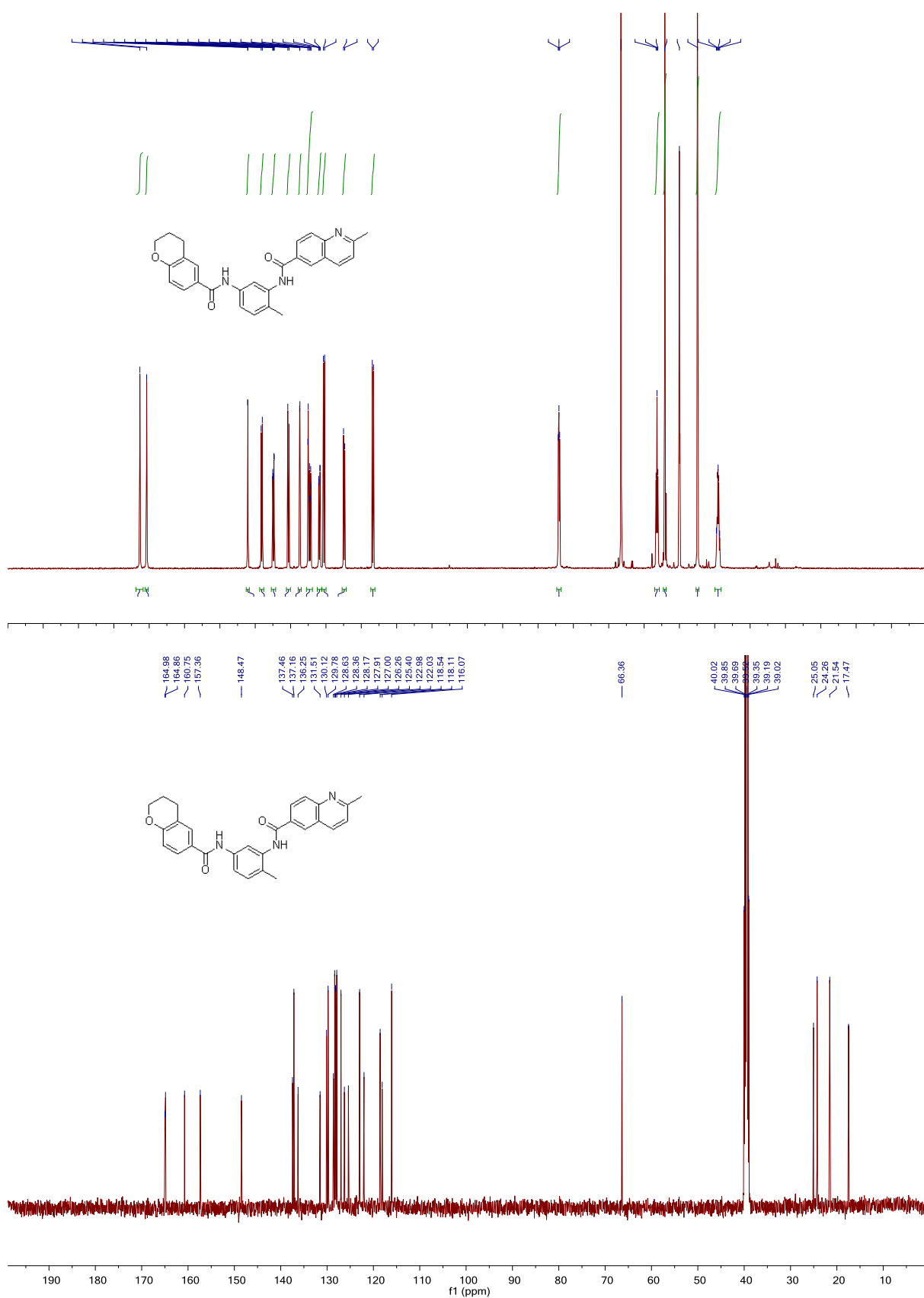
7 ^1H NMR (DMSO- d_6 , 500 MHz) and ^{13}C NMR (DMSO- d_6 , 126 MHz)



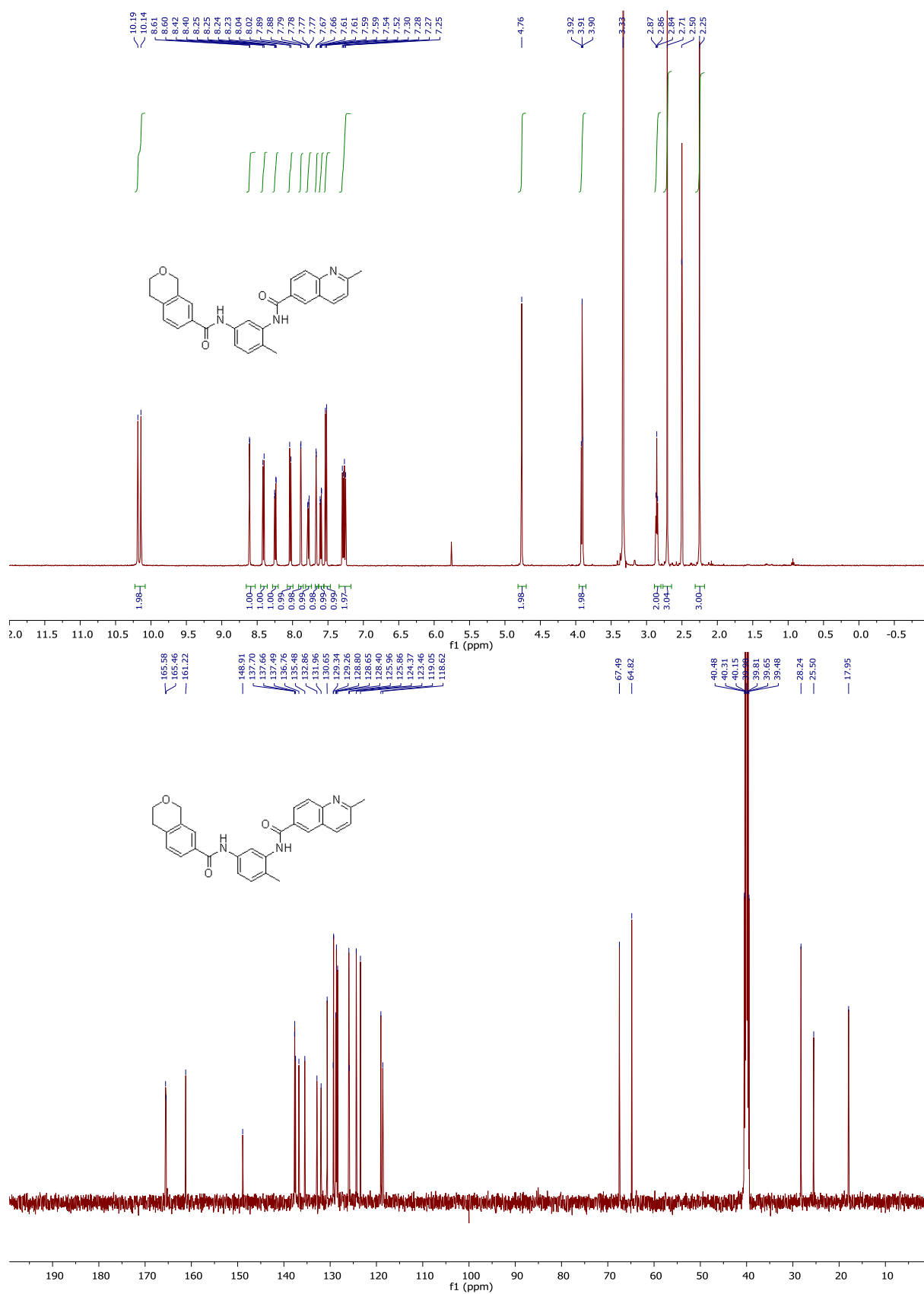
8 ^1H NMR (DMSO- d_6 , 500 MHz) and ^{13}C NMR (DMSO- d_6 , 126 MHz)



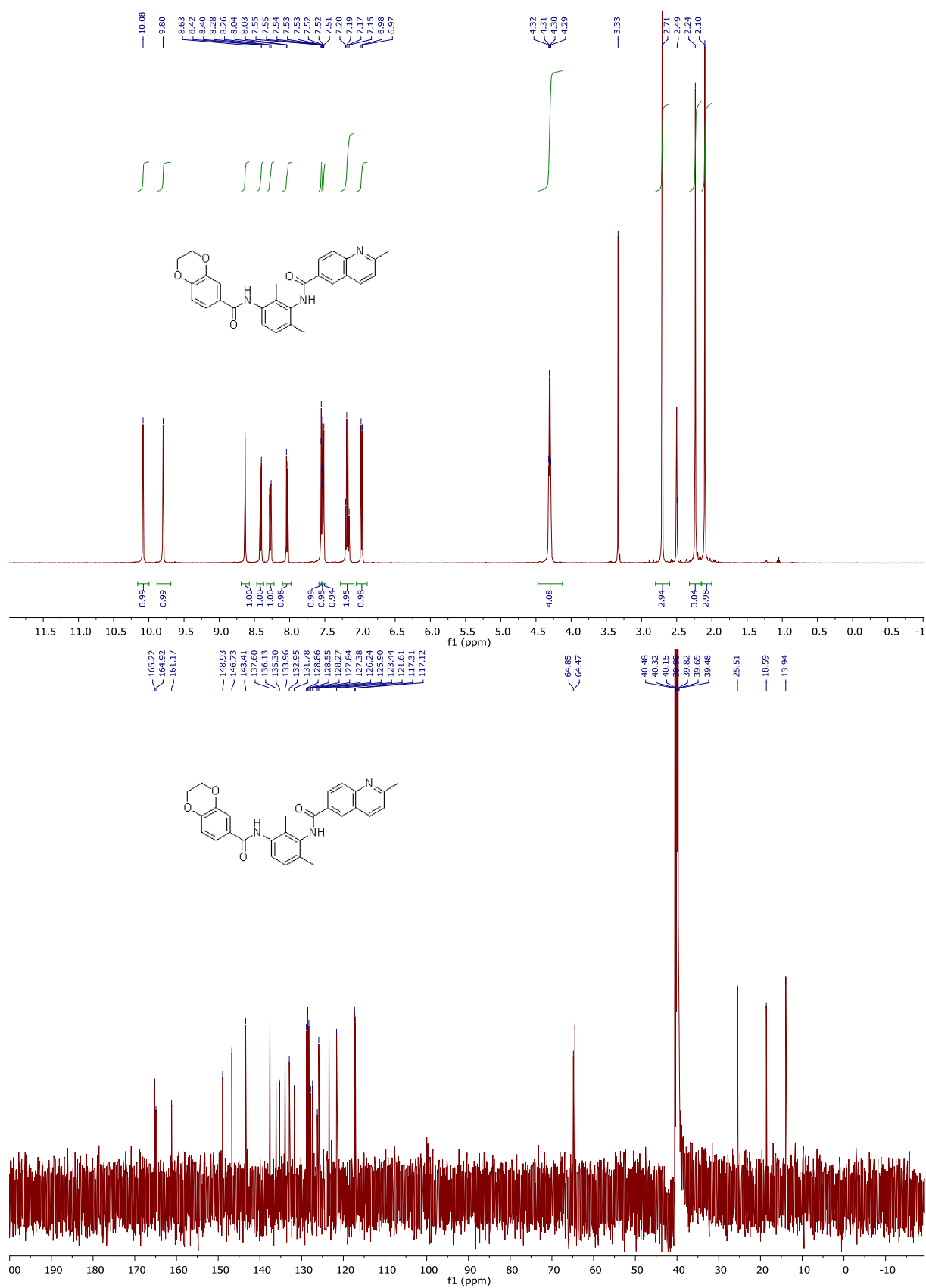
9 ^1H NMR (DMSO- d_6 , 500 MHz) and ^{13}C NMR (DMSO- d_6 , 126 MHz)



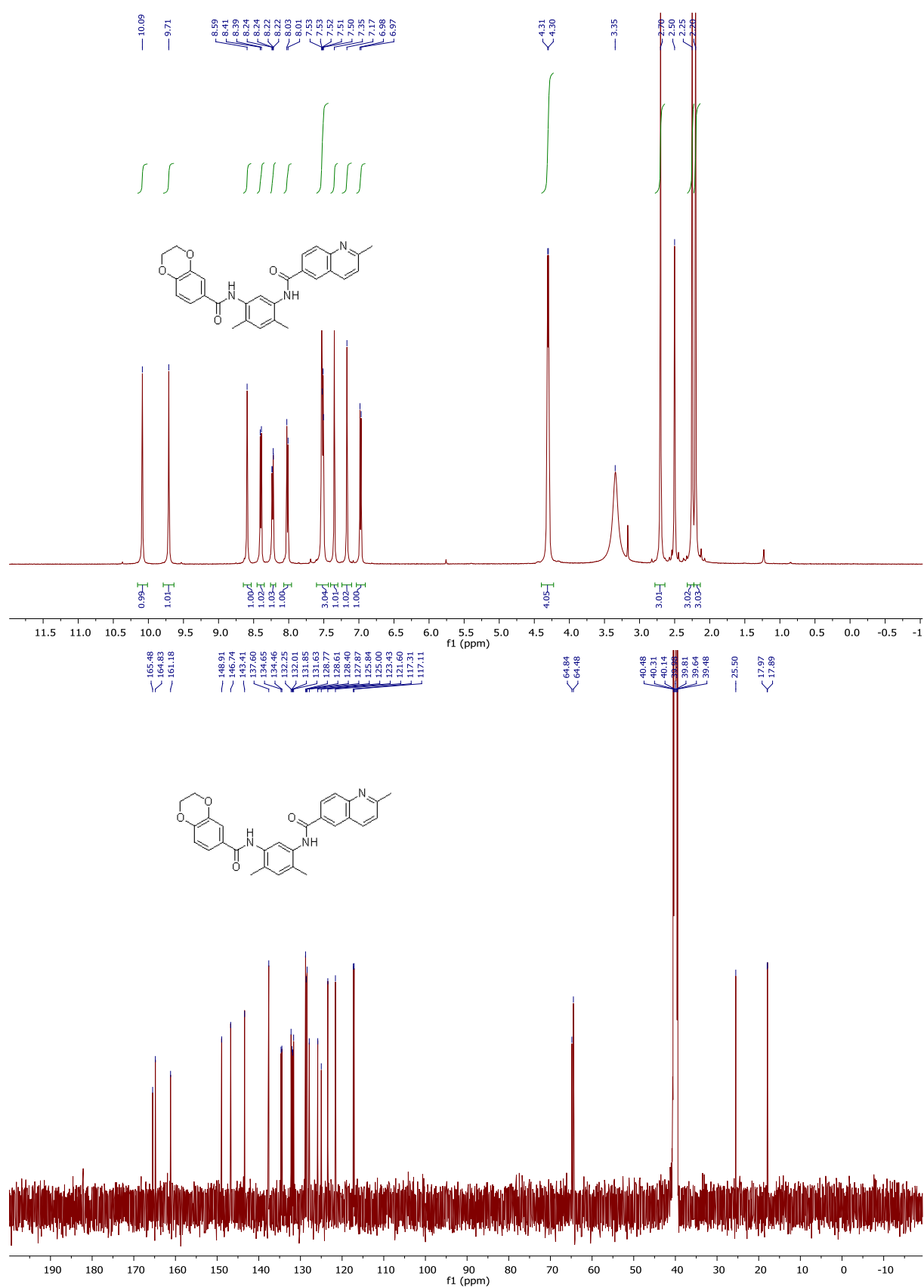
10 ^1H NMR (DMSO- d_6 , 500 MHz) and ^{13}C NMR (DMSO- d_6 , 126 MHz)



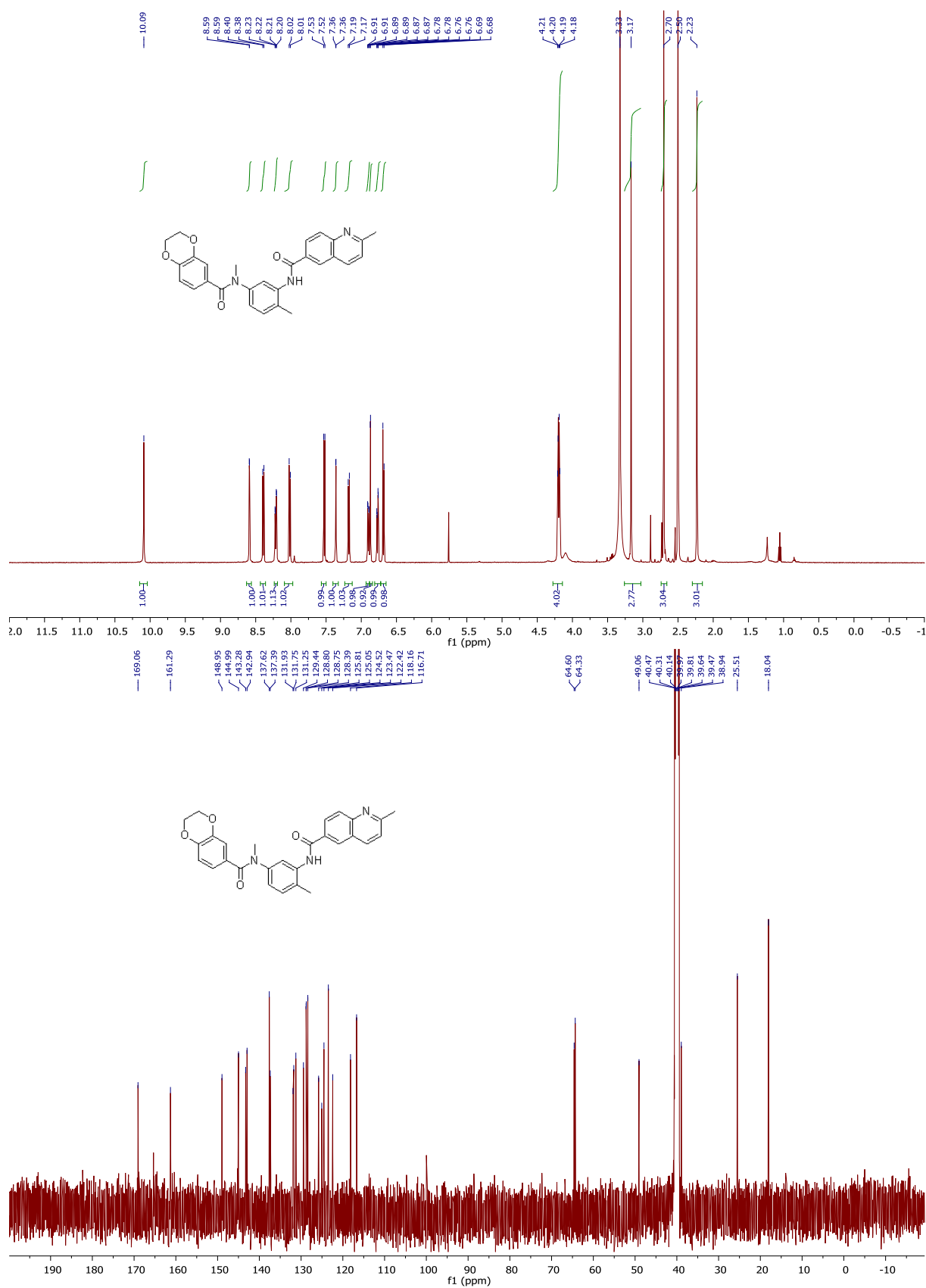
11 ^1H NMR (DMSO- d_6 , 500 MHz) and ^{13}C NMR (DMSO- d_6 , 126 MHz)



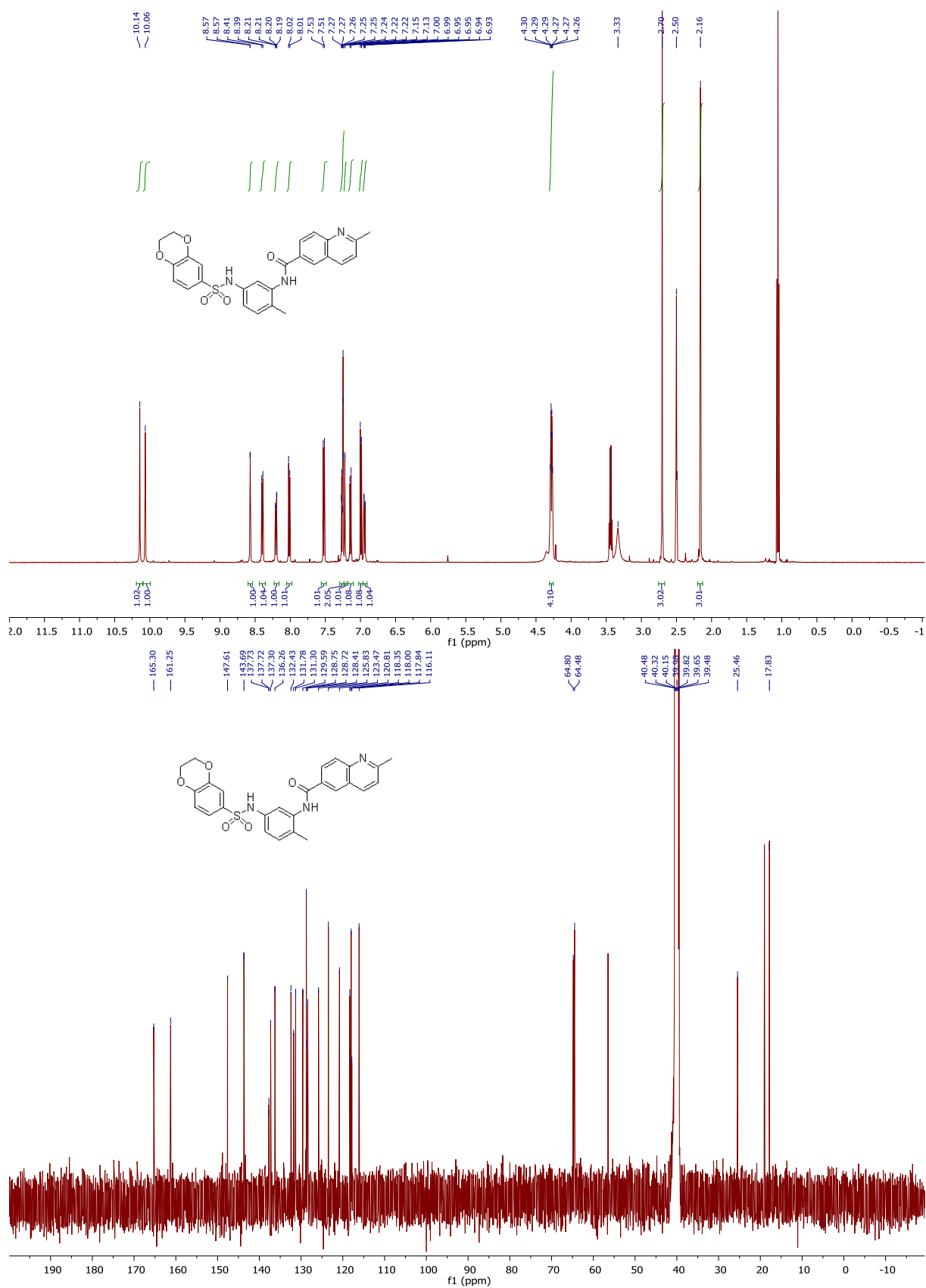
12 ^1H NMR (DMSO- d_6 , 500 MHz) and ^{13}C NMR (DMSO- d_6 , 126 MHz)



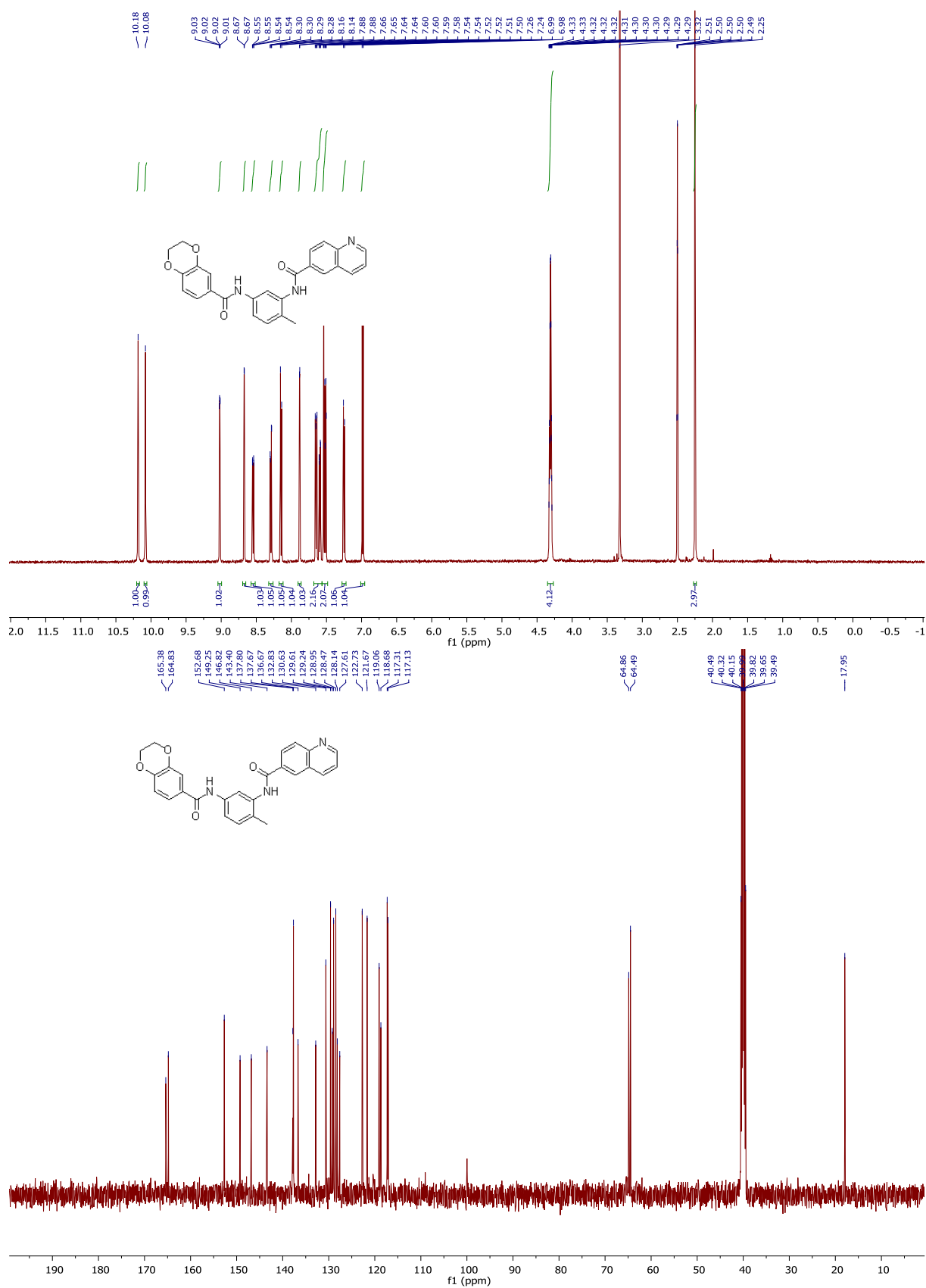
^{13}H NMR (DMSO- d_6 , 500 MHz) and ^{13}C NMR (DMSO- d_6 , 126 MHz)



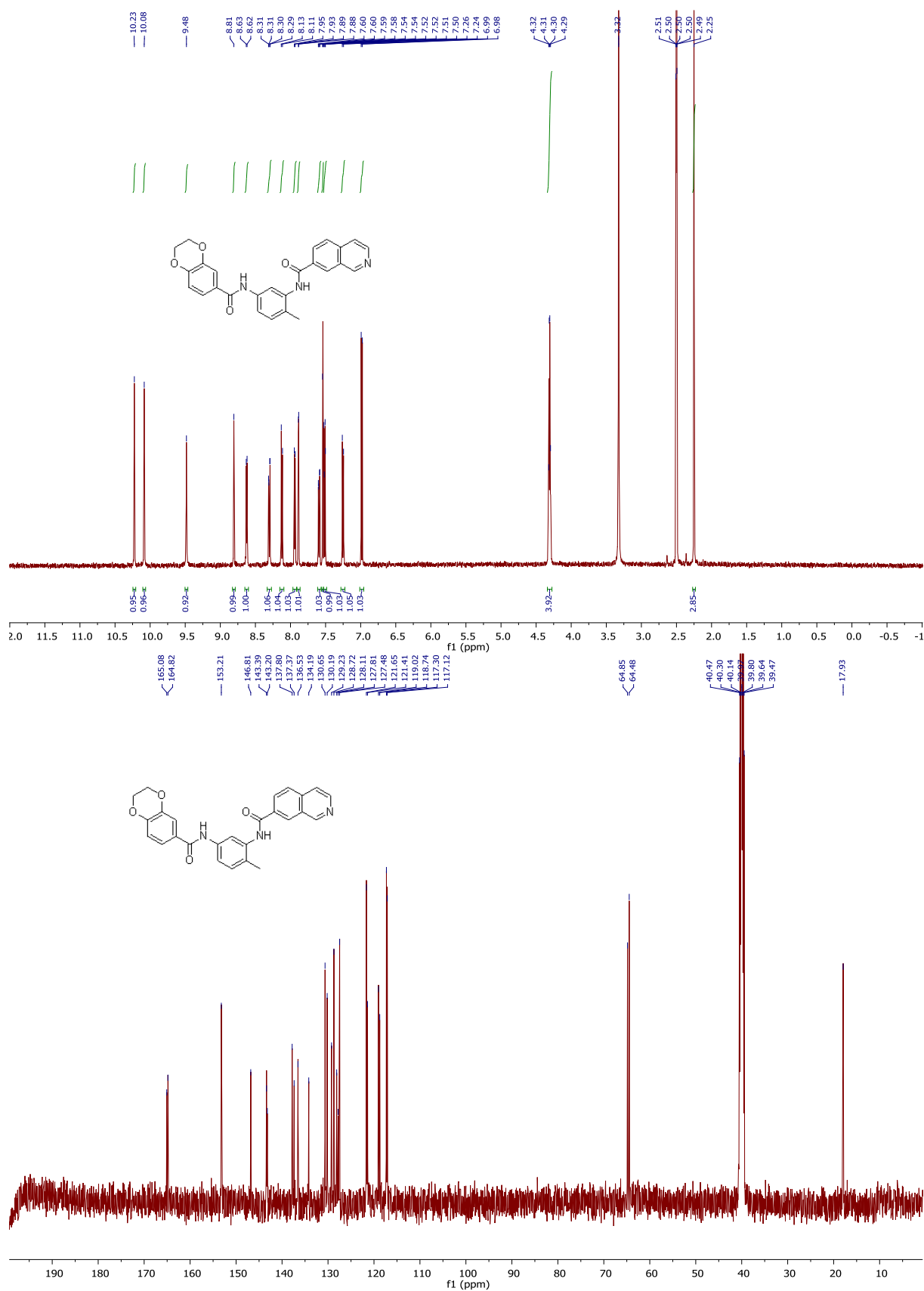
14 ^1H NMR (DMSO- d_6 , 500 MHz) and ^{13}C NMR (DMSO- d_6 , 126 MHz)



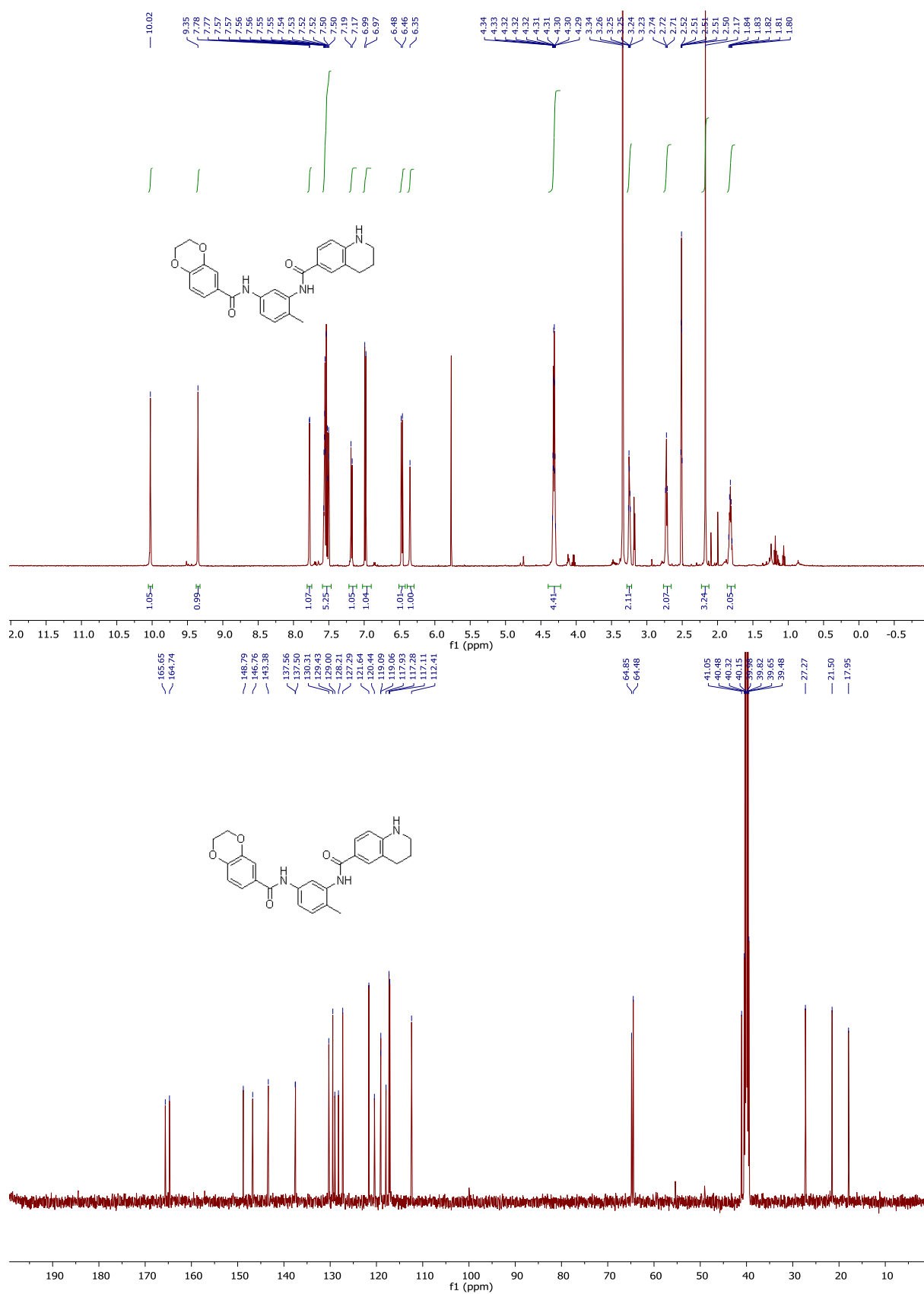
15 ^1H NMR (DMSO- d_6 , 500 MHz) and ^{13}C NMR (DMSO- d_6 , 126 MHz)



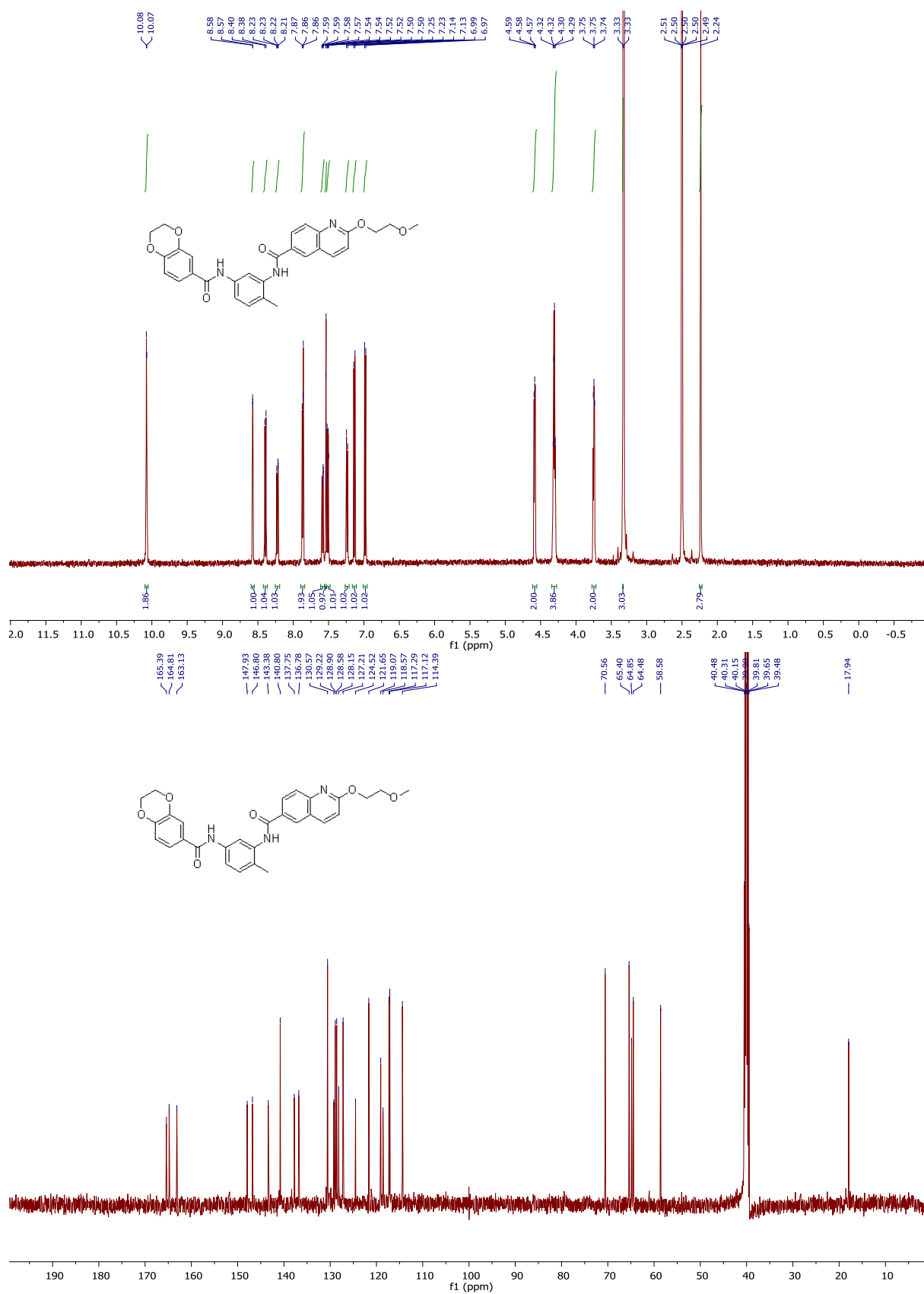
16 ^1H NMR (DMSO- d_6 , 500 MHz) and ^{13}C NMR (DMSO- d_6 , 126 MHz)



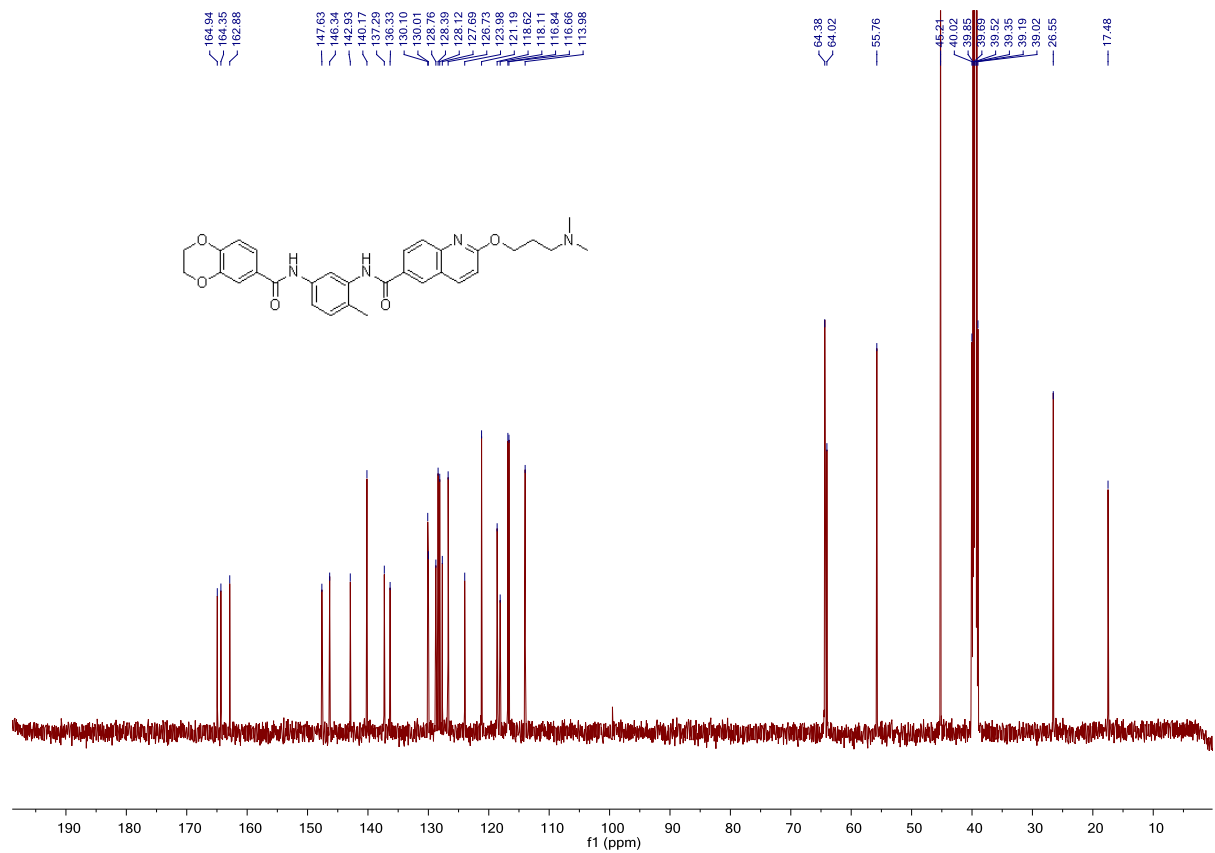
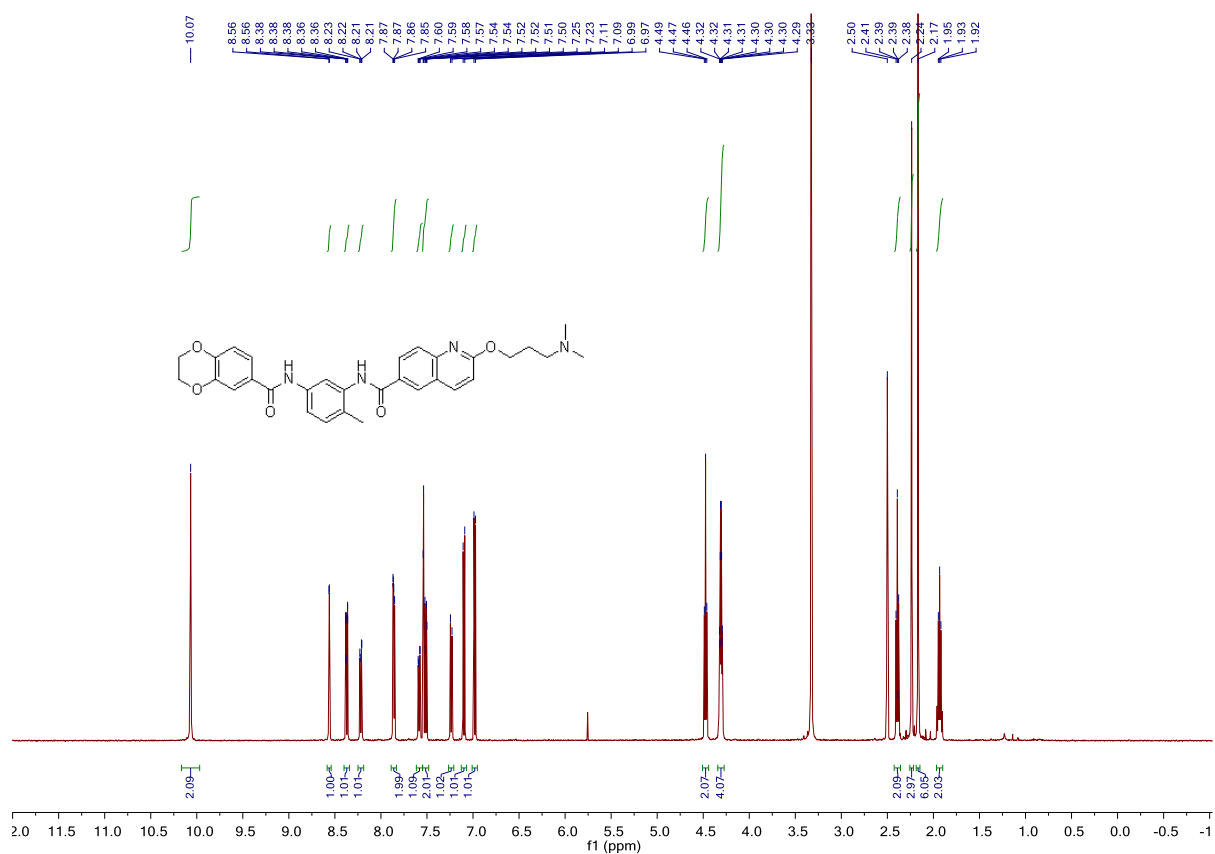
17 ^1H NMR (DMSO- d_6 , 500 MHz) and ^{13}C NMR (DMSO- d_6 , 126 MHz)



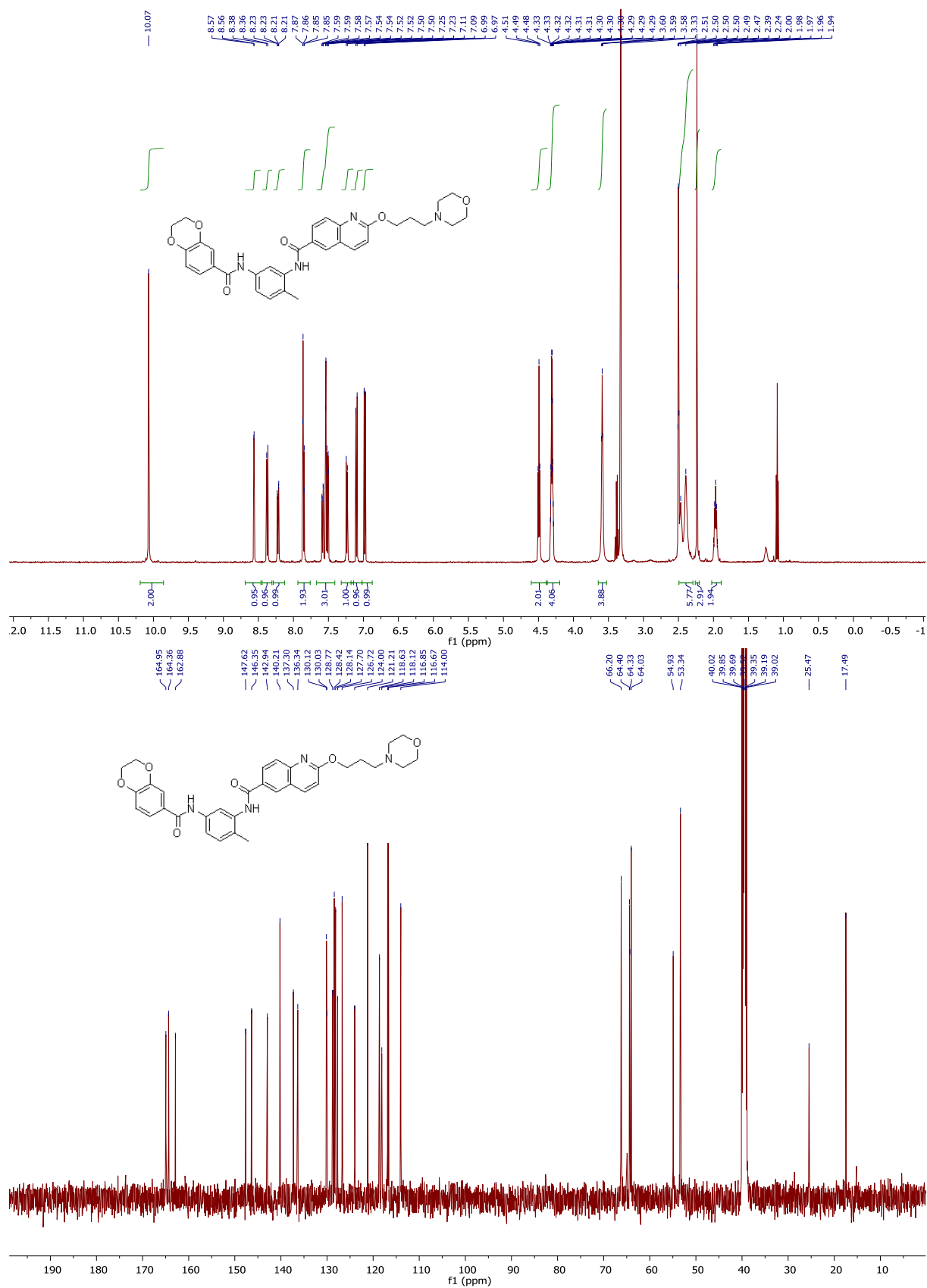
21 ^1H NMR (DMSO- d_6 , 500 MHz) and ^{13}C NMR (DMSO- d_6 , 126 MHz)



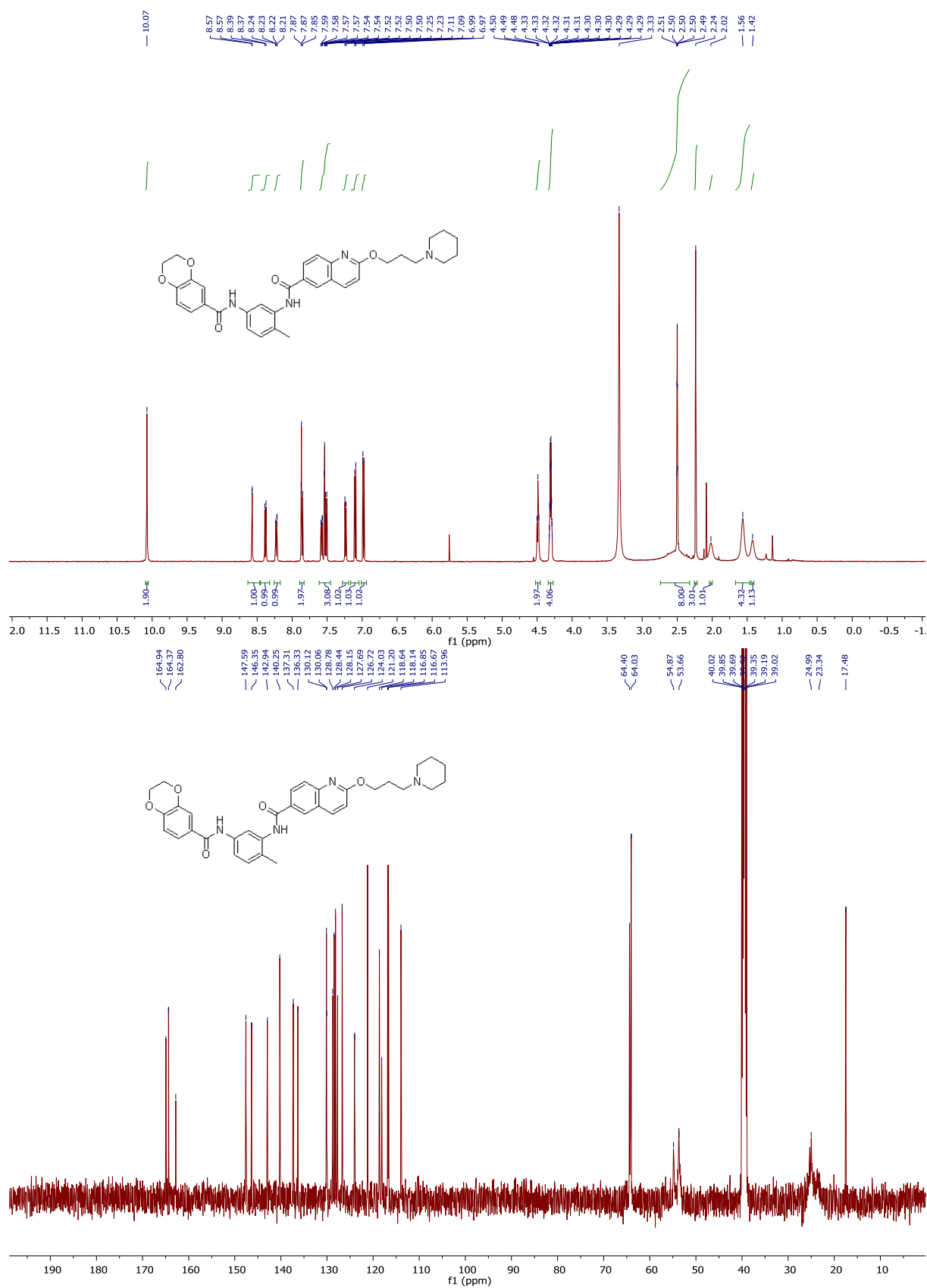
22 ^1H NMR (DMSO- d_6 , 500 MHz) and ^{13}C NMR (DMSO- d_6 , 126 MHz)



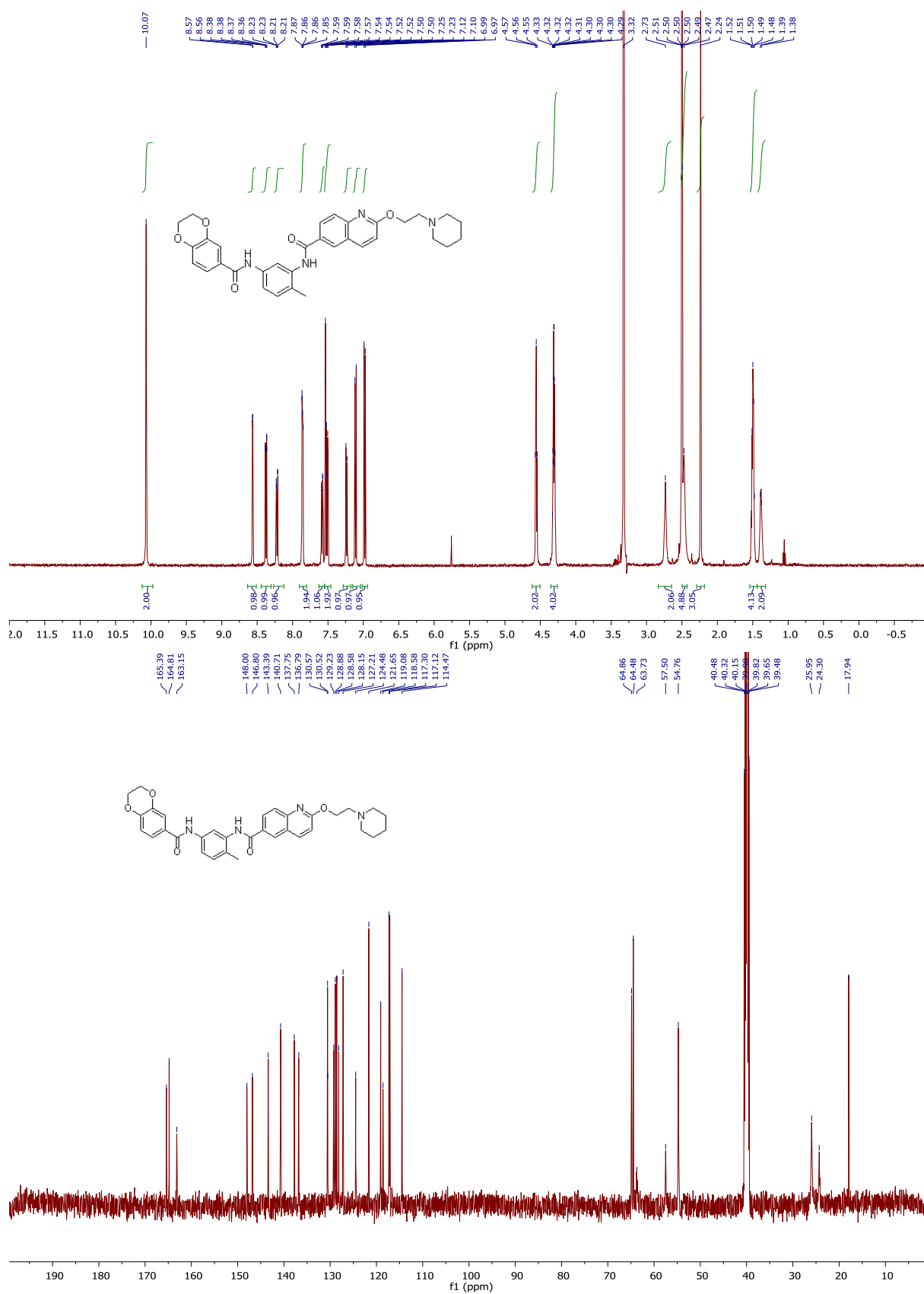
23 ^1H NMR (DMSO- d_6 , 500 MHz) and ^{13}C NMR (DMSO- d_6 , 126 MHz)



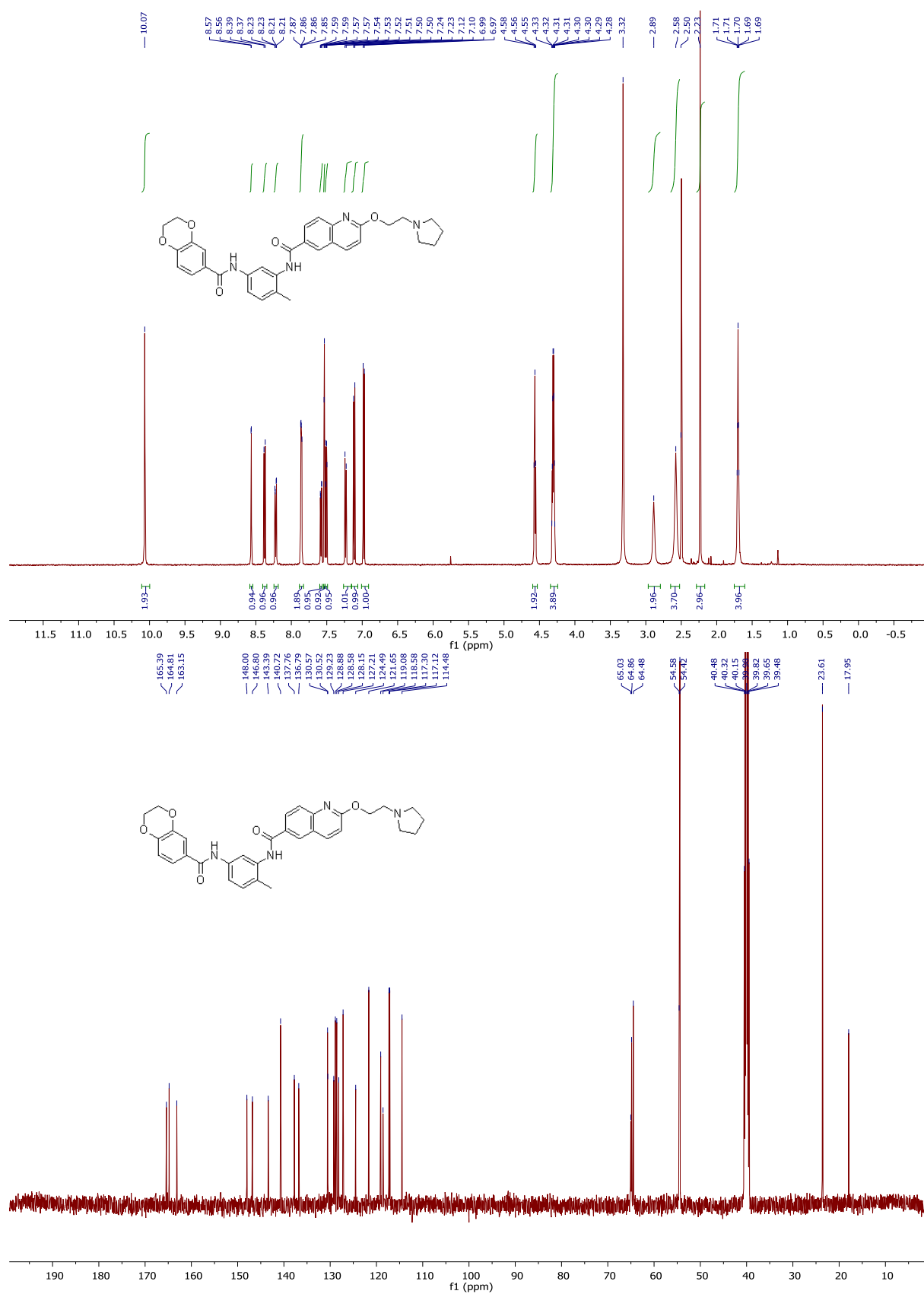
24 ^1H NMR (DMSO- d_6 , 500 MHz) and ^{13}C NMR (DMSO- d_6 , 126 MHz)



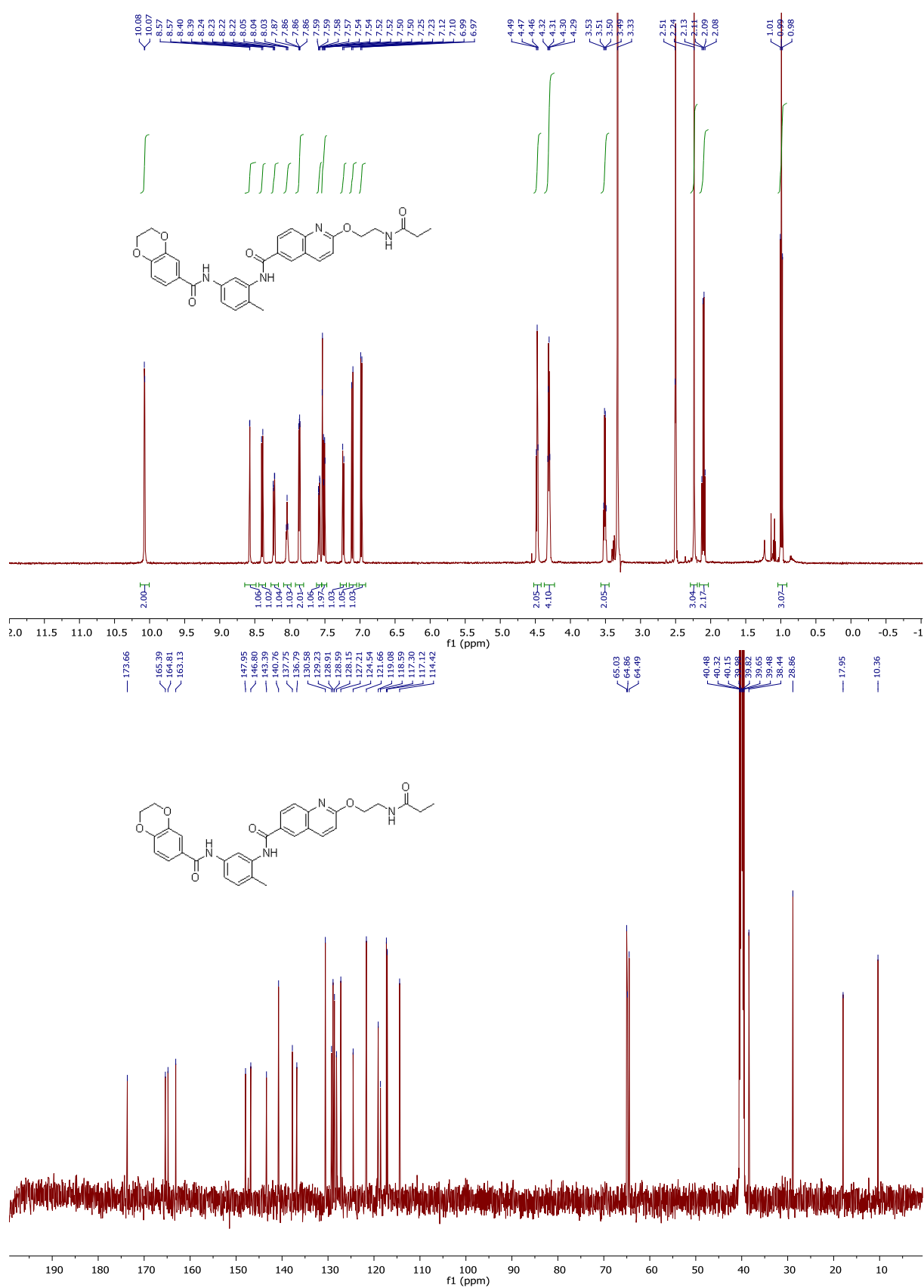
25 ^1H NMR (DMSO- d_6 , 500 MHz) and ^{13}C NMR (DMSO- d_6 , 126 MHz)



26 (CCT251236) ^1H NMR (DMSO- d_6 , 500 MHz) and ^{13}C NMR (DMSO- d_6 , 126 MHz)



27 ^1H NMR (DMSO- d_6 , 500 MHz) and ^{13}C NMR (DMSO- d_6 , 126 MHz)

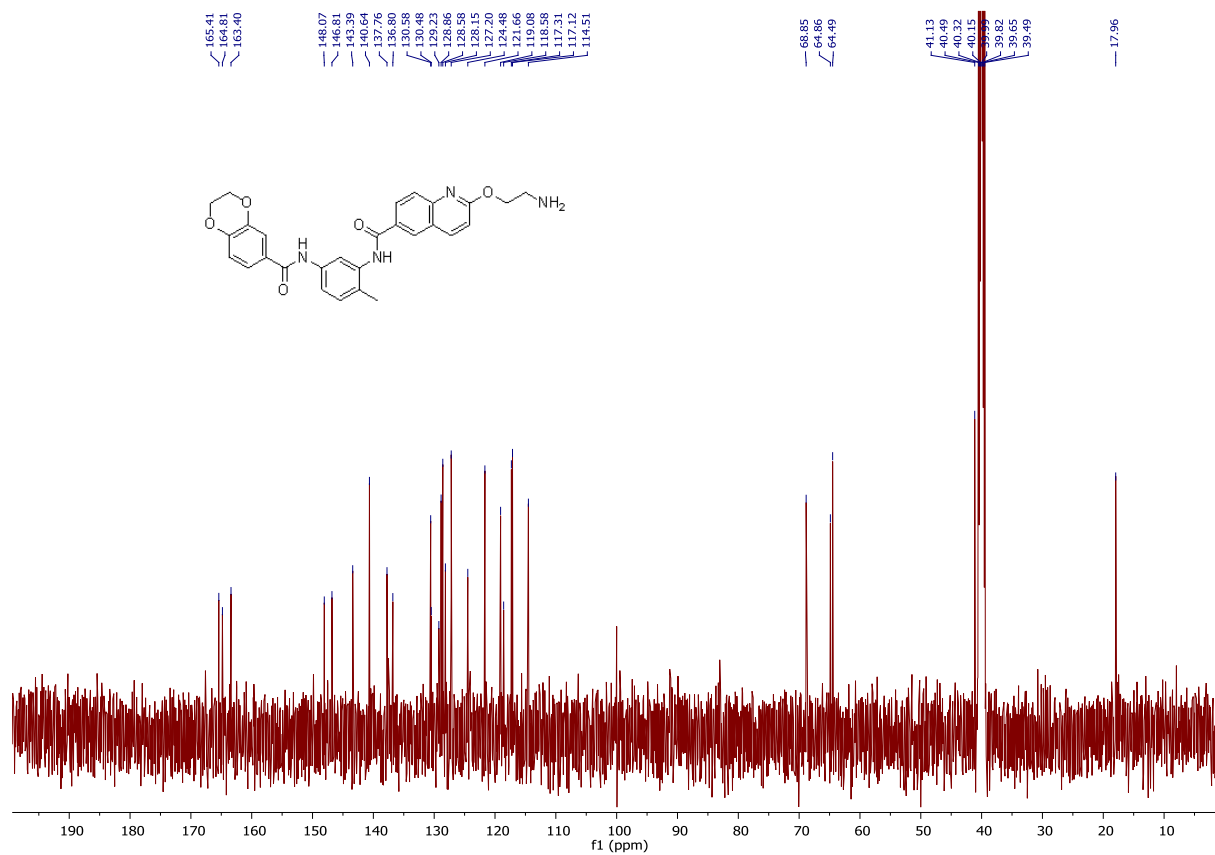
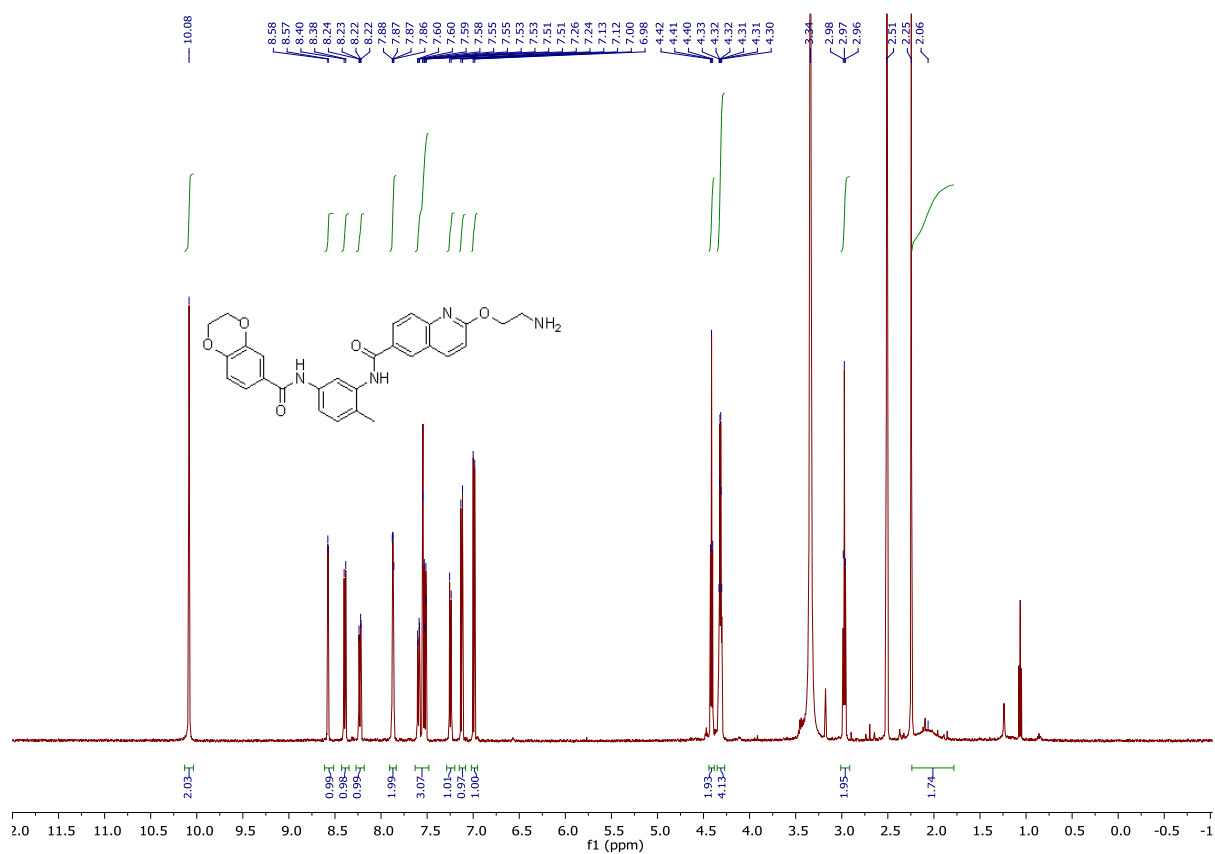


The figure displays the ¹H and ¹³C NMR spectra of compound 10, which is 1-(4-(3-(3,4-dihydro-2H-benzofuran-2-yl)-4-methylphenyl)-3-oxo-1,2,3,4-tetrahydronaphthalen-1-yl)pyrrolidine. The chemical structure is shown above the spectra.

¹H NMR (400 MHz, CDCl₃): The spectrum shows peaks at 10.10 (s, 1H), 10.09 (s, 1H), 8.57 (d, 1H), 8.39 (d, 1H), 8.37 (d, 1H), 8.24 (d, 1H), 8.23 (d, 1H), 8.21 (d, 1H), 7.87 (d, 1H), 7.85 (d, 1H), 7.81 (d, 1H), 7.54 (d, 1H), 7.53 (d, 1H), 7.52 (d, 1H), 7.25 (d, 1H), 7.23 (d, 1H), 7.16 (d, 1H), 7.15 (d, 1H), 7.14 (d, 1H), 7.13 (d, 1H), 7.11 (d, 1H), 7.02 (d, 1H), 7.01 (d, 1H), 7.00 (d, 1H), 6.93 (d, 1H), 6.92 (d, 1H), 6.90 (d, 1H), 4.58 (d, 1H), 4.57 (d, 1H), 4.56 (d, 1H), 4.38 (d, 1H), 4.37 (d, 1H), 4.37 (d, 1H), 4.35 (d, 1H), 4.34 (d, 1H), 4.31 (d, 1H), 4.31 (d, 1H), 4.30 (d, 1H), 4.29 (d, 1H), 2.91 (s, 3H), 2.60 (s, 3H), 2.49 (s, 3H), 2.23 (s, 3H), and 1.71 (s, 3H). Integration values are provided below the peaks.

¹³C NMR (100 MHz, CDCl₃): The spectrum shows peaks at 165.38, 164.26, 163.15, 148.01, 146.85, 141.65, 140.73, 137.51, 136.95, 130.72, 130.45, 129.46, 128.62, 127.20, 126.15, 124.49, 121.72, 121.17, 118.85, 118.45, 117.95, 114.48, 64.93, 64.21, 56.48, 54.55, 54.42, 40.48, 40.32, 40.15, 39.82, 39.65, 39.46, 23.60, and 17.98.

29 ^1H NMR (DMSO- d_6 , 500 MHz) and ^{13}C NMR (DMSO- d_6 , 126 MHz)



CDK Inhibition Assays

Bisamide 1 (CCT245232)

CDK2/Cyclin A: [ATP]=app. K_m

The 2X CDK2/cyclin A/Ser/Thr 12 mixture is prepared in 50 mM HEPES pH 7.5, 0.01 % BRIJ-35, 10 mM MgCl₂, 1 mM EGTA. The final 10 µL Kinase Reaction consists of 1.22 - 10.3 ng CDK2/cyclin A and 2 µM Ser/Thr 12 in 50 mM HEPES pH 7.5, 0.01 % BRIJ-35, 10 mM MgCl₂, 1 mM EGTA. After the 1 hour kinase reaction incubation, 5 µL of a 1:4096 dilution of development reagent A is added.

Life Technologies' SelectScreen® Profiling Service: 10-point Titration Results															
SelectScreen® Scientist:			Derek Johnston			Date:			11-Nov-2015			SSBK-Z-LYTE (Paisley UK)			
Quality Assurance Review:			Theo James			Date:			11-Nov-2015						
% Phosphorylation		Pass													
Z' Determination		Pass													
Project #	Compound Name	Kinase Tested	[ATP] Tested (µM)	IC50 (µM)	Hillslope	R² Value	Conc of Compound (nM)	%Inhibition Point 1	Point 2	Development Reaction Interference	Test Compound Interference Countmin	Fluorescein	Z'	Kinase Part# / Lot#	Graph
SSBK8838_34274	CCT245232	CDK2/cyclin A	Kin app	>1000	0.05	0.3262	✓ 1000	6	11	Pass	Pass	Pass	0.85	PV3267/1626124	
SSBK8838_34274	CCT245232	CDK2/cyclin A	Kin app	>1000	0.05	0.3262	✓ 333	15	13	Pass	Pass	Pass	0.85	PV3267/1626124	
SSBK8838_34274	CCT245232	CDK2/cyclin A	Kin app	>1000	0.05	0.3262	✓ 111	12	22	Pass	Pass	Pass	0.85	PV3267/1626124	
SSBK8838_34274	CCT245232	CDK2/cyclin A	Kin app	>1000	0.05	0.3262	✓ 37.0	5	11	Pass	Pass	Pass	0.85	PV3267/1626124	
SSBK8838_34274	CCT245232	CDK2/cyclin A	Kin app	>1000	0.05	0.3262	✓ 12.3	13	3	Pass	Pass	Pass	0.85	PV3267/1626124	
SSBK8838_34274	CCT245232	CDK2/cyclin A	Kin app	>1000	0.05	0.3262	✓ 4.12	8	12	Pass	Pass	Pass	0.85	PV3267/1626124	
SSBK8838_34274	CCT245232	CDK2/cyclin A	Kin app	>1000	0.05	0.3262	✓ 1.37	7	5	Pass	Pass	Pass	0.85	PV3267/1626124	
SSBK8838_34274	CCT245232	CDK2/cyclin A	Kin app	>1000	0.05	0.3262	✓ 0.457	8	8	Pass	Pass	Pass	0.85	PV3267/1626124	
SSBK8838_34274	CCT245232	CDK2/cyclin A	Kin app	>1000	0.05	0.3262	✓ 0.152	0	11	Pass	Pass	Pass	0.85	PV3267/1626124	
SSBK8838_34274	CCT245232	CDK2/cyclin A	Kin app	>1000	0.05	0.3262	✓ 0.0495	12	4	Pass	Pass	Pass	0.85	PV3267/1626124	

For the screening protocol and assay conditions see:

<https://www.thermofisher.com/uk/en/home/life-science/drug-discovery/target-and-lead-identification-and-validation/kinasebiology/kinase-activity-assays/z-lyte.html> (August 31, 2016).

CDK9/Cyclin T1: [ATP]=app. K_m

The 2X CDK9/cyclin T1/CDK7/9 tide mixture is prepared in 50 mM HEPES pH 7.5, 0.01 % BRIJ-35, 10 mM MgCl₂, 1 mM EGTA. The final 10 µL kinase re action consists of 4-40 ng CDK9/cyclin T1 and 200 µM CDK7/9 tide in 32.5 mM HEPES pH 7.5, 0.005 % BRIJ-35, 5 mM MgCl₂, 0.5 mM EGTA. After the 1 hour kinase reaction incubation, 5 µL of detection mix is added.

Life Technologies' SelectScreen® Profiling Service: 10-point Titration Results														
SelectScreen® Scientist:			Graham Murdoch			Date:			10-Nov-2015			SSBK-Adapta (Paisley UK)		
Quality Assurance Review:			Theo James			Date:			10-Nov-2015					
% Conversion			Pass											
Z' Determination			Pass											
Project #	Compound Name	Kinase Tested	[ATP] Tested (µM)	IC50 (nM)	Hillslope	R ² Value	Conc of Compound (nM)	%Inhibition Point 1	%Inhibition Point 2	Test Compound Interference Donor	Test Compound Interference Acceptor	Z'	Kinase Part# / Lot#	Graph
SSBK8838_34274	CCT245232	CDK9/cyclin T1	Kin app	>1000	-0.06	0.0821	1000	-11	23	Pass	Pass	0.86	PV4131/1650325	
SSBK8838_34274	CCT245232	CDK9/cyclin T1	Kin app	>1000	-0.06	0.0821	333	-41	12	Pass	Pass	0.86	PV4131/1650325	
SSBK8838_34274	CCT245232	CDK9/cyclin T1	Kin app	>1000	-0.06	0.0821	111	-2	6	Pass	Pass	0.86	PV4131/1650325	
SSBK8838_34274	CCT245232	CDK9/cyclin T1	Kin app	>1000	-0.06	0.0821	37.0	-13	4	Pass	Pass	0.86	PV4131/1650325	
SSBK8838_34274	CCT245232	CDK9/cyclin T1	Kin app	>1000	-0.06	0.0821	12.3	11	6	Pass	Pass	0.86	PV4131/1650325	
SSBK8838_34274	CCT245232	CDK9/cyclin T1	Kin app	>1000	-0.06	0.0821	4.12	1	9	Pass	Pass	0.86	PV4131/1650325	
SSBK8838_34274	CCT245232	CDK9/cyclin T1	Kin app	>1000	-0.06	0.0821	1.37	-9	12	Pass	Pass	0.86	PV4131/1650325	
SSBK8838_34274	CCT245232	CDK9/cyclin T1	Kin app	>1000	-0.06	0.0821	0.457	-1	12	Pass	Pass	0.86	PV4131/1650325	
SSBK8838_34274	CCT245232	CDK9/cyclin T1	Kin app	>1000	-0.06	0.0821	0.152	7	-9	Pass	Pass	0.86	PV4131/1650325	
SSBK8838_34274	CCT245232	CDK9/cyclin T1	Kin app	>1000	-0.06	0.0821	0.0495	2	6	Pass	Pass	0.86	PV4131/1650325	

For the screening protocol and assay conditions see:

<https://www.thermofisher.com/uk/en/home/life-science/drug-discovery/target-and-lead-identification-and-validation/kinasebiology/kinase-activity-assays/adapta-universal-kinase-assay.htm> (August 31, 2016).

Cancerxgene Cell Line Profiling

Table S1. Cell line profiling for bisamide 1 (CCT245232)

Cell Line	Tissue	GI ₅₀ (μM)	pGI ₅₀
SW948	GI tract	15.568	4.81
NCI-H2029	lung	13.897	4.86
SW1463	GI tract	3.437	5.46
T84	GI tract	2.685	5.57
NCI-H630	GI tract	1.702	5.77
SIMA	CNS	1.097	5.96
KP-N-YN	CNS	1.091	5.96
RCC10RGB	kidney	0.796	6.10
COLO-680N	upper aerodigestive	0.731	6.14
GAK	skin	0.728	6.14
KURAMOCHI	ovary	0.679	6.17
MFE-280	uterus	0.630	6.20
MDA-MB-453	breast	0.588	6.23
LB373-MEL-D	skin	0.587	6.23
Capan-2	pancreas	0.567	6.25
RT4	bladder	0.505	6.30
EKVX	lung	0.499	6.30
COLO-678	GI tract	0.498	6.30
MKN7	GI tract	0.454	6.34
Hep G2	liver	0.445	6.35
HCC38	breast	0.444	6.35
MCF7	breast	0.440	6.36
MKN1	GI tract	0.428	6.37
PAMC82	GI tract	0.404	6.39
LS-123	GI tract	0.397	6.40
NB17	CNS	0.388	6.41
LS-1034	GI tract	0.384	6.42
COLO-824	breast	0.366	6.44
ChaGo-K-1	lung	0.364	6.44
HT55	GI tract	0.363	6.44
SW1116	GI tract	0.358	6.45
UMC-11	lung	0.345	6.46
HT-29	GI tract	0.341	6.47
OAW-28	ovary	0.337	6.47
SiHa	uterus	0.323	6.49
Raji	blood	0.319	6.50
ZR-75-30	breast	0.315	6.50
OE19	upper aerodigestive	0.309	6.51
SHP-77	lung	0.300	6.52
HCC2998	GI tract	0.295	6.53
HCC1419	breast	0.294	6.53
HCC1937	breast	0.290	6.54
BEN	lung	0.281	6.55
M059J	CNS	0.278	6.56
NCI-H1573	lung	0.278	6.56
BT-20	breast	0.267	6.57
HT-1197	bladder	0.260	6.59
NCI-H522	lung	0.257	6.59
HCC1569	breast	0.253	6.60
NCI-H2170	lung	0.251	6.60
NCI-H596	lung	0.251	6.60

KYSE-520	upper aerodigestive	0.246	6.61
EFM-19	breast	0.245	6.61
MSTO-211H	lung	0.244	6.61
22RV1	other	0.241	6.62
HCC1395	breast	0.235	6.63
RT-112	bladder	0.234	6.63
DMS-114	lung	0.234	6.63
SW837	GI tract	0.227	6.64
SNU-C2B	GI tract	0.224	6.65
RMG-I	ovary	0.224	6.65
HCE-4	upper aerodigestive	0.224	6.65
MKN74	GI tract	0.222	6.65
HCC1954	breast	0.222	6.65
SMMC-7721	liver	0.221	6.66
MZ7-mel	skin	0.221	6.66
TE-1	upper aerodigestive	0.219	6.66
VMRC-RCZ	kidney	0.218	6.66
HCC1806	breast	0.213	6.67
GCIY	GI tract	0.210	6.68
NCI-H1623	lung	0.208	6.68
SW1783	CNS	0.205	6.69
NCI-H2228	lung	0.205	6.69
WM-115	skin	0.203	6.69
Calu-3	lung	0.202	6.70
J82	bladder	0.195	6.71
ESS-1	uterus	0.193	6.71
MES-SA	soft tissue	0.192	6.72
NCI-H2085	lung	0.185	6.73
EVSA-T	breast	0.184	6.74
GP5d	GI tract	0.179	6.75
SCC-15	upper aerodigestive	0.177	6.75
NCI-H1581	lung	0.177	6.75
HCC70	breast	0.175	6.76
HT-1376	bladder	0.175	6.76
NCI-H520	lung	0.174	6.76
639-V	bladder	0.173	6.76
DMS-53	lung	0.172	6.77
HT-29	GI tract	0.170	6.77
Saos-2	bone	0.167	6.78
SNU-423	other	0.166	6.78
TGBC1TKB	GI tract	0.165	6.78
NCI-H1650	lung	0.164	6.78
NCI-H1975	lung	0.164	6.79
AN3-CA	uterus	0.162	6.79
005B	upper aerodigestive	0.162	6.79
SW948	GI tract	0.162	6.79
U-87-MG	CNS	0.159	6.80
NCI-H747	GI tract	0.159	6.80
COLO-668	lung	0.158	6.80
SW900	lung	0.158	6.80
CW-2	GI tract	0.157	6.81
NCI-H650	lung	0.156	6.81
LS-411N	GI tract	0.155	6.81
MDA-MB-175-VII	breast	0.155	6.81
CAPAN-1	pancreas	0.153	6.81
C2BBel	GI tract	0.153	6.82
EFO-21	ovary	0.153	6.82
MKN28	GI tract	0.152	6.82

KNS-42	CNS	0.152	6.82
SNU-387	other	0.150	6.82
KM12	GI tract	0.150	6.82
BT-474	breast	0.148	6.83
AM-38	CNS	0.148	6.83
NCI-H441	lung	0.146	6.84
LB831-BLC	bladder	0.143	6.84
HLF	liver	0.141	6.85
KYSE-410	upper aerodigestive	0.141	6.85
NUGC-3	GI tract	0.140	6.85
RCM-1	GI tract	0.140	6.85
KYSE-180	upper aerodigestive	0.138	6.86
SW1417	GI tract	0.137	6.86
HuO-3N1	bone	0.136	6.87
TE-6	upper aerodigestive	0.135	6.87
NCI-H522	lung	0.135	6.87
KLE	uterus	0.135	6.87
no-11	CNS	0.134	6.87
LS-513	GI tract	0.134	6.87
NCI-H727	lung	0.133	6.88
CAL-72	bone	0.131	6.88
KYSE-270	upper aerodigestive	0.131	6.88
SNU-668	GI tract	0.130	6.89
SKG-IIIa	uterus	0.130	6.89
PANC-10-05	pancreas	0.129	6.89
NCI-H226	lung	0.127	6.90
NCI-H2126	lung	0.127	6.90
NCI-H810	lung	0.126	6.90
PC-3	other	0.125	6.90
Ramos	blood	0.122	6.91
SW626	ovary	0.122	6.92
HT-3	uterus	0.121	6.92
HSC-2	upper aerodigestive	0.121	6.92
NCI-H2126	lung	0.121	6.92
NCI-H1793	lung	0.121	6.92
M14	skin	0.120	6.92
COLO-741	GI tract	0.120	6.92
NCI-H1355	lung	0.119	6.92
NB6	CNS	0.118	6.93
PANC-08-13	pancreas	0.118	6.93
NCI-H1651	lung	0.118	6.93
GOTO	CNS	0.118	6.93
MFM-223	breast	0.117	6.93
SW780	bladder	0.115	6.94
CAMA-1	breast	0.115	6.94
HOP-92	lung	0.114	6.94
NCI-N87	GI tract	0.114	6.94
HCC1954	breast	0.114	6.94
HX147	lung	0.114	6.94
OE33	upper aerodigestive	0.114	6.94
KYSE-70	upper aerodigestive	0.113	6.95
SK-UT-1	soft tissue	0.113	6.95
NCI-H23	lung	0.113	6.95
SJRH30	soft tissue	0.113	6.95
DJM-1	skin	0.112	6.95
SW756	uterus	0.112	6.95
HuO9	bone	0.110	6.96
NCI-H358	lung	0.109	6.96

RD	soft tissue	0.109	6.96
SNU-620	GI tract	0.109	6.96
CAL-27	upper aerodigestive	0.109	6.96
LB771-HNC	upper aerodigestive	0.108	6.97
D-392MG	CNS	0.108	6.97
HLE	liver	0.107	6.97
SW1990	pancreas	0.106	6.97
K-562	blood	0.106	6.97
MDA-MB-157	breast	0.105	6.98
SW403	GI tract	0.105	6.98
CGTH-W-1	thyroid	0.104	6.98
SNU-484	GI tract	0.103	6.99
CAS-1	CNS	0.101	6.99
G-401	kidney	0.101	7.00
D-247MG	CNS	0.101	7.00
OCUB-M	breast	0.100	7.00
OVCAR-4	ovary	0.099	7.00
D-283MED	CNS	0.098	7.01
MCF7	breast	0.098	7.01
SCC-4	upper aerodigestive	0.097	7.01
SJSA-1	bone	0.095	7.02
MDA-MB-361	breast	0.095	7.02
PANC-03-27	pancreas	0.094	7.02
DMS 114	lung	0.094	7.03
YKG-1	CNS	0.093	7.03
KNS-81-FD	CNS	0.093	7.03
SK-MG-1	CNS	0.093	7.03
HuH-7	liver	0.093	7.03
BB49-HNC	upper aerodigestive	0.093	7.03
IA-LM	lung	0.092	7.04
NCI-H2087	lung	0.091	7.04
LC-2-ad	lung	0.091	7.04
SW684	soft tissue	0.091	7.04
OE19	GI tract	0.091	7.04
S-117	soft tissue	0.091	7.04
LNcaP-Clone-FGC	other	0.090	7.04
NCI-H1703	lung	0.090	7.05
SW48	GI tract	0.090	7.05
RH-18	soft tissue	0.088	7.06
FTC-133	thyroid	0.088	7.06
CAL-62	thyroid	0.088	7.06
LK-2	lung	0.087	7.06
NCI-H226	lung	0.087	7.06
SW13	other	0.087	7.06
no-10	CNS	0.087	7.06
TE-5	upper aerodigestive	0.087	7.06
SNU-449	other	0.086	7.06
JJN-3	blood	0.086	7.07
SW962	uterus	0.086	7.07
LN-405	CNS	0.085	7.07
D-502MG	CNS	0.085	7.07
CC20	GI tract	0.085	7.07
UACC-257	skin	0.084	7.07
NCI-H1437	lung	0.084	7.07
MDA-MB-453	breast	0.084	7.08
SK-CO-1	GI tract	0.083	7.08
DoTc2-4510	uterus	0.082	7.08
NCI-H28	lung	0.082	7.09

647-V	bladder	0.081	7.09
C3A	other	0.080	7.10
MZ2-MEL	skin	0.080	7.10
COLO-829	skin	0.080	7.10
BT-20	breast	0.080	7.10
LAN-6	CNS	0.080	7.10
HCE-T	upper aerodigestive	0.079	7.10
Becker	CNS	0.079	7.10
HMV-II	skin	0.078	7.11
SBC-5	lung	0.077	7.11
OMC-1	uterus	0.077	7.11
C32	skin	0.077	7.11
NCI-H2122	lung	0.077	7.11
ES6	bone	0.076	7.12
IST-MES1	lung	0.076	7.12
HCC1187	breast	0.076	7.12
COR-L105	lung	0.076	7.12
NCI-H2342	lung	0.076	7.12
U-118-MG	CNS	0.076	7.12
NCI-H1993	lung	0.076	7.12
PFSK-1	CNS	0.075	7.12
COLO 205	GI tract	0.075	7.12
CaR-1	GI tract	0.074	7.13
KINGS-1	CNS	0.074	7.13
MLMA	blood	0.074	7.13
T98G	CNS	0.073	7.13
TE-9	upper aerodigestive	0.073	7.13
CCK-81	GI tract	0.073	7.13
PC9	lung	0.073	7.14
SNU-886	liver	0.073	7.14
NCI-H2291	lung	0.073	7.14
SK-MEL-30	skin	0.073	7.14
TE-8	upper aerodigestive	0.072	7.14
AZ-521	GI tract	0.072	7.14
HCCC9810	liver	0.072	7.14
HuP-T3	pancreas	0.072	7.14
Hs-578-T	breast	0.072	7.14
NB12	CNS	0.072	7.14
A253	other	0.072	7.14
LCLC-103H	lung	0.072	7.15
A673	soft tissue	0.071	7.15
D-336MG	CNS	0.071	7.15
SW48	GI tract	0.071	7.15
MDA-MB-436	breast	0.071	7.15
OE33	GI tract	0.071	7.15
QGY7703	liver	0.071	7.15
Calu-6	lung	0.071	7.15
Detroit562	upper aerodigestive	0.071	7.15
SF126	CNS	0.071	7.15
NCI-H2347	lung	0.070	7.15
SK-MEL-2	skin	0.070	7.15
HuH-1	liver	0.070	7.15
RPMI-2650	upper aerodigestive	0.070	7.16
KYSE-510	upper aerodigestive	0.070	7.16
TCCSUP	bladder	0.070	7.16
NCI-H661	lung	0.070	7.16
LB2518-MEL	skin	0.069	7.16
OS-RC-2	kidney	0.069	7.16

TGBC24TKB	GI tract	0.068	7.16
SCC-9	upper aerodigestive	0.068	7.17
IST-SL1	lung	0.068	7.17
RVH-421	skin	0.068	7.17
NUGC-4	GI tract	0.067	7.17
SNU-739	liver	0.067	7.17
G-361	skin	0.067	7.18
EW-11	bone	0.067	7.18
MDA-MB-231	breast	0.066	7.18
GTL16	GI tract	0.066	7.18
005A	upper aerodigestive	0.066	7.18
RO82-W-1	thyroid	0.066	7.18
YAPC	pancreas	0.065	7.19
D-423MG	CNS	0.065	7.19
AMO-1	blood	0.065	7.19
HCT-116	GI tract	0.065	7.19
SW480	GI tract	0.065	7.19
NB5	CNS	0.065	7.19
TK10	kidney	0.065	7.19
OVCAR-8	ovary	0.063	7.20
BEL7404	liver	0.063	7.20
MKN1	GI tract	0.063	7.20
NCI-N87	GI tract	0.063	7.20
LS 180	GI tract	0.062	7.20
BxPC-3	pancreas	0.062	7.20
DSH1	bladder	0.062	7.21
T47D	breast	0.062	7.21
NUGC-3	GI tract	0.062	7.21
BFTC-909	kidney	0.061	7.21
OCUM-1	GI tract	0.061	7.21
RPMI-7951	skin	0.061	7.22
SK-MEL-3	skin	0.061	7.22
MMAC-SF	skin	0.061	7.22
KP-4	pancreas	0.061	7.22
MPP-89	lung	0.061	7.22
AGS	GI tract	0.060	7.22
CAL-85-1	breast	0.060	7.22
KYSE-150	upper aerodigestive	0.060	7.22
SNU-354	liver	0.060	7.22
SNU-368	liver	0.060	7.22
SNU-601	GI tract	0.060	7.22
MG-63	bone	0.059	7.23
KALS-1	CNS	0.059	7.23
NEC8	other	0.059	7.23
NCI-H1395	lung	0.059	7.23
COLO-679	skin	0.059	7.23
SF268	CNS	0.058	7.23
C-33-A	uterus	0.058	7.23
SNU-449	liver	0.058	7.24
THP-1	blood	0.058	7.24
CFPAC-1	pancreas	0.057	7.24
HSC-3	upper aerodigestive	0.057	7.24
HUTU-80	GI tract	0.057	7.24
HOS	bone	0.057	7.24
SK-N-AS	CNS	0.057	7.24
NCI-H526	lung	0.057	7.24
Calu-1	lung	0.057	7.25
HRA19	GI tract	0.057	7.25

DBTRG-05MG	CNS	0.056	7.25
NH-12	CNS	0.056	7.25
HEL	blood	0.056	7.25
HPAF-II	pancreas	0.056	7.25
SNU-5	GI tract	0.056	7.25
MEC-1	blood	0.056	7.25
A498	kidney	0.055	7.26
ES5	bone	0.055	7.26
NCI-H23	lung	0.055	7.26
ES8	bone	0.055	7.26
006/1	upper aerodigestive	0.055	7.26
NCI-H1666	lung	0.055	7.26
DMS-273	lung	0.055	7.26
EW-1	bone	0.054	7.27
NCI-H1793	lung	0.054	7.27
SNU-878	liver	0.054	7.27
JEG-3	other	0.054	7.27
RKO	GI tract	0.054	7.27
ACN	CNS	0.054	7.27
MKN45	GI tract	0.053	7.27
MDA-MB-468	breast	0.053	7.28
EPLC-272H	lung	0.053	7.28
SK-MEL-24	skin	0.053	7.28
OVCAR-3	ovary	0.052	7.28
NCI-H1792	lung	0.051	7.29
SCH	GI tract	0.051	7.29
Hep 3B	liver	0.051	7.29
H-EMC-SS	bone	0.051	7.29
NCI-H1693	lung	0.051	7.30
NTERA-S-cl-D1	other	0.051	7.30
BHY	upper aerodigestive	0.050	7.30
CP66-MEL	skin	0.050	7.30
HOP-62	lung	0.050	7.30
A172	CNS	0.050	7.30
A2058	skin	0.050	7.30
AU565	breast	0.050	7.30
COLO 320DM	GI tract	0.050	7.30
UACC-62	skin	0.050	7.30
LoVo	GI tract	0.050	7.31
NCI-H1299	lung	0.050	7.31
SK-MEL-28	skin	0.049	7.31
SK-HEP-1	liver	0.049	7.31
SNU-398	liver	0.049	7.31
NMC-G1	CNS	0.049	7.31
KNS-62	lung	0.049	7.31
HCC1569	breast	0.048	7.32
SCC-25	upper aerodigestive	0.048	7.32
KGN	ovary	0.048	7.32
NB14	CNS	0.048	7.32
SF295	CNS	0.047	7.32
MHCC97-L	liver	0.047	7.33
CAL-12T	lung	0.047	7.33
HCA7	GI tract	0.047	7.33
MHH-ES-1	bone	0.047	7.33
SK-HEP-1	other	0.047	7.33
NCI-H1838	lung	0.047	7.33
IGROV-1	ovary	0.047	7.33
786-0	kidney	0.047	7.33

SW620	GI tract	0.047	7.33
C99	GI tract	0.046	7.33
OAW-42	ovary	0.046	7.34
NCI-H2452	lung	0.045	7.34
HCC1806	breast	0.045	7.35
Reh	blood	0.045	7.35
COLO-800	skin	0.045	7.35
SK-MEL-5	skin	0.045	7.35
SW620	GI tract	0.044	7.35
NCI-H2405	lung	0.044	7.35
NCI-H1648	lung	0.044	7.36
A549	lung	0.044	7.36
HCC1937	breast	0.044	7.36
NCI-H838	lung	0.044	7.36
MIA-PaCa-2	pancreas	0.044	7.36
HEC-1	uterus	0.043	7.36
GI-1	CNS	0.043	7.37
SH-4	skin	0.043	7.37
NCI-H1437	lung	0.043	7.37
D-263MG	CNS	0.043	7.37
SW1088	CNS	0.043	7.37
KS-1	CNS	0.043	7.37
EW-7	bone	0.042	7.37
ETK-1	GI tract	0.042	7.37
U937	blood	0.042	7.37
Hs746T	GI tract	0.042	7.38
GAMG	CNS	0.042	7.38
D-542MG	CNS	0.041	7.38
NCI-H2052	lung	0.041	7.39
SNU-216	GI tract	0.041	7.39
SNU-761	liver	0.041	7.39
HuP-T4	pancreas	0.041	7.39
MEL-HO	skin	0.041	7.39
RXF393	kidney	0.041	7.39
RKO	GI tract	0.040	7.39
SF539	CNS	0.040	7.39
JIMT-1	breast	0.040	7.40
HN15	upper aerodigestive	0.040	7.40
RH-1	soft tissue	0.040	7.40
A388	other	0.040	7.40
CAL-33	upper aerodigestive	0.039	7.41
SK-N-DZ	CNS	0.039	7.41
SNU-638	GI tract	0.039	7.41
SAS	upper aerodigestive	0.039	7.41
UM-UC-3	bladder	0.038	7.42
NB10	CNS	0.038	7.42
MEL-JUSO	skin	0.038	7.42
KATOIII	GI tract	0.038	7.42
NCI-H1703	lung	0.038	7.42
SC-1	blood	0.038	7.42
Detroit562	upper aerodigestive	0.038	7.42
MDA-MB-157	breast	0.037	7.43
OCI-AML2	blood	0.037	7.43
ZR-75-1	breast	0.037	7.43
LU-99A	lung	0.037	7.43
CP50-MEL-B	skin	0.037	7.43
A431	skin	0.037	7.43
ES7	bone	0.037	7.43

8505C	thyroid	0.037	7.44
ES4	bone	0.036	7.44
G-402	soft tissue	0.036	7.44
COR-L23	lung	0.036	7.44
BT-549	breast	0.036	7.44
HCC1395	breast	0.036	7.44
NCI-H1975	lung	0.036	7.44
SK-BR-3	breast	0.036	7.44
SUM52PE	breast	0.036	7.44
SK-N-FI	CNS	0.036	7.44
EGI-1	GI tract	0.035	7.45
NCI-H1048	lung	0.035	7.46
EC-GI-10	upper aerodigestive	0.035	7.46
BB65-RCC	kidney	0.034	7.47
IGR-1	skin	0.034	7.47
NCI-H358	lung	0.034	7.47
23132-87	GI tract	0.034	7.47
IST-MEL1	skin	0.034	7.47
HCT-8	GI tract	0.033	7.48
NCI-H1755	lung	0.033	7.48
HCT-15	GI tract	0.033	7.48
DOK	upper aerodigestive	0.033	7.48
HGC-27	GI tract	0.033	7.48
A101D	skin	0.033	7.48
Ca9-22	upper aerodigestive	0.033	7.48
A204	soft tissue	0.033	7.48
NAMALWA	blood	0.033	7.48
SN12C	kidney	0.033	7.48
8305C	thyroid	0.033	7.49
AsPC-1	pancreas	0.033	7.49
CHP-212	CNS	0.032	7.49
NB13	CNS	0.032	7.49
SK-OV-3	ovary	0.032	7.49
AGS	GI tract	0.032	7.49
BT-549	breast	0.032	7.49
EW-16	bone	0.032	7.50
BPH-1	other	0.032	7.50
SK-LU-1	lung	0.032	7.50
O13	upper aerodigestive	0.031	7.51
ARH-77	blood	0.031	7.51
CAL27	upper aerodigestive	0.031	7.51
Daoy	CNS	0.031	7.51
PSN1	pancreas	0.030	7.52
NB7	CNS	0.030	7.52
NCI-H2030	lung	0.030	7.52
IM95m	GI tract	0.030	7.52
MOLM-13	blood	0.030	7.52
NCI-H460	lung	0.030	7.53
HD-MY-Z	blood	0.030	7.53
SW954	uterus	0.029	7.53
HLE	other	0.029	7.53
Mewo	skin	0.029	7.54
SNU-16	GI tract	0.029	7.54
NCI-H1299	lung	0.029	7.54
HN5	upper aerodigestive	0.029	7.54
MOLP-8	blood	0.029	7.54
COLO-792	skin	0.029	7.54
5637	bladder	0.029	7.54

CAL-39	uterus	0.028	7.55
HuH-7	other	0.028	7.55
LCLC-97TM1	lung	0.028	7.55
HCT-15	GI tract	0.028	7.55
23132/87	GI tract	0.028	7.55
CAMA-1	breast	0.028	7.55
CAL-54	kidney	0.028	7.56
ES1	bone	0.027	7.56
JAR	other	0.027	7.57
BEL7405	liver	0.027	7.57
NCI-H322	lung	0.027	7.57
BHT-101	thyroid	0.027	7.57
NY	bone	0.027	7.57
SW1573	lung	0.026	7.58
EW-22	bone	0.026	7.58
CAL-120	breast	0.026	7.58
GB-1	CNS	0.026	7.58
UACC-893	breast	0.026	7.59
MC-IXC	CNS	0.026	7.59
TE-10	upper aerodigestive	0.026	7.59
NB69	CNS	0.025	7.59
ONS-76	CNS	0.025	7.60
GI-ME-N	CNS	0.025	7.60
MonoMac6	blood	0.025	7.60
MZ1-PC	pancreas	0.025	7.61
LOXIMVI	skin	0.024	7.62
A2780	ovary	0.024	7.62
FADU	upper aerodigestive	0.024	7.62
SNU-1	GI tract	0.024	7.62
EFO-27	ovary	0.024	7.62
TE-11	upper aerodigestive	0.024	7.62
HSC-4	upper aerodigestive	0.024	7.62
DU-145	other	0.024	7.63
RERF-LC-MS	lung	0.024	7.63
OVCAR-5	ovary	0.023	7.63
WSU DLCL2	blood	0.023	7.63
LB2241-RCC	kidney	0.023	7.63
RPMI-8226	blood	0.023	7.64
SK-MES-1	lung	0.023	7.64
ES3	bone	0.023	7.64
NCI-H2009	lung	0.023	7.64
Nomo-1	blood	0.023	7.64
GT3TKB	GI tract	0.023	7.64
ABC-1	lung	0.023	7.64
L-363	blood	0.022	7.66
HTC-C3	thyroid	0.022	7.66
U-2-OS	bone	0.022	7.66
GMS-10	CNS	0.022	7.67
HT-144	skin	0.021	7.67
KU-19-19	bladder	0.021	7.67
VA-ES-BJ	soft tissue	0.021	7.67
HEL 92.1.7	blood	0.021	7.68
BFTC-905	bladder	0.021	7.68
769-P	kidney	0.021	7.69
BCPAP	thyroid	0.020	7.69
NCI-H292	lung	0.020	7.69
T-47D	breast	0.020	7.70
HN6	upper aerodigestive	0.020	7.70

TYK-nu	ovary	0.019	7.71
8-MG-BA	CNS	0.019	7.72
HGC-27	GI tract	0.019	7.72
NCI-H2291	lung	0.019	7.72
JVM-3	blood	0.019	7.72
SK-LMS-1	soft tissue	0.019	7.72
LXF-289	lung	0.019	7.73
HCC1187	breast	0.018	7.74
Jurkat	blood	0.018	7.74
SW872	soft tissue	0.018	7.75
NCI-H1563	lung	0.018	7.76
SW1710	bladder	0.017	7.76
HCC1419	breast	0.017	7.77
MV-4-11	blood	0.017	7.77
NCI-H1869	lung	0.017	7.77
JEKO-1	blood	0.017	7.77
DK-MG	CNS	0.017	7.78
T-24	bladder	0.016	7.80
KG-1	blood	0.016	7.80
ACHN	kidney	0.016	7.80
HO-1-N-1	upper aerodigestive	0.016	7.80
A549	lung	0.016	7.81
HN	upper aerodigestive	0.015	7.81
PA-1	ovary	0.015	7.82
CMK	blood	0.015	7.82
RS4;11	blood	0.015	7.82
CAL-51	breast	0.015	7.82
BB30-HNC	upper aerodigestive	0.015	7.83
OC-314	ovary	0.014	7.85
YH-13	CNS	0.014	7.85
LoVo	GI tract	0.014	7.86
U251	CNS	0.014	7.86
HuCCCT1	GI tract	0.014	7.86
GCT	soft tissue	0.013	7.88
U031	kidney	0.013	7.88
NOS-1	bone	0.013	7.89
CHL-1	skin	0.013	7.90
LB1047-RCC	kidney	0.012	7.90
PJ34	upper aerodigestive	0.012	7.92
A375	skin	0.012	7.94
A427	lung	0.011	7.94
IM-9	blood	0.011	7.95
HCT-116	GI tract	0.011	7.97
KYSE-140	upper aerodigestive	0.010	7.99
KYSE-450	upper aerodigestive	0.010	8.01
CAKI-1	kidney	0.010	8.02
Molm 16	blood	0.009	8.03
HN3	upper aerodigestive	0.009	8.04
OCI-LY-19	blood	0.009	8.06
PC-14	lung	0.009	8.07
HT-1080	soft tissue	0.008	8.10
011B	upper aerodigestive	0.008	8.12
KOSC-2	upper aerodigestive	0.007	8.14
LB996-RCC	kidney	0.007	8.18
PJ41	upper aerodigestive	0.006	8.20
011A	upper aerodigestive	0.006	8.22
H4	CNS	0.006	8.26
HN4	upper aerodigestive	0.005	8.30

015B	upper aerodigestive	0.004	8.44
SW982	soft tissue	0.003	8.47
D-566MG	CNS	0.003	8.51
K5	thyroid	0.002	8.65

DiscoverX KinomeScan

Single-point determination with bisamide **1** (CCT245232) at 1 μ M.

For screening protocol and assay conditions see: <https://www.discoverx.com/technologies-platforms/competitive-binding-technology/kinomescan-technology-platform> (August 31, 2016).

Table S2. Single-Point KinomeScan for Bisamide **1**

Compound Name	Ambit Gene Symbol	Entrez Gene Symbol	Percent Control
CCT245232	KIT(L576P)	KIT	0
CCT245232	KIT(V559D)	KIT	0.05
CCT245232	KIT	KIT	0.1
CCT245232	PDGFRA	PDGFRA	0.7
CCT245232	PDGFRB	PDGFRB	0.95
CCT245232	BRAF(V600E)	BRAF	6
CCT245232	DDR1	DDR1	13
CCT245232	KIT(V559D,V654A)	KIT	15
CCT245232	BRAF	BRAF	22
CCT245232	CSF1R	CSF1R	23
CCT245232	BMPR1B	BMPR1B	29
CCT245232	ABL1(F317I)-nonphosphorylated	ABL1	38
CCT245232	IRAK1	IRAK1	44
CCT245232	IRAK4	IRAK4	46
CCT245232	ABL1(F317I)-phosphorylated	ABL1	52
CCT245232	ABL1-nonphosphorylated	ABL1	52
CCT245232	KIT(A829P)	KIT	52
CCT245232	ABL1(F317L)-nonphosphorylated	ABL1	55
CCT245232	MKNK1	MKNK1	56
CCT245232	RAF1	RAF1	56
CCT245232	ABL1(Q252H)-nonphosphorylated	ABL1	62
CCT245232	NDR2	STK38L	63
CCT245232	SRPK1	SRPK1	65
CCT245232	PIM2	PIM2	68
CCT245232	ABL1(H396P)-nonphosphorylated	ABL1	69
CCT245232	p38-alpha	MAPK14	69
CCT245232	CDKL3	CDKL3	70
CCT245232	ABL1(F317L)-phosphorylated	ABL1	71
CCT245232	AKT1	AKT1	71
CCT245232	CTK	MATK	71
CCT245232	HPK1	MAP4K1	72
CCT245232	PIK3CA(I800L)	PIK3CA	72
CCT245232	SGK3	SGK3	72
CCT245232	PIK3C2G	PIK3C2G	73
CCT245232	PKNB(M.tuberculosis)	pknB	73
CCT245232	SNRK	SNRK	73
CCT245232	ABL1(M351T)-phosphorylated	ABL1	75
CCT245232	MEK5	MAP2K5	75
CCT245232	RIOK3	RIOK3	75
CCT245232	ERN1	ERN1	76
CCT245232	RPS6KA4(Kin. Dom. 2-C-terminal)	RPS6KA4	76
CCT245232	MINK	MINK1	78
CCT245232	ABL1(T315I)-nonphosphorylated	ABL1	79
CCT245232	BMX	BMX	79
CCT245232	ADCK3	CABC1	79
CCT245232	PIK3CG	PIK3CG	79
CCT245232	NDR1	STK38	79
CCT245232	CAMK2D	CAMK2D	80
CCT245232	TIE1	TIE1	80
CCT245232	HIPK3	HIPK3	81
CCT245232	JAK1(JH1 domain-catalytic)	JAK1	81
CCT245232	TLK2	TLK2	81
CCT245232	KIT(V559D,T670I)	KIT	82
CCT245232	LRRK2	LRRK2	82
CCT245232	EPHA3	EPHA3	83
CCT245232	FLT3(N841I)	FLT3	83
CCT245232	RSK3(Kin. Dom. 1-N-terminal)	RPS6KA2	83
CCT245232	STK39	STK39	83
CCT245232	CAMK1	CAMK1	84
CCT245232	HIPK2	HIPK2	84
CCT245232	SNARK	NUAK2	84
CCT245232	YSK1	STK25	84
CCT245232	ABL2	ABL2	85
CCT245232	CDC2L1	CDC2L1	85
CCT245232	EPHB6	EPHB6	85
CCT245232	KIT(D816H)	KIT	85

CCT245232	MEK1	MAP2K1	85
CCT245232	MKK7	MAP2K7	85
CCT245232	JNK3	MAPK10	85
CCT245232	MUSK	MUSK	85
CCT245232	NEK7	NEK7	85
CCT245232	PRKCE	PRKCE	85
CCT245232	ACVR2A	ACVR2A	86
CCT245232	ACVR2B	ACVR2B	86
CCT245232	CAMK2G	CAMK2G	86
CCT245232	DYRK2	DYRK2	86
CCT245232	EPHA2	EPHA2	86
CCT245232	EPHA8	EPHA8	86
CCT245232	IRAK3	IRAK3	86
CCT245232	MEK2	MAP2K2	86
CCT245232	MARK3	MARK3	86
CCT245232	PIK3CA	PIK3CA	86
CCT245232	RIOK2	RIOK2	86
CCT245232	ULK1	ULK1	86
CCT245232	CDK4-cyclinD3	CDK4	87
CCT245232	DYRK1B	DYRK1B	87
CCT245232	ERBB3	ERBB3	87
CCT245232	ERBB4	ERBB4	87
CCT245232	JAK3(JH1dom ain-catalytic)	JAK3	87
CCT245232	MEK3	MAP2K3	87
CCT245232	NEK4	NEK4	87
CCT245232	ARK5	NUAK1	87
CCT245232	PRKCI	PRKCI	87
CCT245232	PRKG2	PRKG2	87
CCT245232	CDK4-cyclinD1	CDK4	88
CCT245232	CSNK2A1	CSNK2A1	88
CCT245232	FLT3(D835Y)	FLT3	88
CCT245232	NEK1	NEK1	88
CCT245232	PIK3CA(M104 3I)	PIK3CA	88
CCT245232	PKAC-alpha	PRKACA	88
CCT245232	ROCK2	ROCK2	88
CCT245232	TAOK3	TAOK3	88
CCT245232	TNIK	TNIK	88
CCT245232	CDK11	CDC2L6	89
CCT245232	CDKL2	CDKL2	89
CCT245232	EPHA4	EPHA4	89
CCT245232	INSRR	INSRR	89
CCT245232	KIT(D816V)	KIT	89
CCT245232	MAPKAPK5	MAPKAPK 5	89
CCT245232	MET(M1250T)	MET	89

CCT245232	MYLK	MYLK	89
CCT245232	NEK5	NEK5	89
CCT245232	PAK6	PAK6	89
CCT245232	PIK3C2B	PIK3C2B	89
CCT245232	TEC	TEC	89
CCT245232	CSK	CSK	90
CCT245232	CSNK1D	CSNK1D	90
CCT245232	FLT3(K663Q)	FLT3	90
CCT245232	GSK3A	GSK3A	90
CCT245232	ITK	ITK	90
CCT245232	LIMK2	LIMK2	90
CCT245232	NEK3	NEK3	90
CCT245232	TRKC	NTRK3	90
CCT245232	PRKCH	PRKCH	90
CCT245232	LKB1	STK11	90
CCT245232	TESK1	TESK1	90
CCT245232	TSSK1B	TSSK1B	90
CCT245232	AAK1	AAK1	91
CCT245232	ABL1(T315I)- phosphorylated	ABL1	91
CCT245232	EGFR(L747- S752del, P753S)	EGFR	91
CCT245232	EGFR(L861Q)	EGFR	91
CCT245232	GRK7	GRK7	91
CCT245232	JAK2(JH1dom ain-catalytic)	JAK2	91
CCT245232	MYLK4	MYLK4	91
CCT245232	PIK3CA(Q546 K)	PIK3CA	91
CCT245232	PIP5K2C	PIP4K2C	91
CCT245232	PRKD2	PRKD2	91
CCT245232	RSK2(Kin.Do m.1-N- terminal)	RPS6KA3	91
CCT245232	MST2	STK3	91
CCT245232	TTK	TTK	91
CCT245232	TYK2(JH1dom ain-catalytic)	TYK2	91
CCT245232	WEE1	WEE1	91
CCT245232	MRCKA	CDC42BPA	92
CCT245232	CDK2	CDK2	92
CCT245232	RPS6KA5(Kin. Dom.1-N- terminal)	RPS6KA5	92
CCT245232	RSK4(Kin.Do m.1-N- terminal)	RPS6KA6	92
CCT245232	TRPM6	TRPM6	92
CCT245232	AURKA	AURKA	93
CCT245232	BIKE	BMP2K	93
CCT245232	DYRK1A	DYRK1A	93
CCT245232	EGFR(L747- E749del, A750P)	EGFR	93
CCT245232	FGFR2	FGFR2	93
CCT245232	PFPK5(P.falcip arum)	MAL13P1.2 79	93

CCT245232	TAK1	MAP3K7	93
CCT245232	p38-beta	MAPK11	93
CCT245232	SRMS	SRMS	93
CCT245232	LOK	STK10	93
CCT245232	YANK1	STK32A	93
CCT245232	ZAK	ZAK	93
CCT245232	CHEK2	CHEK2	94
CCT245232	EGFR(L858R)	EGFR	94
CCT245232	GCN2(Kin.Do m.2,S808G)	EIF2AK4	94
CCT245232	FGFR3	FGFR3	94
CCT245232	FGFR3(G697C)	FGFR3	94
CCT245232	NEK11	NEK11	94
CCT245232	PDPK1	PDPK1	94
CCT245232	PIK3CB	PIK3CB	94
CCT245232	ROCK1	ROCK1	94
CCT245232	SBK1	SBK1	94
CCT245232	VRK2	VRK2	94
CCT245232	YES	YES1	94
CCT245232	ABL1(Y253F)- phosphorylated	ABL1	95
CCT245232	AURKB	AURKB	95
CCT245232	DAPK2	DAPK2	95
CCT245232	FLT3(R834Q)	FLT3	95
CCT245232	LATS2	LATS2	95
CCT245232	LTK	LTK	95
CCT245232	MAP4K2	MAP4K2	95
CCT245232	MAP4K4	MAP4K4	95
CCT245232	RIPK1	RIPK1	95
CCT245232	STK35	STK35	95
CCT245232	TAOK1	TAOK1	95
CCT245232	TAOK2	TAOK2	95
CCT245232	TNK2	TNK2	95
CCT245232	ULK2	ULK2	95
CCT245232	AKT2	AKT2	96
CCT245232	AXL	AXL	96
CCT245232	CDK5	CDK5	96
CCT245232	CDK8	CDK8	96
CCT245232	FLT3(D835H)	FLT3	96
CCT245232	IKK-beta	IKBKB	96
CCT245232	INSR	INSR	96
CCT245232	MEK6	MAP2K6	96
CCT245232	MLK2	MAP3K10	96
CCT245232	MLK1	MAP3K9	96
CCT245232	JNK2	MAPK9	96
CCT245232	TRKA	NTRK1	96

CCT245232	OSR1	OXSRI	96
CCT245232	PCTK1	PCTK1	96
CCT245232	PHKG1	PHKG1	96
CCT245232	PIP5K1A	PIP5K1A	96
CCT245232	PLK2	PLK2	96
CCT245232	PKAC-beta	PRKACB	96
CCT245232	RET(V804L)	RET	96
CCT245232	RIPK4	RIPK4	96
CCT245232	SRC	SRC	96
CCT245232	ABL1- phosphorylated	ABL1	97
CCT245232	CAMK1G	CAMK1G	97
CCT245232	CDK3	CDK3	97
CCT245232	CSNK1G2	CSNK1G2	97
CCT245232	EPHA1	EPHA1	97
CCT245232	EPHA7	EPHA7	97
CCT245232	FLT3(ITD)	FLT3	97
CCT245232	p38-delta	MAPK13	97
CCT245232	ERK1	MAPK3	97
CCT245232	PAK3	PAK3	97
CCT245232	PLK1	PLK1	97
CCT245232	TYRO3	TYRO3	97
CCT245232	ACVR1B	ACVR1B	98
CCT245232	DMPK2	CDC42BPG	98
CCT245232	FLT1	FLT1	98
CCT245232	IKK-epsilon	IKBKE	98
CCT245232	MAP4K5	MAP4K5	98
CCT245232	MAPKAPK2	MAPKAPK 2	98
CCT245232	TRKB	NTRK2	98
CCT245232	PIK3CA(E542 K)	PIK3CA	98
CCT245232	FAK	PTK2	98
CCT245232	RET(V804M)	RET	98
CCT245232	STK16	STK16	98
CCT245232	BMPRI1A	BMPRI1A	99
CCT245232	CDC2L2	CDC2L2	99
CCT245232	CDC2L5	CDC2L5	99
CCT245232	CDKL5	CDKL5	99
CCT245232	MAP3K1	MAP3K1	99
CCT245232	PAK7	PAK7	99
CCT245232	PIK3CA(E545 A)	PIK3CA	99
CCT245232	PIK3CD	PIK3CD	99
CCT245232	PIP5K1C	PIP5K1C	99
CCT245232	PKMYT1	PKMYT1	99
CCT245232	PRKCQ	PRKCQ	99
CCT245232	RSK4(Kin.Do m.2-C- terminal)	RPS6KA6	99

CCT245232	DRAK2	STK17B	99
CCT245232	YANK3	STK32C	99
CCT245232	TXK	TXK	99
CCT245232	ULK3	ULK3	99
CCT245232	ABL1(E255K)-phosphorylated	ABL1	100
CCT245232	ABL1(H396P)-phosphorylated	ABL1	100
CCT245232	ABL1(Q252H)-phosphorylated	ABL1	100
CCT245232	ACVR1	ACVR1	100
CCT245232	ACVRL1	ACVRL1	100
CCT245232	ADCK4	ADCK4	100
CCT245232	AKT3	AKT3	100
CCT245232	ALK	ALK	100
CCT245232	ANKK1	ANKK1	100
CCT245232	AURKC	AURKC	100
CCT245232	BLK	BLK	100
CCT245232	BMPR2	BMPR2	100
CCT245232	BRSK1	BRSK1	100
CCT245232	BRSK2	BRSK2	100
CCT245232	BTK	BTK	100
CCT245232	CAMK1D	CAMK1D	100
CCT245232	CAMK2A	CAMK2A	100
CCT245232	CAMK2B	CAMK2B	100
CCT245232	CAMK4	CAMK4	100
CCT245232	CAMKK1	CAMKK1	100
CCT245232	CAMKK2	CAMKK2	100
CCT245232	CASK	CASK	100
CCT245232	MRCKB	CDC42BPB	100
CCT245232	CDK7	CDK7	100
CCT245232	CDK9	CDK9	100
CCT245232	CDKL1	CDKL1	100
CCT245232	CHEK1	CHEK1	100
CCT245232	IKK-alpha	CHUK	100
CCT245232	CIT	CIT	100
CCT245232	CLK1	CLK1	100
CCT245232	CLK2	CLK2	100
CCT245232	CLK3	CLK3	100
CCT245232	CLK4	CLK4	100
CCT245232	CSNK1A1	CSNK1A1	100
CCT245232	CSNK1A1L	CSNK1A1L	100
CCT245232	CSNK1E	CSNK1E	100
CCT245232	CSNK1G1	CSNK1G1	100
CCT245232	CSNK1G3	CSNK1G3	100
CCT245232	CSNK2A2	CSNK2A2	100
CCT245232	DAPK1	DAPK1	100

CCT245232	DAPK3	DAPK3	100
CCT245232	DCAMKL1	DCLK1	100
CCT245232	DCAMKL2	DCLK2	100
CCT245232	DCAMKL3	DCLK3	100
CCT245232	DDR2	DDR2	100
CCT245232	DMPK	DMPK	100
CCT245232	RIPK5	DSTKY	100
CCT245232	EGFR	EGFR	100
CCT245232	EGFR(E746-A750del)	EGFR	100
CCT245232	EGFR(G719C)	EGFR	100
CCT245232	EGFR(G719S)	EGFR	100
CCT245232	EGFR(L747-T751del,Sins)	EGFR	100
CCT245232	EGFR(L858R, T790M)	EGFR	100
CCT245232	EGFR(S752-I759del)	EGFR	100
CCT245232	EGFR(T790M)	EGFR	100
CCT245232	EIF2AK1	EIF2AK1	100
CCT245232	PRKR	EIF2AK2	100
CCT245232	EPHA5	EPHA5	100
CCT245232	EPHA6	EPHA6	100
CCT245232	EPHB1	EPHB1	100
CCT245232	EPHB2	EPHB2	100
CCT245232	EPHB3	EPHB3	100
CCT245232	EPHB4	EPHB4	100
CCT245232	ERBB2	ERBB2	100
CCT245232	FER	FER	100
CCT245232	FES	FES	100
CCT245232	FGFR1	FGFR1	100
CCT245232	FGFR4	FGFR4	100
CCT245232	FGR	FGR	100
CCT245232	FLT3	FLT3	100
CCT245232	FLT4	FLT4	100
CCT245232	MTOR	FRAP1	100
CCT245232	FRK	FRK	100
CCT245232	FYN	FYN	100
CCT245232	GAK	GAK	100
CCT245232	GRK1	GRK1	100
CCT245232	GRK4	GRK4	100
CCT245232	GSK3B	GSK3B	100
CCT245232	HCK	HCK	100
CCT245232	HIPK1	HIPK1	100
CCT245232	HIPK4	HIPK4	100
CCT245232	HUNK	HUNK	100
CCT245232	ICK	ICK	100
CCT245232	IGF1R	IGF1R	100

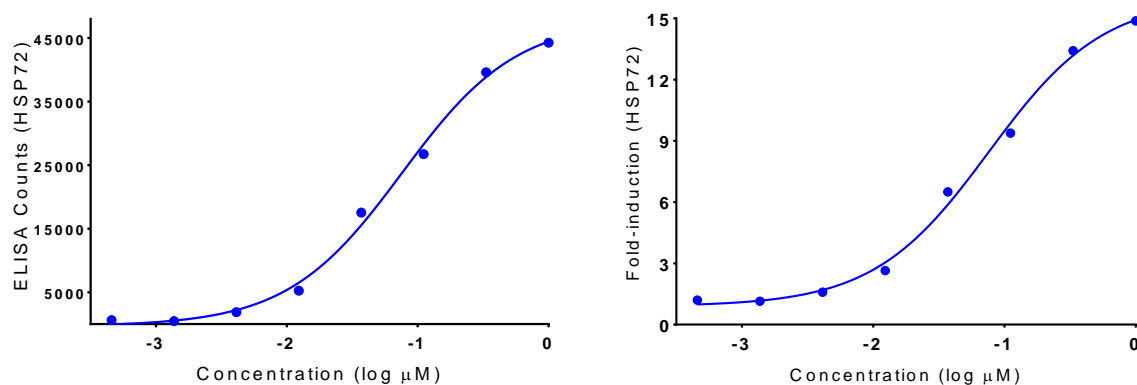
CCT245232	JAK1(JH2domain-pseudokinase)	JAK1	100
CCT245232	VEGFR2	KDR	100
CCT245232	QSK	KIAA0999	100
CCT245232	LATS1	LATS1	100
CCT245232	LCK	LCK	100
CCT245232	LIMK1	LIMK1	100
CCT245232	LRRK2(G2019S)	LRRK2	100
CCT245232	LYN	LYN	100
CCT245232	MAK	MAK	100
CCT245232	MEK4	MAP2K4	100
CCT245232	MLK3	MAP3K11	100
CCT245232	DLK	MAP3K12	100
CCT245232	LZK	MAP3K13	100
CCT245232	MAP3K15	MAP3K15	100
CCT245232	MAP3K2	MAP3K2	100
CCT245232	MAP3K3	MAP3K3	100
CCT245232	MAP3K4	MAP3K4	100
CCT245232	ASK1	MAP3K5	100
CCT245232	ASK2	MAP3K6	100
CCT245232	MAP4K3	MAP4K3	100
CCT245232	ERK2	MAPK1	100
CCT245232	p38-gamma	MAPK12	100
CCT245232	ERK8	MAPK15	100
CCT245232	ERK4	MAPK4	100
CCT245232	ERK3	MAPK6	100
CCT245232	ERK5	MAPK7	100
CCT245232	JNK1	MAPK8	100
CCT245232	MARK1	MARK1	100
CCT245232	MARK2	MARK2	100
CCT245232	MARK4	MARK4	100
CCT245232	MAST1	MAST1	100
CCT245232	MELK	MELK	100
CCT245232	MERTK	MERTK	100
CCT245232	MET	MET	100
CCT245232	MET(Y1235D)	MET	100
CCT245232	NIM1	MGC42105	100
CCT245232	MKNK2	MKNK2	100
CCT245232	MST1R	MST1R	100
CCT245232	MST4	MST4	100
CCT245232	MYLK2	MYLK2	100
CCT245232	MLCK	MYLK3	100
CCT245232	MYO3A	MYO3A	100
CCT245232	MYO3B	MYO3B	100
CCT245232	NEK2	NEK2	100

CCT245232	NEK6	NEK6	100
CCT245232	NEK9	NEK9	100
CCT245232	NLK	NLK	100
CCT245232	PAK1	PAK1	100
CCT245232	PAK2	PAK2	100
CCT245232	PAK4	PAK4	100
CCT245232	PCTK2	PCTK2	100
CCT245232	PCTK3	PCTK3	100
CCT245232	PFCDPK1(P.falciparum)	PFB0815w	100
CCT245232	PFTK1	PFTK1	100
CCT245232	PFTAIRE2	PFTK2	100
CCT245232	PHKG2	PHKG2	100
CCT245232	PIK4CB	PI4KB	100
CCT245232	PIK3CA(C420R)	PIK3CA	100
CCT245232	PIK3CA(E545K)	PIK3CA	100
CCT245232	PIK3CA(H1047L)	PIK3CA	100
CCT245232	PIK3CA(H1047Y)	PIK3CA	100
CCT245232	PIM1	PIM1	100
CCT245232	PIM3	PIM3	100
CCT245232	PIP5K2B	PIP4K2B	100
CCT245232	PKN1	PKN1	100
CCT245232	PKN2	PKN2	100
CCT245232	PLK3	PLK3	100
CCT245232	PLK4	PLK4	100
CCT245232	AMPK-alpha1	PRKAA1	100
CCT245232	AMPK-alpha2	PRKAA2	100
CCT245232	PRKCD	PRKCD	100
CCT245232	PRKD1	PRKD1	100
CCT245232	PRKD3	PRKD3	100
CCT245232	PRKG1	PRKG1	100
CCT245232	PRKX	PRKX	100
CCT245232	PRP4	PRPF4B	100
CCT245232	PYK2	PTK2B	100
CCT245232	BRK	PTK6	100
CCT245232	RET	RET	100
CCT245232	RET(M918T)	RET	100
CCT245232	RIOK1	RIOK1	100
CCT245232	RIPK2	RIPK2	100
CCT245232	ROS1	ROS1	100
CCT245232	RSK1(Kin.Dom.1-N-terminal)	RPS6KA1	100
CCT245232	RSK1(Kin.Dom.2-C-terminal)	RPS6KA1	100
CCT245232	RSK3(Kin.Dom.2-C-terminal)	RPS6KA2	100
CCT245232	RPS6KA4(Kin.Dom.1-N-terminal)	RPS6KA4	100

CCT245232	RPS6KA5(Kin. Dom.2-C-terminal)	RPS6KA5	100
CCT245232	S6K1	RPS6KB1	100
CCT245232	SgK110	SgK110	100
CCT245232	SIK	SIK1	100
CCT245232	SIK2	SIK2	100
CCT245232	SLK	SLK	100
CCT245232	SRPK2	SRPK2	100
CCT245232	SRPK3	SRPK3	100
CCT245232	DRAK1	STK17A	100
CCT245232	MST3	STK24	100
CCT245232	YANK2	STK32B	100
CCT245232	STK33	STK33	100
CCT245232	STK36	STK36	100

CCT245232	MST1	STK4	100
CCT245232	SYK	SYK	100
CCT245232	TBK1	TBK1	100
CCT245232	TIE2	TEK	100
CCT245232	TGFB1	TGFB1	100
CCT245232	TGFB2	TGFB2	100
CCT245232	TLK1	TLK1	100
CCT245232	TNK1	TNK1	100
CCT245232	TNNI3K	TNNI3K	100
CCT245232	TYK2(JH2dom ain-pseudokinase)	TYK2	100
CCT245232	WEE2	WEE2	100
CCT245232	YSK4	YSK4	100
CCT245232	ZAP70	ZAP70	100

SK-OV-3 HSP72 Cell-Based ELISA



$$EC_F = \left(\frac{F}{100 - F} \right)^{1/H} * EC_{50}$$

17-AAG:

E_{max}=48000 or 16-fold

Hill Slope, H=0.99

EC₅₀=76 nM

17-AAG: EC₇₆=250 nM

17-AAG, n=1. See experimental section for methods. The data was analyzed using Graphpad Prism Version 6 (Non-linear regression, variable slope, 4 parameters).

Figure S1. Induction of the heat-shock response by HSP90 (17-AAG) inhibitor in SK-OV-3 cells.

Example Dataset: Bisamide **26**

Table S3. HSP72 Cell-based ELISA data

BCA Protein Read	Heat-Shock Inducer	HSP72 ELISA Counts	Normalized HSP72 ELISA Counts	[Bisamide 26] (μM)	HSP72 ELISA Counts	Normalized HSP72 ELISA Counts
0.3153	Medium	2150	4277	1.000	1172	3717
0.3135	Medium	2133	4218	0.333	1183	3773
0.3296	Medium	2289	4563	0.111	2094	6353
0.3580	Medium	2091	4147	0.037	5245	14650
0.3888	17-AAG	20523	50375	0.012	9440	24279
0.3972	17-AAG	18838	43748	0.004	15063	37922
0.4339	17-AAG	20766	50872	0.001	18057	41615
0.4201	17-AAG	19724	52836	0.0004	19994	47593

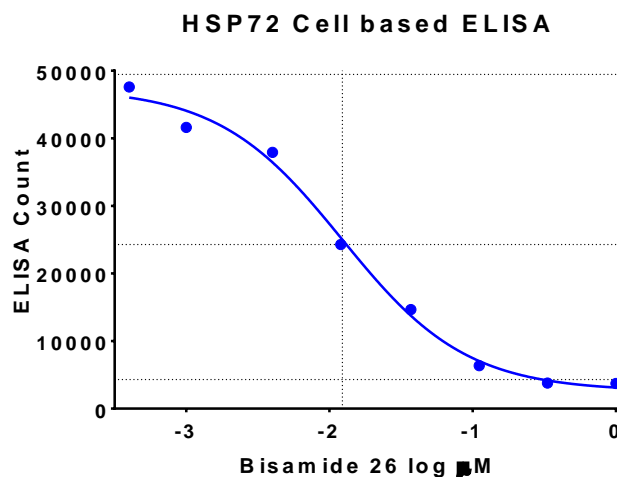


Figure S2. Example Cell-based ELISA data

See experimental section for methods. The data was analyzed using Graphpad Prism Version 6 (Non-linear regression, variable slope, 4 parameters).

The HSP72 cell-based ELISA is used to quantify the induced expression of the heat-shock protein, HSP72. The ELISA assay is a standard commercially available assay format for quantifying protein expression. Potential HSF1-mediated transcription inhibitors were added to cells 1 h before the addition of the validated HSP90 inhibitor, 17-AAG, which in a separate experiment was shown to induce HSP72 expression to $EC_{76}@250$ nM after 18 h exposure. HSF1-mediated transcription inhibitors were then defined by their ability to block the induction of HSP72 at a particular inhibitor concentration. A dose-response curve was plotted with the IC_{50} defined as the concentration at which half the expected expression of 17-AAG-induced HSP72 occurred after 18 h exposure to the inhibitor. 18 h exposure to the medium alone represented the baseline control response, while exposure to both the medium and 17-AAG (250 nM) represented the maximum induction.

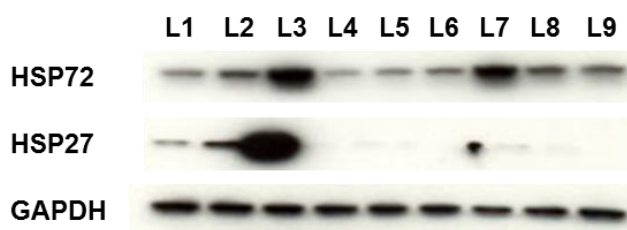


Figure S3. Induction of the HSF1-mediated heat-shock proteins, HSP72 and HSP27, with the HSP90 inhibitor 17-AAG is blocked by treatment with the active tool compound. L1=Control, L2=17-AAG (250 nM, 2 h), L3=17-AAG (250 nM, 24 h), L4=**26** (10 nM, 24 h), L5=**26** (100 nM, 24 h), L6=**26** (1000 nM, 24 h), L7=**26**+17-AAG (10 nM, 250 nM, 24 h), L8=**26**+17-AAG (100 nM, 250 nM, 24 h), L9=**26**+17-AAG (1000 nM, 250 nM, 24 h).

SK-OV-3 cells were treated with 17-AAG alone or compounds +/- 17-AAG for 2 or 24 h. The cells were then trypsinized, washed with PBS and lysed for 1 h at 4 °C in lysis buffer

(Cell Signaling) supplemented with complete protease inhibitor cocktail tablets (Roche). Lysates were centrifuged (MSE Microcentrifuge; 13500 rpm for 15 minutes at 4 °C) and protein concentration was determined using a bicinchoninic acid (BCA) protein assay kit (Thermo Fisher Scientific). Samples (30 µg protein/well) were run on a 4-20% Tris-Glycine gel (Life Technologies), transferred onto nitrocellulose membrane and immunoblotted for HSP72 (Stressgen, SPA810), HSP27 (Stressgen, SPA800) and the loading control GAPDH (Chemicon, MAB374). Protein was then detected using horseradish peroxidase-labelled secondary antibodies combined with enhanced chemiluminescence reagents (Thermo Scientific) and autoradiography.

TAQman HSPA1A 17-AAG induced qPCR

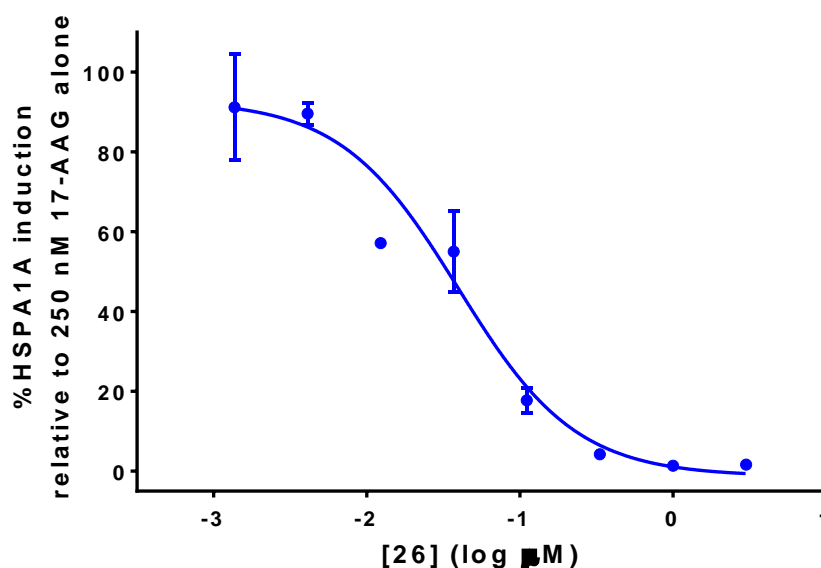


Figure S4. Blocked the induction of HSPA1A mRNA by 17-AAG in a dose-dependent manner

SK-OV-3 cells were seeded in 96 well plates and left to settle for 24 hours. Cells were pre-treated with different concentrations of bisamide **26** for one hour prior to treatment with 250 nM 17-AAG for 6h. Medium was discarded and the cells were washed with ice cold PBS. The cells were lysed in 35 microliter of Cells-to-cDNA II buffer (Thermo Fisher) at 75 °C for 15 min. 1 microliter of DNase I was added to each well, and mixed well before incubation at 37 °C for 15 minutes and heat inactivation at 75 °C for 10 minutes. 5 microliter was reverse transcribed using the high capacity cDNA kit (Thermo Fisher) according to manufacturers instructions. HSPA1A (encoding HSP72) mRNA levels were determined relative to RPLP0 in a multiplex TAQman assay (Hs00359163_s1, Hs99999902_m1, Thermo Fisher). HSPA1A levels of bisamide **26** and 17-AAG co-treated samples were expressed relative to those treated with 17-AAG alone.

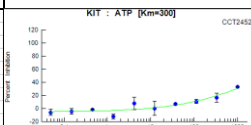
Kinase Inhibition Assays

Bisamide 1 (CCT245232)

For the screening protocol and assay conditions see: <https://www.thermofisher.com/uk/en/home/life-science/drug-discovery/target-and-lead-identification-and-validation/kinasebiology/kinase-activity-assays/z-lyte.html> (August 31, 2016).

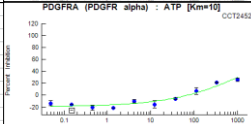
KIT: [ATP]=app. K_m

The 2X KIT/Tyr 06 mixture is prepared in 50 mM HEPES pH 7.5, 0.01 % BRIJ-35, 10 mM $MnCl_2$, 1 mM EGTA, 2 mM DTT, 0.02 % NaN_3 . The final 10 μL kinase reaction consists of 3.17-30 ng KIT and 2 μM Tyr 06 in 50 mM HEPES pH 7.5, 0.01 % BRIJ-35, 5 mM $MgCl_2$, 5 mM $MnCl_2$, 1 mM EGTA, 1 mM DTT, 0.01 % NaN_3 . After the 1 hour kinase reaction incubation, 5 μL of a 1:128 dilution of development reagent A is added.

Life Technologies' SelectScreen® Profiling Service: 10-point Titration Results															
SelectScreen® Scientist:			Derek Johnston			Date:			11-Nov-2015			SSBK-Z-LYTE (Paisley UK)			
Quality Assurance Review:			Theo James			Date:			11-Nov-2015						
% Phosphorylation		Pass													
Z' Determination		Pass													
Project #	Compound Name	Kinase Tested	[ATP] Tested (uM)	IC50 (uM)	Hillslope	R² Value	Conc of Compound (nM)	% Inhibition		Development Reaction Interference	Test Compound Interference		Z'	Kinase Part# / Lot#	Graph
								Point 1	Point 2		Coumarine	Fluorescein			
SSBK8838_34274	CCT245232	KIT	Km app	>1000	0.47	0.8728	1000	31	34	Pass	Pass	Pass	0.53	P30811/1559213	
SSBK8838_34274	CCT245232	KIT	Km app	>1000	0.47	0.8728	333	9	23	Pass	Pass	Pass	0.53	P30811/1559213	
SSBK8838_34274	CCT245232	KIT	Km app	>1000	0.47	0.8728	111	7	13	Pass	Pass	Pass	0.53	P30811/1559213	
SSBK8838_34274	CCT245232	KIT	Km app	>1000	0.47	0.8728	37.0	8	5	Pass	Pass	Pass	0.53	P30811/1559213	
SSBK8838_34274	CCT245232	KIT	Km app	>1000	0.47	0.8728	12.3	-11	11	Pass	Pass	Pass	0.53	P30811/1559213	
SSBK8838_34274	CCT245232	KIT	Km app	>1000	0.47	0.8728	4.12	17	-2	Pass	Pass	Pass	0.53	P30811/1559213	
SSBK8838_34274	CCT245232	KIT	Km app	>1000	0.47	0.8728	1.37	-16	-9	Pass	Pass	Pass	0.53	P30811/1559213	
SSBK8838_34274	CCT245232	KIT	Km app	>1000	0.47	0.8728	0.457	-3	-1	Pass	Pass	Pass	0.53	P30811/1559213	
SSBK8838_34274	CCT245232	KIT	Km app	>1000	0.47	0.8728	0.152	0	-9	Pass	Pass	Pass	0.53	P30811/1559213	
SSBK8838_34274	CCT245232	KIT	Km app	>1000	0.47	0.8728	0.0495	-2	-11	Pass	Pass	Pass	0.53	P30811/1559213	

PDGFRA: [ATP]=app. K_m

The 2X PDGFRA (PDGFR alpha)/Tyr 04 mixture is prepared in 50 mM HEPES pH 7.5, 0.01 % BRIJ-35, 10 mM $MgCl_2$, 4 mM $MnCl_2$, 1 mM EGTA, 2 mM DTT. The final 10 μL kinase reaction consists of 1.54-22.6 ng PDGFRA (PDGFR alpha) and 2 μM Tyr 04 in 50 mM HEPES pH 7.5, 0.01 % BRIJ-35, 10 mM $MgCl_2$, 2 mM $MnCl_2$, 1 mM EGTA, 1 mM DTT. After the 1 hour kinase reaction incubation, 5 μL of a 1:64 dilution of development reagent B is added.

Life Technologies® SelectScreen® Profiling Service: 10-point Titration Results															
SelectScreen® Scientist:			Derek Johnston			Date:			11-Nov-2015			SSBK-2-LYTE (Paisley UK)			
Quality Assurance Review:			Theo James			Date:			11-Nov-2015						
% Phosphorylation			Pass												
Z' Determination			Pass												
Project #	Compound Name	Kinase Tested	[ATP] Tested (µM)	IC50 (nM)	Hillslope	R² Value	Conc of Compound (nM)	% Inhibition		Development Reaction Interference	Test Compound Interference		Z'	Kinase Part# / Lot#	Graph
								Point 1	Point 2		Coumarine	Fluorescein			
SSBK8838_34274	CCT245232	KIT	Km app	>1000	0.47	0.8728	0.0495	-2	-11	Pass	Pass	Pass	0.53	P30811/1559213	
SSBK8838_34274	CCT245232	PDGFRA (PDGFR alpha)	Km app	>1000	0.49	0.9349	1000	29	23	Pass	Pass	Pass	0.65	PV3811/1269727	
SSBK8838_34274	CCT245232	PDGFRA (PDGFR alpha)	Km app	>1000	0.49	0.9349	333	22	20	Pass	Pass	Pass	0.65	PV3811/1269727	
SSBK8838_34274	CCT245232	PDGFRA (PDGFR alpha)	Km app	>1000	0.49	0.9349	111	13	1	Pass	Pass	Pass	0.65	PV3811/1269727	
SSBK8838_34274	CCT245232	PDGFRA (PDGFR alpha)	Km app	>1000	0.49	0.9349	37.0	-7	-5	Pass	Pass	Pass	0.65	PV3811/1269727	
SSBK8838_34274	CCT245232	PDGFRA (PDGFR alpha)	Km app	>1000	0.49	0.9349	12.3	-9	-21	Pass	Pass	Pass	0.65	PV3811/1269727	
SSBK8838_34274	CCT245232	PDGFRA (PDGFR alpha)	Km app	>1000	0.49	0.9349	4.12	-13	-7	Pass	Pass	Pass	0.65	PV3811/1269727	
SSBK8838_34274	CCT245232	PDGFRA (PDGFR alpha)	Km app	>1000	0.49	0.9349	1.37	-21	-21	Pass	Pass	Pass	0.65	PV3811/1269727	
SSBK8838_34274	CCT245232	PDGFRA (PDGFR alpha)	Km app	>1000	0.49	0.9349	0.457	-25	-17	Pass	Pass	Pass	0.65	PV3811/1269727	
SSBK8838_34274	CCT245232	PDGFRA (PDGFR alpha)	Km app	>1000	0.49	0.9349	0.152	-15	-25	Pass	Pass	Pass	0.65	PV3811/1269727	

PDGFRB: [ATP]=app. K_m

The 2X PDGFRB (PDGFR beta)/Tyr 04 mixture is prepared in 50 mM HEPES pH 7.5, 0.01 % BRIJ-35, 10 mM $MgCl_2$, 4 mM $MnCl_2$, 1 mM EGTA, 2 mM DTT. The final 10 μL kinase

reaction consists of 7-50 ng PDGFRB (PDGFR beta) and 2 μ M Tyr 04 in 50 mM HEPES pH 7.5, 0.01 % BRIJ-35, 10 mM MgCl₂, 2 mM MnCl₂, 1 mM EGTA, 1 mM DTT. After the 1 hour kinase reaction incubation, 5 μ L of a 1:64 dilution of development reagent B is added.

Life Technologies' SelectScreen® Profiling Service: 10-point Titration Results														
SelectScreen® Scientist:			Derek Johnston			Date:			11-Nov-2015			SSBK-Z-LYTE (Paisley UK)		
Quality Assurance Review:			Theo James			Date:			11-Nov-2015					
% Phosphorylation			Pass											
Z' Determination			Pass											

Project #	Compound Name	Kinase Tested	[ATP] Tested μ M	IC50 (nM)	Hilllope	R ² Value	Conc of Compound nM	%Inhibition		Development Reaction Interference	Test Compound Interference		Z'	Kinase Part# / Lot#	Graph
								Point 1	Point 2		Compound	Fluorescence			
SSBK8838_34274	CCT245232	PDGFRB (PDGFR beta)	Kin app	>1000	0.99	0.9321	1000	17	27	Pass	Pass	Pass	0.55	P3082/27567	
SSBK8838_34274	CCT245232	PDGFRB (PDGFR beta)	Kin app	>1000	0.99	0.9321	333	4	8	Pass	Pass	Pass	0.55	P3082/27567	
SSBK8838_34274	CCT245232	PDGFRB (PDGFR beta)	Kin app	>1000	0.99	0.9321	111	-3	4	Pass	Pass	Pass	0.55	P3082/27567	
SSBK8838_34274	CCT245232	PDGFRB (PDGFR beta)	Kin app	>1000	0.99	0.9321	37.0	-12	-6	Pass	Pass	Pass	0.55	P3082/27567	
SSBK8838_34274	CCT245232	PDGFRB (PDGFR beta)	Kin app	>1000	0.99	0.9321	12.3	-14	4	Pass	Pass	Pass	0.55	P3082/27567	
SSBK8838_34274	CCT245232	PDGFRB (PDGFR beta)	Kin app	>1000	0.99	0.9321	4.12	-8	-4	Pass	Pass	Pass	0.55	P3082/27567	
SSBK8838_34274	CCT245232	PDGFRB (PDGFR beta)	Kin app	>1000	0.99	0.9321	1.37	-13	-1	Pass	Pass	Pass	0.55	P3082/27567	
SSBK8838_34274	CCT245232	PDGFRB (PDGFR beta)	Kin app	>1000	0.99	0.9321	0.457	3	-16	Pass	Pass	Pass	0.55	P3082/27567	
SSBK8838_34274	CCT245232	PDGFRB (PDGFR beta)	Kin app	>1000	0.99	0.9321	0.152	-4	-7	Pass	Pass	Pass	0.55	P3082/27567	
SSBK8838_34274	CCT245232	PDGFRB (PDGFR beta)	Kin app	>1000	0.99	0.9321	0.0485	2	-4	Pass	Pass	Pass	0.55	P3082/27567	

GSK3 β Kinase Assay

Assay for Glycogen Synthase Kinase 3beta (GSK-3beta)

The LanthaScreen Eu Kinase Binding assay (NP_002084 from Thermo Fisher Scientific, Paisley, UK) was used to test if the bisamides bind to human recombinant GSK-3beta (PR5074A). The assays were based on the binding of a proprietary Alexa Fluor 647-labelled ATP-competitive inhibitor to the kinase of interest. Binding of the tracer is detected using a Europium-labelled anti-tag antibody, so simultaneous binding of tracer and antibody leads to a fluorescence resonance energy transfer (FRET) signal. Inhibitor binding to the kinase competes with the tracer leading to a decrease in the FRET signal.

The experimental procedure was as described in the manual and optimization of the tracer signal was carried out with GSK-3beta at 5 nM and the Eu-Anti-His Ab at 2 nM. This gave a K_D of 11 nM \pm 2.8 for the Kinase tracer 236 (PV5592), which is close to the published value of 12nM.

The bisamides, CCT245232 (bisamide **1**), CCT251236 (pyrrolidine **26**) and CCT250879 (tetrahydroquinoline **17**) were tested across an eight point concentration range together with the established GSK-3beta inhibitor, 6BIO, (ALX-430-156-M005, Enzo Life Sciences) under the assay conditions described above.

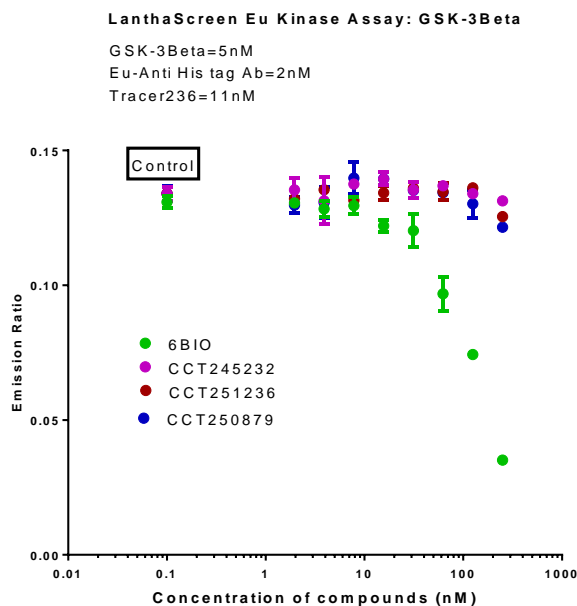


Figure S5. Lanthascreen GSK-3beta kinase inhibition assay


BRAF Kinase Inhibition

Bisamide **1** (CCT245232)

For the screening protocol and assay conditions see:
<https://www.thermofisher.com/uk/en/home/life-science/drug-discovery/target-and-lead-identification-and-validation/kinasebiology/kinase-activity-assays/z-lyte.html>

BRAF: [ATP]=100 μ M Cascade

The 2X BRAF/inactive MAP2K1 (MEK1)/inactive MAPK1 (ERK2)/Ser/Thr 03 mixture is prepared in 50 mM HEPES pH 7.5, 0.01 % BRIJ-35, 10 mM MgCl₂, 1 mM EGTA. The final 10 μ L kinase reaction consists of 0.03-0.1 ng BRAF, 1X inactive MAP2K1 (MEK1)/inactive MAPK1 (ERK2), and 2 μ M Ser/Thr 03 in 50 mM HEPES pH 7.5, 0.01 % BRIJ-35, 10 mM MgCl₂, 1 mM EGTA. After the 1 hour kinase reaction incubation, 5 μ L of a 1:1024 dilution of development reagent A is added.

Life Technologies® SelectScreen® Profiling Service: 10-point Titration Results															
SelectScreen® Scientist:			Andrew Heuze			Date:		01-Oct-2014							
Quality Assurance Review:			Theo James			Date:		01-Oct-2014							
% Phosphorylation			Pass												
Z' Determination			Pass												
Project #	Compound Name	Kinase Tested	[ATP] Tested (µM)	IC50 (nM)	Hillslope	R² Value	Conc of Compound (nM)	%Inhibition Point 1	Point 2	Development Reaction Interference	Test Compound Interference Coumarin	Fluorescein	Z'	Kinase Part# / Lot#	Graph
Project #	Compound Name	Kinase Tested	[ATP] Tested (µM)	IC50 (nM)	Hillslope	R² Value	Compound (nM)	%Inhibition Point 1	Point 2	Reaction	Interference Coumarin	Fluorescein	Z'	Part# / Lot#	Graph
SSBK9431_23647	CCT245232	BRAF	100	415	0.59	0.9853	50000	91	94	Pass	Pass	Pass	0.55	PV3848/34486	
SSBK9431_23647	CCT245232	BRAF	100	415	0.59	0.9853	16700	82	94	Pass	Pass	Pass	0.55	PV3848/34486	
SSBK9431_23647	CCT245232	BRAF	100	415	0.59	0.9853	5560	82	81	Pass	Pass	Pass	0.55	PV3848/34486	
SSBK9431_23647	CCT245232	BRAF	100	415	0.59	0.9853	1850	62	79	Pass	Pass	Pass	0.55	PV3848/34486	
SSBK9431_23647	CCT245232	BRAF	100	415	0.59	0.9853	617	41	54	Pass	Pass	Pass	0.55	PV3848/34486	
SSBK9431_23647	CCT245232	BRAF	100	415	0.59	0.9853	206	40	30	Pass	Pass	Pass	0.55	PV3848/34486	
SSBK9431_23647	CCT245232	BRAF	100	415	0.59	0.9853	69.0	9	21	Pass	Pass	Pass	0.55	PV3848/34486	
SSBK9431_23647	CCT245232	BRAF	100	415	0.59	0.9853	23.0	19	15	Pass	Pass	Pass	0.55	PV3848/34486	
SSBK9431_23647	CCT245232	BRAF	100	415	0.59	0.9853	7.70	-19	5	Pass	Pass	Pass	0.55	PV3848/34486	
SSBK9431_23647	CCT245232	BRAF	100	415	0.59	0.9853	2.57	6	-12	Pass	Pass	Pass	0.55	PV3848/34486	

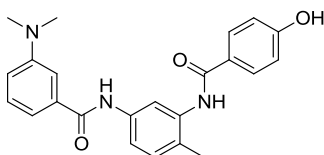
BRAF Inhibitors

All BRAF inhibitors were purchased from SelleckChem and used without further purification.

All compounds displayed $IC_{50} > 10 \mu M$ in the HSP72 cell-based ELISA assay to measure HSF1 pathway inhibition.

ZM336372

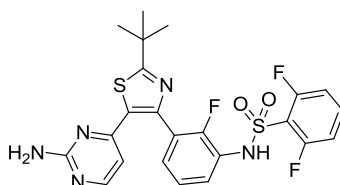
<http://www.selleckchem.com/products/zm-336372.html> (August 31, 2016).



Paradoxical activation of Raf by a novel Raf inhibitor. Hall-Jackson, C. A.; Eysers, P. A.; Cohen, P.; Goedert, M.; Boyle, F. T.; Hewitt, N.; Plant, H.; Hedge, P. *Chem. Biol.* **1999**, *6*, 559-568.

Dabrafenib

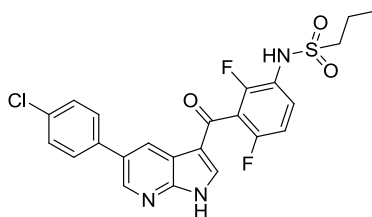
<http://www.selleckchem.com/products/dabrafenib-gsk2118436.html> (August 31, 2016).



Targeting ER stress-induced autophagy overcomes BRAF inhibitor resistance in melanoma. Ma, X. H.; Piao, S. F.; Dey, S.; McAfee, Q.; Karakousis, G.; Villanueva, J.; Hart, L. S.; Levi, S.; Hu, J.; Zhang, G.; Lazova, R.; Klump, V.; Pawelek, J. M.; Xu, X.; Xu, W.; Schuchter, L. M.; Davies, M. A.; Herlyn, M.; Winkler, J.; Koumenis, C.; Amaravadi, R. K. *J. Clin. Invest.* **2014**, *124*, 1406-1417.

Vemurafenib

<http://www.selleckchem.com/products/PLX-4032.html> (August 31, 2016).

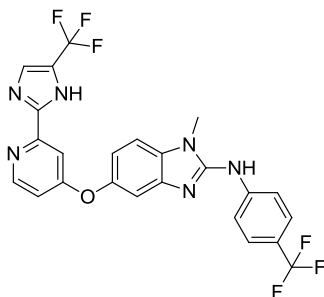


Clinical efficacy of a RAF inhibitor needs broad target blockade in BRAF-mutant melanoma. Bollag, G.; Hirth, P.; Tsai, J.; Zhang, J.; Ibrahim, P. N.; Cho, H.; Spevak, W.; Zhang, C.;

Zhang, Y.; Habets, G.; Burton, E. A.; Wong, B.; Tsang, G.; West, B. L.; Powell, B.; Shellooe, R.; Marimuthu, A.; Nguyen, H.; Zhang, K. Y.; Artis, D. R.; Schlessinger, J.; Su, F.; Higgins, B.; Iyer, R.; D'Andrea, K.; Koehler, A.; Stumm, M.; Lin, P. S.; Lee, R. J.; Grippo, J.; Puzanov, I.; Kim, K. B.; Ribas, A.; McArthur, G. A.; Sosman, J. A.; Chapman, P. B.; Flaherty, K. T.; Xu, X.; Nathanson, K. L.; Nolop, K. *Nature* **2010**, 467, 596-599.

RAF265

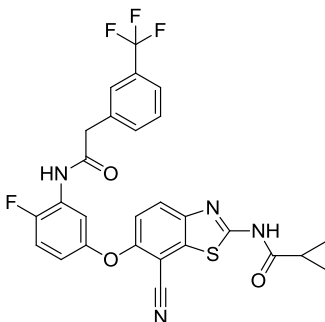
[http://www.selleckchem.com/products/RAF265\(CHIR-265\).html](http://www.selleckchem.com/products/RAF265(CHIR-265).html) (August 31, 2016).



Dependence on phosphoinositide 3-kinase and RAS-RAF pathways drive the activity of RAF265, a novel RAF/VEGFR2 inhibitor, and RAD001 (Everolimus) in combination. Mordant, P.; Lorient, Y.; Leteur, C.; Calderaro, J.; Bourhis, J.; Wislez, M.; Soria, J. C.; Deutsch, E. *Mol. Cancer Ther.* **2010**, 9, 358-368.

TAK632

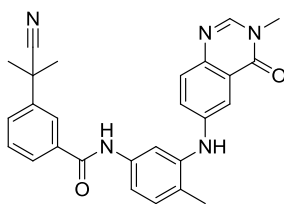
<http://www.selleckchem.com/products/tak-632.html> (August 31, 2016).



Discovery of a selective kinase inhibitor (TAK-632) targeting pan-RAF inhibition: design, synthesis, and biological evaluation of C-7-substituted 1,3-benzothiazole derivatives. Okaniwa, M.; Hirose, M.; Arita, T.; Yabuki, M.; Nakamura, A.; Takagi, T.; Kawamoto, T.; Uchiyama, N.; Sumita, A.; Tsutsumi, S.; Tottori, T.; Inui, Y.; Sang, B. C.; Yano, J.; Aertgeerts, K.; Yoshida, S.; Ishikawa, T. *J. Med. Chem.* **2013**, 56, 6478-6494.

AZ628

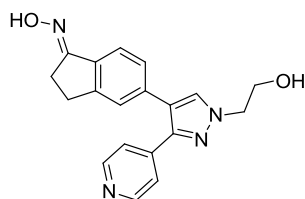
<http://www.selleckchem.com/products/az628.html> (August 31, 2016).



Selective Raf inhibition in cancer therapy. Khazak, V.; Astsaturov, I.; Serebriiskii, I. G.; Golemis, E. A. *Expert Opin. Ther. Targets* **2007**, *11*, 1587-1609.

GDC-0879

<http://www.selleckchem.com/products/GDC-0879.html> (August 31, 2016).



Pharmacodynamics of 2-[4-[(1*E*)-1-(hydroxyimino)-2,3-dihydro-1*H*-inden-5-yl]-3-(pyridine-4-yl)-1*H*-pyrazol-1-yl]ethan-1-ol (GDC-0879), a potent and selective B-Raf kinase inhibitor: understanding relationships between systemic concentrations, phosphorylated mitogen-activated protein kinase kinase 1 inhibition, and efficacy. Wong, H.; Belvin, M.; Herter, S.; Hoeflich, K. P.; Murray, L. J.; Wong, L.; Choo, E. F. *J. Pharmacol. Exp. Ther.* **2009**, *329*, 360-367.

Solubilizing Group Optimization

Microsomal Stability Assay:

For the screening protocol and assay conditions see: <http://www.cypotex.com/admepk/in-vitro-metabolism/microsomal-stability> (August 31, 2016).

Test compound (1 μ M) is incubated with pooled liver microsomes. Test compound is incubated at 5 time points over the course of a 45 min experiment and the test compound is analyzed by LC MS/MS.

Experimental Procedure:

Pooled mouse liver microsomes (male CD1 mice) are purchased from a reputable commercial supplier. Microsomes are stored at -80 °C prior to use.

Microsomes (final protein concentration 0.5 mg/mL), 0.1 M phosphate buffer pH 7.4 and test compound (final substrate concentration 1 μ M; final DMSO concentration 0.25 %) are pre incubated at 37 °C prior to the addition of NADPH (final concentration 1 mM) to initiate the reaction. The final incubation volume is 50 μ L. A control incubation is included for each compound tested where 0.1 M phosphate buffer pH 7.4 is added instead of NADPH (minus NADPH). Two control compounds are included with each species. All incubations are performed singularly for each test compound.

Each compound is incubated for 0, 5, 15, 30 and 45 min. The control (minus NADPH) is incubated for 45 min only. The reactions are stopped by transferring 25 μ L of incubate to 50 μ L methanol at the appropriate time points. The termination plates are centrifuged at 2,500 rpm for 20 min at 4 °C to precipitate the protein.

Quantitative Analysis:

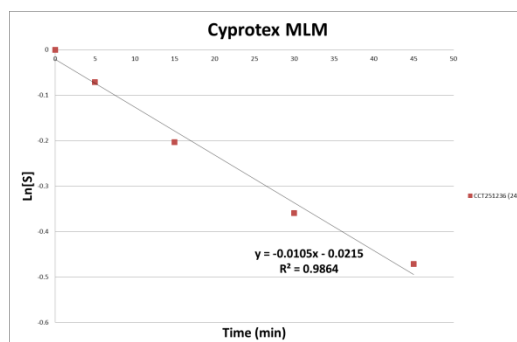
Following protein precipitation, the sample supernatants are combined in cassettes of up to 4 compounds, internal standard is added and samples analyzed using Cypotex generic LC MS/MS conditions.

Data Analysis:

From a plot of \ln peak area ratio (compound peak area/internal standard peak area) against time, the gradient of the line is determined. Subsequently, half-life and intrinsic clearance are calculated.

Two control compounds are included in the assay and if the values for these compounds are not within the specified limits the results are rejected and the experiment repeated.

Compound			Metabolic Stability (Species=Mouse, SubstrateConc=1µM)								
CypotrexId	Customer Id	Customer Batch Id	Compound Remaining (% of 0 min)						Comments	Supplier Test Id	Control Group Id
			0 min	5 min	15 min	30 min	45 min	Control			
CY0000082701	CCT251236	7	100	93.1	81.6	69.8	62.4	83.6		1952823	55213



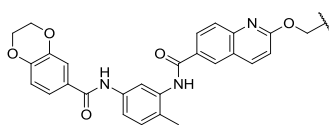
$$\ln[S]_t = -k * t + \ln[S]_0$$

$$V = \frac{\text{volume of incubation}}{\text{protein in the incubation}}$$

$$\text{In vitro Intrinsic Clearance (Cl}_{\text{int}}) = V * k$$

Figure S6. Mouse Liver Microsome Stability

Table S4. HSF1 pathway inhibition



Entry	Compd	Sol. Group	SK-OV-3 pIC ₅₀ ±SEM (IC ₅₀ , n) ^a
1	21		7.01±0.05 (98 nM, n=3)
2	22		8.19±0.20 (6.5 nM, n=3)
3	23		6.01±0.06 (980 nM, n=3)
4	24		7.74±0.14 (18 nM, n=3)
5	25		7.10±0.15 (799 nM, n=3)
6	26		7.73±0.07 (19 nM, n=15)

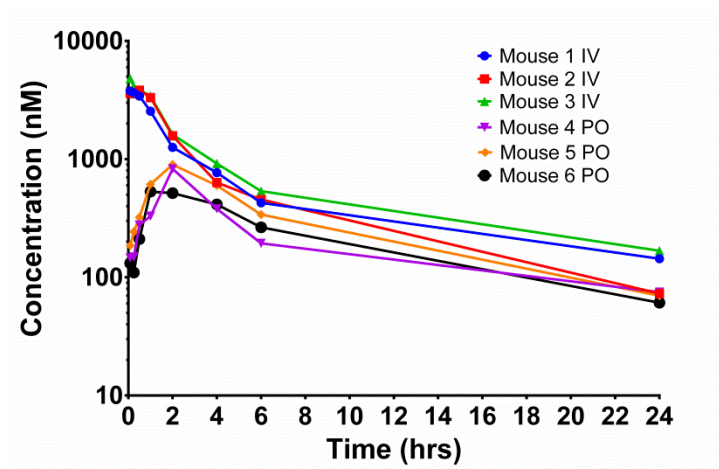
^aThe IC₅₀ was measured using the HSP72 cell-based ELISA as described in the experimental procedure. pIC₅₀=-log IC₅₀ (M); geometric mean±SEM, n=number of biological repeats in parenthesis.

Assay Free-Fraction:

Titre Blue Growth Inhibition Assay free fraction (f_{ua}) for Pyrrolidine **26** (CCT251236) in 10 % Foetal Calf Serum 0.436, 0.507, 0.474, n=3.

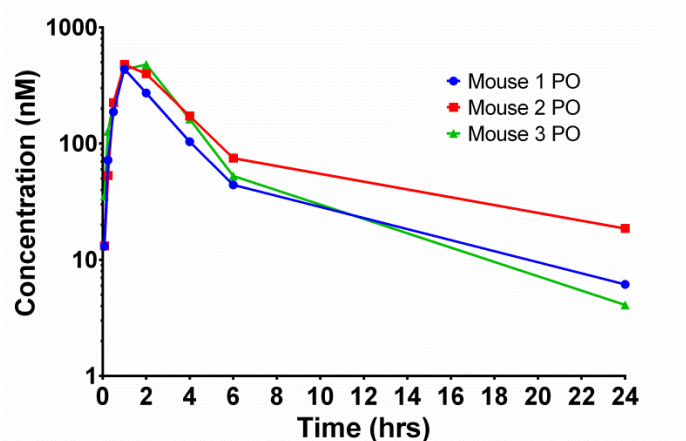
Mouse Pharmacokinetics

Pyrrolidine **26** (CCT251236)



Route	Dose (mg/kg)	Animal	Animal Wt (g)	T _{max} (h)	C _{max} (nmol/L)	AUC _{last} (h*nmol/L)	AUC _{inf} (h*nmol/L)	Cl (ml/min/kg)	HL Lambda z (h)	V _z (L/kg)	V _{ss} (L/kg)	F (AUC _{last})
IV	5	1	21.6	0.083	3771	13579	15510	10.031	9.297	7.824	5.324	
		2	18.7	0.5	3832	14123	14815	9.804	6.565	5.775	3.262	
		3	17	0.083	4815	16836	19022	7.843	9.019	6.176	4.118	
PO	5	4	19.8	2	828	5018	6090	9.121	9.913	8.384		0.39
		5	19	2	901	7234	7937	7.895	6.959	4.526		
		6	20.1	1	532	5319	5964	9.950	7.332	6.318		

Figure S7. Blood PK of bisamide **26** in immunocompetent BALB/c mice– 5 mg/kg po and 5 mg/kg iv bolus



Route	Dose (mg/kg)	Animal	Animal Wt (g)	T _{max} (h)	C _{max} (nmol/L)	AUC _{last} (h*nmol/L)	AUC _{inf} (h*nmol/L)	HL Lambda z (h)
PO	20	1	23.8	1	439	1531	1579	5.38
		2	25.6	1	480	2318	2508	7.07
		3	23.5	2	480	2053	2077	4.14

Figure S8. Blood PK of bisamide **26** in immunodeprived athymic mice – 20 mg/kg po

Table S5. Mouse Blood to Plasma Ratios for Pyrrolidine **26** (CCT251236)

Concentration	Immunocompetent BALB/c Mice	Immunodeprived Athymic Mice
1 μ M	1.18	1.69
1 μ M	1.29	1.72
1 μ M	1.07	1.69
10 μ M	1.27	1.26
10 μ M	1.25	1.36
10 μ M	1.25	1.32

Table S6. Mouse Plasma Protein Binding for Pyrrolidine **26** (CCT251236)

Immunocompetent BALB/c Mice (%unbound)	Immunodeprived Athymic Mice (%unbound)
1.01	2.39
1.06	2.28
1.05	2.88

In Vivo Mouse Efficacy Studies

Pyrrolidine **26** (CCT251236)

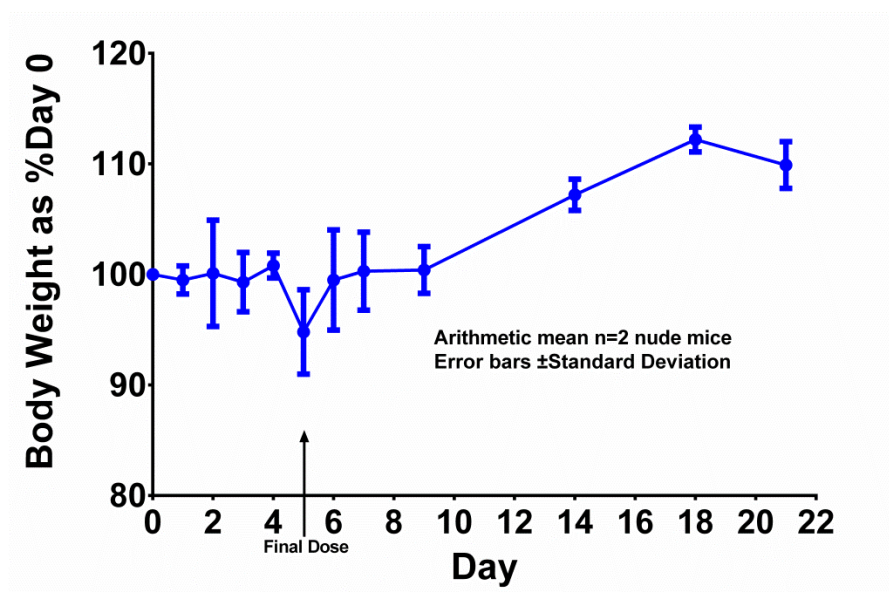
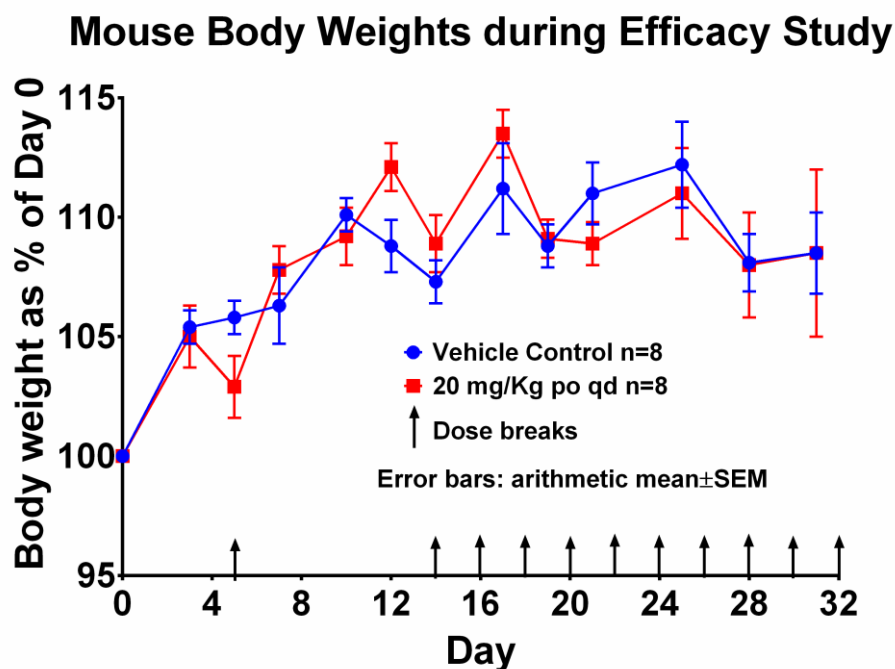
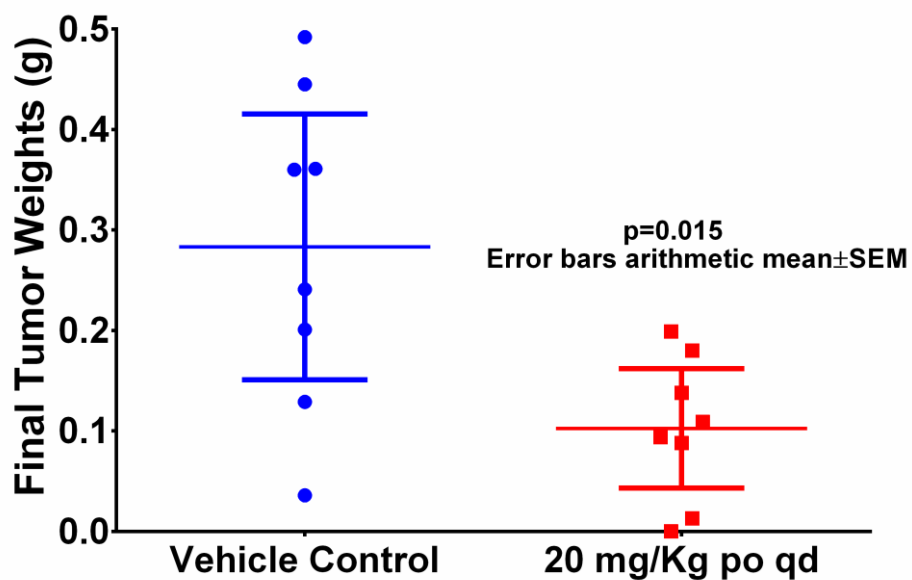


Figure S9. Mouse tolerability study of bisamide **26** in immunodeprived athymic mice – 30 mg/Kg po qd



Dosing breaks were carried out on days 5-12, 14, 16, 18, 20, 22, 24, 26, 29, 31.

Figure S10. Mouse body weights during bisamide **26** efficacy study – 20 mg/Kg po qd



All *p*-values calculated using unpaired two-tailed Student's *t*-test with Welch's correction of the untransformed data.

Figure S11. Tumor weights at the end of bisamide **26** efficacy study – 20 mg/Kg po qd

Total tumor concentrations of bisamide **24** were measured 2 and 6 h post final dose in the efficacy study:

Compound	Dose (mg/Kg)	Time (h)	Total Tumor Conc. (nM)
26	20	2	540
26	20	2	440
26	20	6	960
26	20	6	610

Cerep Diversity Screen

Pyrrolidine **26** (CCT251236)

For the screening protocol and assay conditions see:

<http://www.cerep.fr/cerep/users/pages/catalog/profiles/DetailProfile.asp?profile=2121>
(August 31, 2016).

http://www.cerep.fr/cerep/users/pages/catalog/p_Catalogue.asp?profile=2121&TypCall=profile
(August 31, 2016).

Table S7. Binding Assays

Assay	Catalog Ref	Test Concentration (M)	% Inhibition of Control Specific Binding	% of Control Specific Binding			Reference Compound
				1st	2nd	Mean	
A1 (h) (antagonist radioligand)	0002	1.0E-05	13	91.5	81.5	86.5	DPCPX
A2A (h) (agonist radioligand)	0004	1.0E-05	88	15.7	9.0	12.4	NECA
A3 (h) (agonist radioligand)	0006	1.0E-05	85	12.2	17.3	14.7	IB-MECA
alpha 1 (non-selective) (antagonist radioligand)	0008	1.0E-05	33	73.5	60.7	67.1	prazosin
alpha 2 (non-selective) (antagonist radioligand)	0011	1.0E-05	74	31.2	21.5	26.4	yohimbine
beta 1 (h) (agonist radioligand)	0018	1.0E-05	6	88.0	99.3	93.7	atenolol
beta 2 (h) (agonist radioligand)	0020	1.0E-05	18	85.2	79.7	82.5	ICI 118551
AT1 (h) (antagonist radioligand)	0024	1.0E-05	-20	123.0	116.2	119.6	saralasin
AT2 (h) (agonist radioligand)	0026	1.0E-05	-3	104.7	101.4	103.0	angiotensin-II
BZD (central) (agonist radioligand)	0028	1.0E-05	-6	117.7	95.0	106.3	diazepam
B1 (h) (agonist radioligand)	1189	1.0E-05	7	97.9	88.4	93.1	desArg10-KD
B2 (h) (agonist radioligand)	0033	1.0E-05	-3	103.5	102.7	103.1	NPC 567
CB1 (h) (agonist radioligand)	0036	1.0E-05	8	96.1	88.5	92.3	CP 55940
CB2 (h) (agonist radioligand)	0037	1.0E-05	44	57.4	54.0	55.7	WIN 55212-2
CCK1 (CCKA) (h) (agonist radioligand)	0039	1.0E-05	19	85.9	75.8	80.9	CCK-8s
CCK2 (CCKB) (h) (agonist radioligand)	0041	1.0E-05	1	91.4	106.0	98.7	CCK-8s
CRF1 (h) (agonist radioligand)	1467	1.0E-05	-22	140.3	103.2	121.8	sauvagine
D1 (h) (antagonist radioligand)	0044	1.0E-05	36	64.7	63.1	63.9	SCH 23390
D2S (h) (antagonist radioligand)	0046	1.0E-05	23	75.4	77.9	76.7	(+)butaclamol
D3 (h) (antagonist radioligand)	0048	1.0E-05	63	34.8	38.9	36.9	(+)butaclamol
D4.4 (h) (antagonist radioligand)	0049	1.0E-05	16	84.6	83.7	84.2	clozapine
ETA (h) (agonist radioligand)	0054	1.0E-05	-4	96.5	111.8	104.2	endothelin-1
ETB (h) (agonist radioligand)	0056	1.0E-05	-1	102.6	100.1	101.4	endothelin-3
GABA (non-selective) (agonist radioligand)	0057	1.0E-05	-3	103.2	103.2	103.2	GABA
AMPA (agonist radioligand)	0064	1.0E-05	1	104.4	93.0	98.7	L-glutamate
kainate (agonist radioligand)	0065	1.0E-05	2	99.1	96.0	97.5	kainic acid
NMDA (antagonist radioligand)	0066	1.0E-05	9	89.6	92.7	91.2	CGS 19755
H1 (h) (antagonist radioligand)	0870	1.0E-05	27	63.6	83.1	73.4	pyrilamine
H2 (h) (antagonist radioligand)	1208	1.0E-05	95	1.1	8.1	4.6	cimetidine

H3 (h) (agonist radioligand)	1332	1.0E-05	93	8.6	5.3	6.9	(R)alpha -Me-histamine
I2 (antagonist radioligand)	0081	1.0E-05	77	20.3	26.6	23.4	idazoxan
BLT1 (LTB4) (h) (agonist radioligand)	1209	1.0E-05	17	80.4	84.9	82.6	LTB4
CysLT1 (LTD4) (h) (agonist radioligand)	0086	1.0E-05	12	93.5	83.1	88.3	LTD4
MC4 (h) (agonist radioligand)	0420	1.0E-05	18	87.8	77.0	82.4	NDP-alpha -MSH
MT1 (ML1A) (h) (agonist radioligand)	1538	1.0E-05	42	60.5	55.9	58.2	melatonin
M (non-selective) (antagonist radioligand)	0089	1.0E-05	92	6.3	10.0	8.2	atropine
NK1 (h) (agonist radioligand)	0100	1.0E-05	10	72.5	106.6	89.6	[Sar9, Met(02)11]-SP
NK2 (h) (agonist radioligand)	0102	1.0E-05	39	55.2	67.2	61.2	[Nleu10]-NKA (4-10)
NK3 (h) (antagonist radioligand)	0104	1.0E-05	14	81.9	90.3	86.1	SB 222200
Y (non-selective) (agonist radioligand)	0105	1.0E-05	39	63.0	59.4	61.2	NPY
N neuronal alpha 4beta 2 (h) (agonist radioligand)	3029	1.0E-05	24	73.5	79.2	76.4	nicotine
opioid (non-selective) (antagonist radioligand)	0112	1.0E-05	77	23.5	21.6	22.5	naloxone
NOP (ORL1) (h) (agonist radioligand)	0358	1.0E-05	5	92.6	97.0	94.8	nociceptin
PPARgamma (h) (agonist radioligand)	0641	1.0E-05	21	81.9	75.4	78.7	rosiglitazone
PCP (antagonist radioligand)	0124	1.0E-05	6	95.1	92.5	93.8	MK 801
EP2 (h) (agonist radioligand)	1955	1.0E-05	-1	99.3	101.9	100.6	PGE2
IP (PGI2) (h) (agonist radioligand)	2230	1.0E-05	-6	96.0	116.0	106.0	iloprost
P2X (agonist radioligand)	0127	1.0E-05	-5	103.8	106.2	105.0	alpha ,beta -MeATP
P2Y (agonist radioligand)	0128	1.0E-05	38	64.1	59.4	61.7	dATPalph S
5-HT (non-selective) (agonist radioligand)	0129	1.0E-05	17	84.9	80.8	82.9	serotonin
sigma (non-selective) (h) (agonist radioligand)	3500	1.0E-05	74	28.9	23.2	26.1	haloperidol
GR (h) (agonist radioligand)	0469	1.0E-05	19	83.8	77.4	80.6	dexamethasone
ER (non-selective) (h) (agonist radioligand)	0152	1.0E-05	-6	105.1	106.3	105.7	17-beta -estradiol
PR (h) (agonist radioligand)	2341	1.0E-05	3	95.9	97.7	96.8	promegestone
AR (h) (agonist radioligand)	0933	1.0E-05	-2	103.8	99.3	101.6	mibolerone
TRH1 (h) (agonist radioligand)	1616	1.0E-05	-14	111.4	117.1	114.2	TRH
V1a (h) (agonist radioligand)	0159	1.0E-05	66	36.7	31.9	34.3	[d(CH2)51, Tyr(Me)2]-AVP
V2 (h) (agonist radioligand)	0497	1.0E-05	9	99.6	82.1	90.9	AVP
Ca2+ channel (L, dihydropyridine site) (antagonist radioligand)	0161	1.0E-05	4	92.5	100.1	96.3	nitrendipine
Ca2+ channel (L, diltiazem site) (benzothiazepines) (antagonist radioligand)	0162	1.0E-05	19	74.9	86.5	80.7	diltiazem
Ca2+ channel (L, verapamil site) (phenylalkylamine) (antagonist radioligand)	0163	1.0E-05	33	66.2	68.1	67.1	D 600
KATP channel (antagonist radioligand)	0165	1.0E-05	0	104.5	95.9	100.2	glibenclamide
KV channel (antagonist radioligand)	0166	1.0E-05	-16	113.5	117.9	115.7	alpha -dendrotoxin
SKCa channel (antagonist radioligand)	0167	1.0E-05	26	67.8	80.4	74.1	apamin
Na+ channel (site 2) (antagonist radioligand)	0169	1.0E-05	49	50.4	51.2	50.8	veratridine
Cl- channel (GABA-gated) (antagonist radioligand)	0170	1.0E-05	-4	99.9	108.9	104.4	picrotoxinin
norepinephrine transporter (h) (antagonist radioligand)	0355	1.0E-05	37	63.5	62.1	62.8	protriptyline
dopamine transporter (h) (antagonist radioligand)	0052	1.0E-05	31	71.9	66.6	69.3	BTCP
GABA transporter (antagonist radioligand)	0060	1.0E-05	-5	109.0	101.4	105.2	nipecotic acid
choline transporter (CHT1) (h) (antagonist radioligand)	1552	1.0E-05	55	46.2	44.5	45.3	hemicholinium-3

5-HT transporter (h) (antagonist radioligand)	0439	1.0E-05	16	86.2	82.2	84.2	imipramine
--	------	---------	----	------	------	------	------------

Table S8. Enzyme and Cell Based Assays

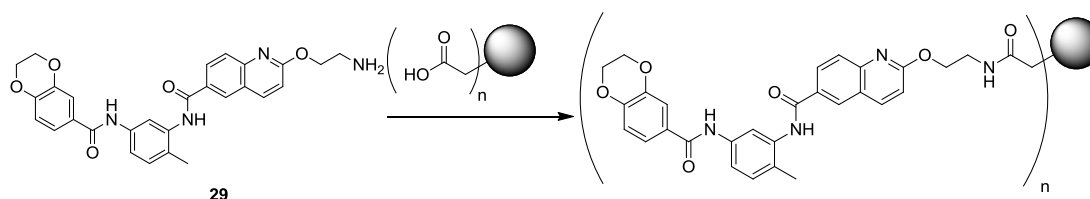
Assay	Catalog Ref	Test Concentration (M)	% Inhibition of Control Values	% of Control Values			Reference Compound
				1st	2nd	Mean	
COX1 (h)	0726	1.0E-05	-24	114.4	134.3	124.4	diclofenac
5-lipoxygenase (h)	0772	1.0E-05	25	77.5	72.8	75.2	NDGA
PDE1B (h)	2431	1.0E-05	-8	103.0	112.2	107.6	nitrendipine
PDE2A1 (h)	2426	1.0E-05	10	88.6	91.9	90.2	EHNA
PDE3A (h)	2432	1.0E-05	22	83.6	71.5	77.5	milrinone
PDE4D2 (h)	2434	1.0E-05	22	64.5	90.7	77.6	rolipram
PDE5 (h) (non-selective)	0204	1.0E-05	10	86.7	92.4	89.5	dipyridamole
phosphatase 1B (h) (PTP1B)	2593	1.0E-05	-8	108.0	108.8	108.4	NSC87877
phosphatase CDC25A (h)	2561	1.0E-05	2	107.2	89.3	98.3	NSC 663284
PKCalpha (h)	0348	1.0E-05	-23	109.5	137.4	123.4	Bis 10
acetylcholinesterase (h)	0363	1.0E-05	84	18.0	14.1	16.1	neostigmine
COMT (catechol- O-methyl transferase)	0457	1.0E-05	-5	103.8	106.8	105.3	Ro 41-0960
GABA transaminase	0461	1.0E-05	-5	119.5	90.8	105.2	O-(Carboxyméthyl) hydroxylamine hémihydrochloride
MAO-A (h)	0191	1.0E-05	12	85.9	90.5	88.2	clorgyline
MAO-B (h) recombinant enzyme	3477	1.0E-05	4	96.4	95.1	95.7	deprenyl
tyrosine hydroxylase	0214	1.0E-05	4	91.8	99.6	95.7	3-iodo L-tyrosine
ATPase (Na ⁺ /K ⁺)	2009	1.0E-05	0	100.9	99.6	100.2	ouabain
CENP-E (h)	2150	1.0E-05	0	99.8	99.8	99.8	rose bengal
Eg5 (h)	2151	1.0E-05	-15	120.1	109.6	114.8	S-trityl-L-cysteine
HDAC3 (h)	2083	1.0E-05	5	93.4	97.3	95.3	trichostatin A
HDAC4 (h)	2493	1.0E-05	-4	105.8	101.3	103.5	trichostatin A
HDAC6 (h)	2495	1.0E-05	4	98.0	93.2	95.6	trichostatin A
HDAC11 (h)	2663	1.0E-05	4	97.0	94.7	95.8	scriptaid
sirtuin 1 (h) (inhibitor effect)	2581	1.0E-05	27	74.7	72.0	73.4	suramin
sirtuin 2 (h) (inhibitor effect)	2582	1.0E-05	-9	107.5	111.1	109.3	suramin

Table S9. Enzyme and Cell Based Assays

Assay	Catalog Ref	Test Concentration (M)	% Stimulation Relative to Control	% Stimulation Relative to Control			Reference Compound
				1st	2nd	Mean	
adenylyl cyclase (activator effect)	3002	1.0E-05	0	0.2	0.2	0.2	forskolin
guanylyl cyclase (h) (activator effect)	3004	1.0E-05	0	-0.8	1.2	0.2	sodium nitroprusside

SILAC Target Identification

Scheme S1 Immobilized Bisamide **29**



Bisamide **29** was coupled to Sepharose beads to give estimated $[29_{imm}]$ from 0 to 100 μM

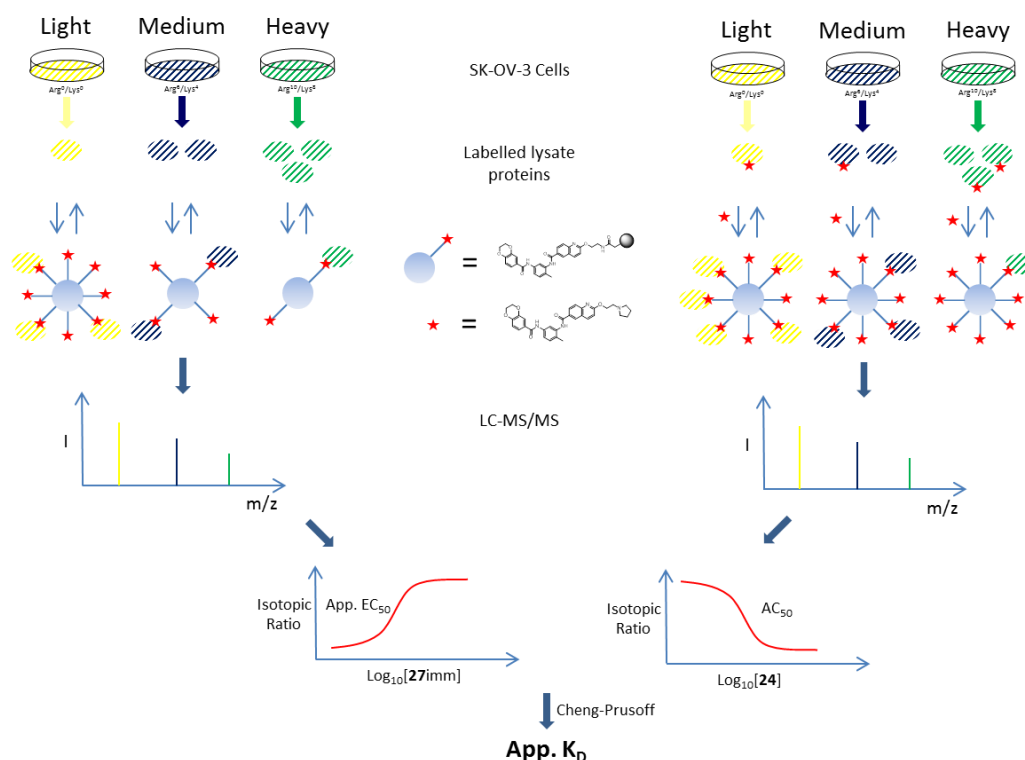


Figure S12. SILAC Target Identification Method

Evotec Target-ID Report:

The aim of this study was to determine quantitative cellular target profiles of the bioactive compounds pyrrolidine **26** (CCT251236) and tetrahydroquinoline **17**. Both profiles were compared to the target profile of the inactive regioisomer **28**.

In order to identify individual cellular target proteins, shared targets and off-targets of both active compounds, one linker derivative of pyrrolidine **26**, amine **29**, served as tool for protein enrichment from SK-OV-3 cells, an ovarian carcinoma cell line. Initially, the linker derivative was immobilized to generate an affinity matrix for the enrichment of potential target proteins. Based on small-scale test experiments the most promising conditions were chosen to conduct Cellular Target Profiling®. The affinity resin was employed in competition experiments in the presence of different concentrations of active “free”

compound to identify compound-specific targets and determine their respective binding constants. Furthermore, this study was complemented by including the inactive regioisomer **26** for target displacement from the immobilized version of pyrrolidine **26**, in order to account for the possibility of shared target proteins between the three small molecules.

Cellular Target Profiling® technology

The Cellular Target Profiling® technology combines state-of-the-art chemical proteomics with SILAC-based quantitative mass spectrometry (MS) in order to obtain the K_D values of free compounds for their specific target proteins present in the investigated cellular proteome (Ong S.E., Mann M. (2005), *Nat. Chem. Biol.*, 252-262.; Sharma K., *et al.* (2009), *Nat. Methods*, 741-744).

In brief, to determine the cellular target profile of a given free compound, an affinity matrix is generated by covalently attaching a linker compound to a Sepharose resin. This matrix is used as a tool to capture potential target proteins from a cell lysate in a dose-dependent manner, thus permitting the determination of apparent binding constants (EC_{50}); dissociation constant for the immobilized compound of all target proteins. In a second experiment, binding is competed by addition of the free compound at various concentrations and the compound concentration for 50 % competition (AC_{50}) is determined. Apparent K_i values for the interaction of target proteins with the free compound in solution are then calculated by the Cheng-Prusoff equation based on the values for the binding constant (EC_{50}), the AC_{50} value and the known concentration of immobilized compound (Cheng Y, Prusoff WH. (1973), *Biochem. Pharmacol.*, 3099-31): Based on these calculations target proteins can then be ranked according to their affinities.

To obtain binding and competition constants, mass spectrometry is used in a quantitative manner. A requirement for this technique is the use of differentially labelled proteomes, which were generated by SILAC (stable isotope labelling with amino acids in cell culture) with either arginine and lysine or heavier isotopic variants of these amino acids. The respective affinity matrix is used to capture cellular proteins and identify proteins exhibiting specific binding compared to a control resin by quantitative mass spectrometry. Binding to immobilized inhibitor is further evaluated by enrichment with different inhibitor resin dilutions. For additional quality control a SILAC label switch experiment is included when performing consecutive in vitro associations with immobilized compound to determine the fraction of resin-bound protein. Here, the binding behavior is required to be consistent irrespective of the SILAC scheme. Furthermore, to monitor for equilibrium binding two quantitative competition experiments are performed in parallel. In the first experiment, the cell lysate is incubated with the free compound and subsequently incubated with the affinity matrix. In the second experiment, affinity matrix and free compound are added to cell lysate simultaneously. Under equilibrium conditions, competition curves from both experiments should be congruent for each target protein.

Cellular Target Profiling® of the compounds of the Bisamide Series

The linker compound and free compounds used in this study were synthesized and provided by the ICR. One linker compound, amine **29**, was immobilized on a solid support to enrich potential target proteins from cell extracts. The compound contained a linker (spacer) moiety with a terminal amino-group suitable for immobilization.

Test immobilizations were performed to identify an optimal coupling density. The compound could be immobilized at high coupling densities up to 5.5 mM. Prior to target profiling experiments, analytical binding and displacement experiments were conducted with matrices of varying immobilization densities to identify conditions of optimal target protein binding and displacement. A resin saturated with ethanolamine served as a negative control to identify unspecific background binding.

Extracts of SILAC-encoded SK-OV-3 cells were used throughout this study. The cell line turned out to be applicable to SILAC (incorporation efficiency of lysine and arginine exceeding 95 % and arginine to proline conversion below 5 %). The cell line was obtained from the ICR. Isotope labelling was conducted by Evotec and the incorporation of the heavier isotopic variants of arginine and lysine was verified to exceed 95 %.

All target deconvolution experiments were performed under low salt conditions (150 mM NaCl). Target enrichment was conducted with affinity matrices consisting of immobilized compound amine **29**. The concentration range for competition experiments with the parental/free compounds was from 300 pM up to 30 μ M. Bound proteins from target profiling experiments were completely eluted from the respective affinity matrix, separated by SDS-PAGE and subjected to tryptic digestion. Recovered peptides were analyzed by LC-MS/MS using a LTQ Orbitrap Velos mass spectrometer (Thermo Fisher). Raw data generated by LC-MS/MS were searched against a combined forward and reverse (decoy) peptide database (Elia *et al.*, (2005), *Nat. Methods*, 667-675). MaxQuant was employed to obtain quantitative protein abundance data for all in vitro associations with immobilized and soluble compounds (Cox J, Mann M., (2008), *Nat. Biotechnol.*, 1367-1372).

Identification of optimal matrix conditions for Cellular Target Profiling®

To enrich potential target proteins from cell extracts the linker compound amine **29** was immobilized on a solid support. According to the ICR, the linker compound is still active in the biological assay, indicating that the linker moiety does not interfere with the biological activity.

To identify the most suitable conditions for subsequent target profiling experiments, analytical in vitro binding experiments were performed. To this end, matrices of the immobilized compound amine **29** were incubated with freshly prepared extracts of SILAC-encoded SK-OV-3 cells. Incubations were performed both in the absence as well as in the presence of the compound pyrrolidine **26** (50 μ M) or vehicle control (DMSO). These experiments were conducted under low salt conditions (150 mM NaCl). Different immobilization densities were analyzed in the analytical test experiments to identify optimal conditions for target protein enrichment and displacement.

Bound proteins were eluted from the affinity resins and analyzed by mass spectrometry for:

1. At least twofold enrichment of proteins compared to the control matrix.
2. Displacement of at least 50 % of the bound protein by incubation with tetrahydroquinoline 17.

Such a binding/displacement pattern would be expected of a specific target protein. It should be bound by the affinity matrix and should be displaced by the parental compound. Only proteins that fulfilled both criteria irrespective of the SILAC labelling scheme in two independent test experiments were considered as potential target proteins.

The results of the aforementioned test experiments suggested employing an affinity matrix with a coupling density of 1.6 mM for the Cellular Target Profiling® experiments.

Table S10. Protein Identified from Cellular Target Profiling®

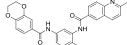
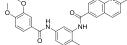
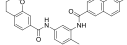
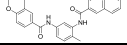
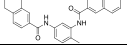
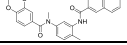
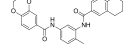
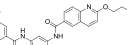
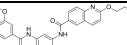
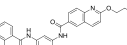
Uniprot ID	Protein Names	Names	Peptides	Sequence Coverage [%]
P49841	Glycogen synthase Kinase 3beta	GSK3β	3	15.5
O00625	PIRIN	PIR	26	45.6
O43924	Retinal rod rhodopsinsensitive cGMP 3,5-cyclic phosphodiesterase subunit delta	PDE6D	4	33.3

Peptides: Number of peptides that were sequenced to identify a target protein. Sequence coverage: the sequence coverage in percent which was determined by razor and unique peptides. Unique peptides unambiguously identifying a target protein and razor peptides are peptides not discriminating between splice variants and close homologues.

Pirin Surface Plasmon Resonance (SPR)

Pirin MW=32113 Da

Table S11. Pirin SPR affinity and apparent stoichiometry

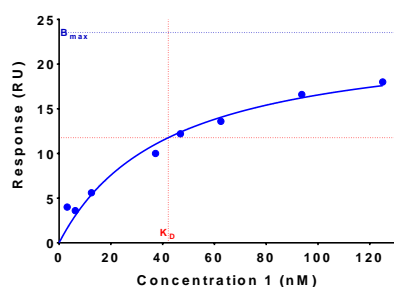
Cd	Structure	Fc2 4327 RU				Fc3 4348 RU				Fc4 4955 RU				Mean pK _D ±SEM	K _D (nM)
		pK _D	T. R _{max}	M. R _{max}	AS	pK _D	T. R _{max}	M. R _{max}	AS	pK _D	T. R _{max}	M. R _{max}	AS		
1		7.38	61	20	0.35	7.41	61	21	0.37	7.38	70	24	0.36	7.42±0.03	38
7		5.66	61	9	0.16	5.65	62	9	0.16	5.66	70	10	0.15	<6.00	>1000
8		7.55	61	21	0.37	7.57	61	22	0.38	7.55	70	24	0.37	7.57±0.01	27
9		7.68	61	28	0.49	7.76	61	28	0.49	7.68	70	29	0.45	7.74±0.03	18
10		7.51	61	26	0.46	7.57	61	28	0.48	7.51	70	31	0.47	7.57±0.03	27
13		4.98	63	24	0.40	5.04	63	22	0.38	4.98	72	21	0.32	<6.00	>1000
17		7.42	60	21	0.37	7.43	60	21	0.38	7.42	68	23	0.36	7.42±0.00	38
24		7.50	78	32	0.43	7.51	79	33	0.45	7.50	89	36	0.43	7.52±0.02	30
26		7.35	74	28	0.40	7.37	75	28	0.41	7.35	85	31	0.39	7.36±0.01	44
28		4.03	74	82	1.18	4.43	75	78	1.11	4.03	85	144	1.80	<6.00	>1000

T. R_{max}=Theoretical R_{max} M. R_{max}=Measured R_{max} AS=Apparent Stoichiometry. All Measured R_{max} and K_D values were calculated using Graphpad Prism 6 using a one-site specific binding model.

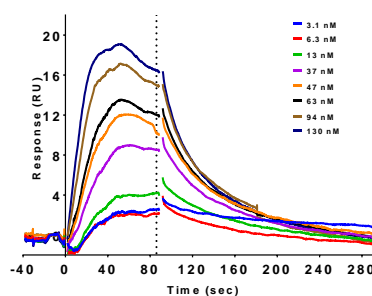
Representative Sensorgrams and Binding Isotherms

All binding isotherms were measured using Graphpad Prism 6 applying a one-site specific binding model.

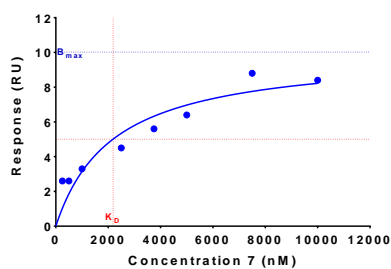
Compound 1 (CCT245232)



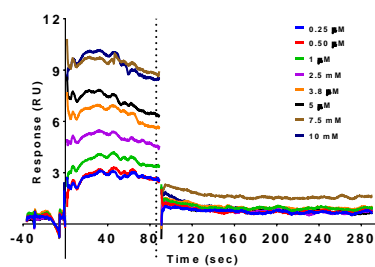
One site -- Specific binding	
Best-fit values	
B _{max}	23.52
K _D	42.14
Std. Error	
B _{max}	2.489
K _D	11.20
95% Confidence Intervals	
B _{max}	17.43 to 29.61
K _D	14.74 to 69.55
Goodness of Fit	
Degrees of Freedom	6
R square	0.9653
Absolute Sum of Squares	7.626
Sy.x	1.127
Number of points analyzed	8



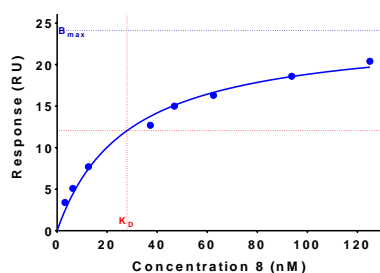
Compound 7



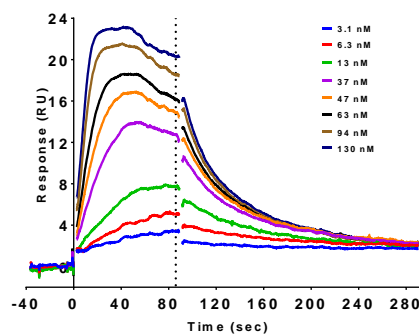
One site -- Specific binding	
Best-fit values	
B _{max}	10.02
K _D	2188
Std. Error	
B _{max}	1.461
K _D	950.6
95% Confidence Intervals	
B _{max}	6.444 to 13.59
K _D	-138.2 to 4514
Goodness of Fit	
Degrees of Freedom	6
R square	0.8649
Absolute Sum of Squares	5.725
Sy.x	0.9768
Number of points analyzed	8



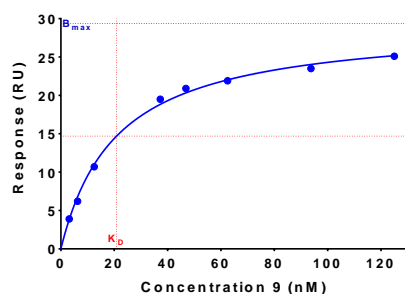
Compound 8



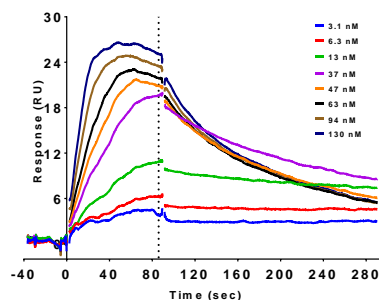
One site -- Specific binding	
Best-fit values	
B _{max}	24.09
K _D	27.93
Std. Error	
B _{max}	1.141
K _D	3.960
95% Confidence Intervals	
B _{max}	21.30 to 26.88
K _D	18.24 to 37.62
Goodness of Fit	
Degrees of Freedom	6
R square	0.9883
Absolute Sum of Squares	3.274
Sy.x	0.7387
Number of points analyzed	8



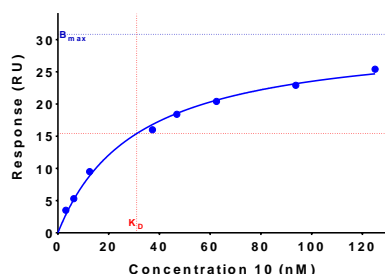
Compound 9



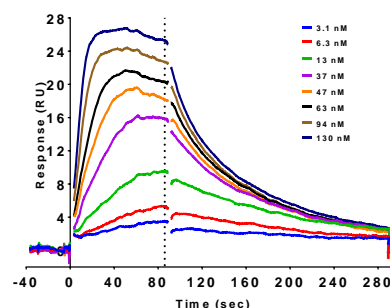
One site -- Specific binding	
Best-fit values	
B _{max}	29.37
K _D	20.86
Std. Error	
B _{max}	0.6159
K _D	1.474
95% Confidence Intervals	
B _{max}	27.87 to 30.88
K _D	17.25 to 24.47
Goodness of Fit	
Degrees of Freedom	6
R square	0.9969
Absolute Sum of Squares	1.502
Sy.x	0.5004
Number of points analyzed	8



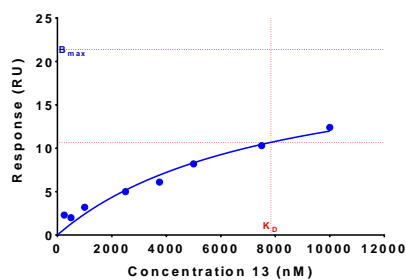
Compound 10



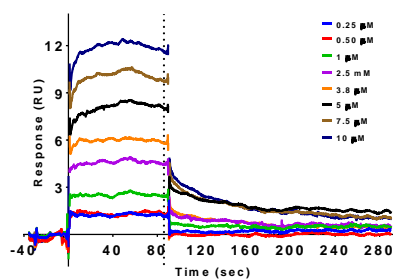
One site -- Specific binding	
Best-fit values	
B _{max}	30.83
K _D	31.07
Std. Error	
B _{max}	1.020
K _D	2.942
95% Confidence Intervals	
B _{max}	28.33 to 33.32
K _D	23.88 to 38.27
Goodness of Fit	
Degrees of Freedom	6
R square	0.9953
Absolute Sum of Squares	2.192
Sy.x	0.6044
Number of points analyzed	8



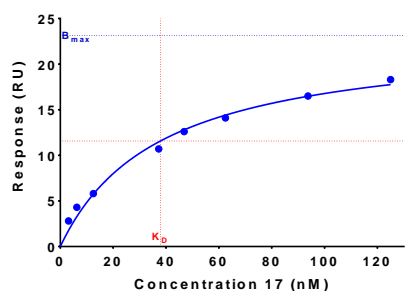
Compound 13



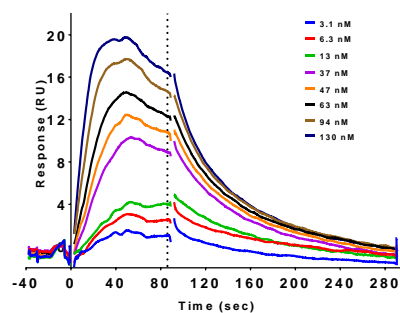
One site -- Specific binding	
Best-fit values	
B _{max}	21.37
K _D	7841
Std. Error	4.692
B _{max}	3088
K _D	3088
95% Confidence Intervals	
B _{max}	9.884 to 32.85
K _D	285.2 to 15397
Goodness of Fit	
Degrees of Freedom	6
R square	0.9539
Absolute Sum of Squares	4.723
Sy.x	0.8872
Number of points analyzed	8



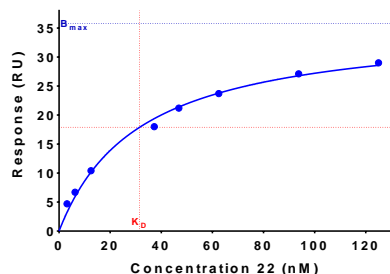
Compound 17



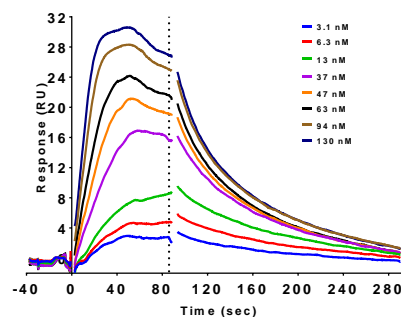
One site -- Specific binding	
Best-fit values	
B _{max}	23.13
K _D	37.86
Std. Error	1.451
B _{max}	6.247
K _D	6.247
95% Confidence Intervals	
B _{max}	19.58 to 26.68
K _D	22.58 to 53.15
Goodness of Fit	
Degrees of Freedom	6
R square	0.9665
Absolute Sum of Squares	3.149
Sy.x	0.7244
Number of points analyzed	8



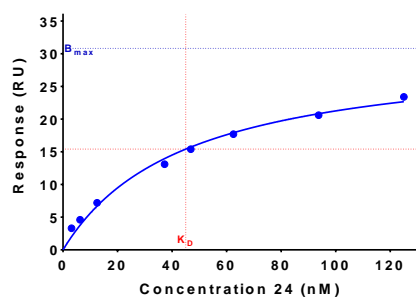
Compound 24



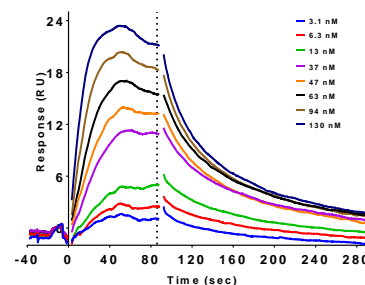
One site -- Specific binding	
Best-fit values	
B _{max}	35.77
K _D	31.50
Std. Error	1.569
B _{max}	3.931
K _D	3.931
95% Confidence Intervals	
B _{max}	31.93 to 39.61
K _D	21.88 to 41.11
Goodness of Fit	
Degrees of Freedom	6
R square	0.9917
Absolute Sum of Squares	5.070
Sy.x	0.9192
Number of points analyzed	8



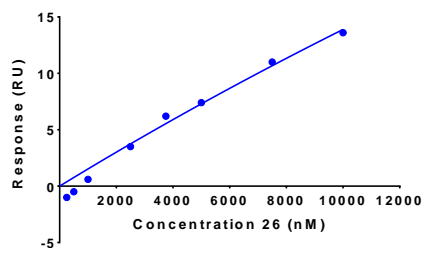
Compound 26 (CCT251236)



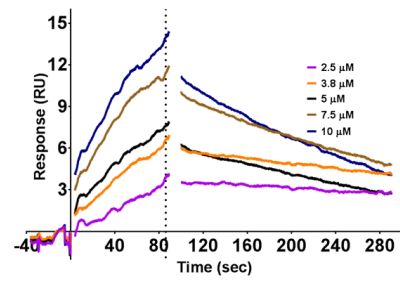
One site -- Specific binding	
Best-fit values	
B _{max}	30.83
K _D	45.03
Std. Error	1.947
B _{max}	6.944
K _D	6.944
95% Confidence Intervals	
B _{max}	26.07 to 35.60
K _D	28.04 to 62.02
Goodness of Fit	
Degrees of Freedom	6
R square	0.9895
Absolute Sum of Squares	4.129
Sy.x	0.8296
Number of points analyzed	8



Compound 28



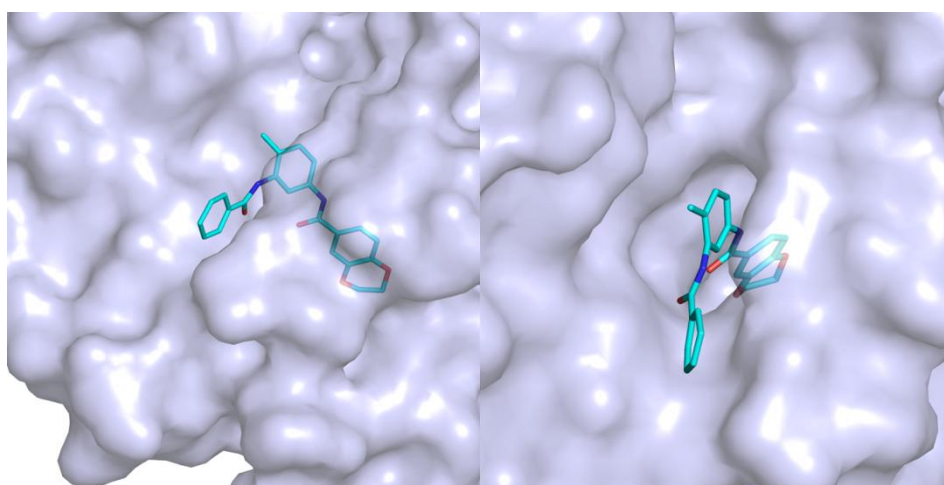
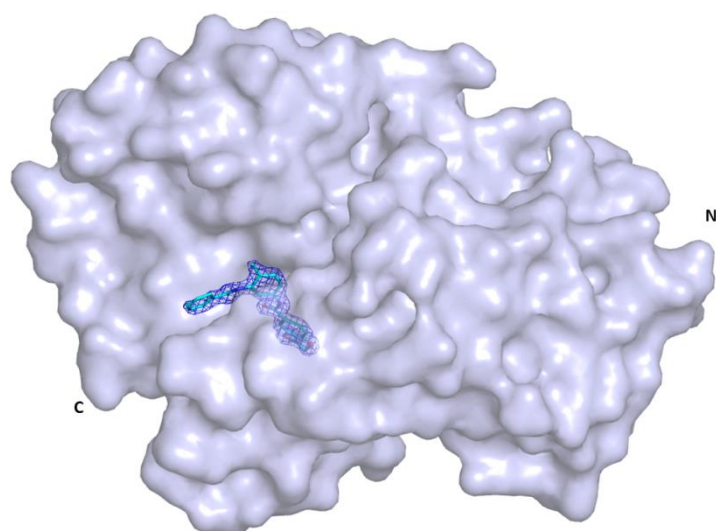
One site -- Specific binding	
Best-fit values	
B_{max}	143.9
K_D	93621
Std. Error	
B_{max}	268.0
K_D	188759
95% Confidence Intervals	
B_{max}	-511.8 to 799.7
K_D	-368256 to 555498
Goodness of Fit	
Degrees of Freedom	6
R square	6
Absolute Sum of Squares	0.9753
Sy.x	5.052
Number of points analyzed	8



Pirin Crystallography

Data were integrated with XDS¹ and scaled and merged with AIMLESS.² The structure was solved by molecular replacement using PHASER³ and a publically available pirin structure (PDB code **4EWA**)⁴ with ligand, metal and water molecules removed as the molecular replacement model. The protein-ligand structure was manually rebuilt in COOT⁵ and refined with BUSTER⁶ in iterative cycles. Ligand restraints were generated using grade.⁷ The quality of the structure was assessed using MOLPROBITY.⁸

<i>Crystals</i>	
Space group	P212121
Lattice constants	
a (Å)	42.15
b (Å)	67.41
c (Å)	107.06
α, β, γ (°)	90
<i>Data collection</i>	
Beamline	ID30A-1/MASSIF-1
Wavelength (Å)	0.965
Resolution range (Å)	42.15–1.73
(highest-resolution shell values)	(1.76–1.73)
Observations	151343 (7956)
Unique reflections	32524 (1758)
Completeness (%)	99.6 (99.6)
Multiplicity	4.7 (4.5)
Rmerge	0.08 (1.379)
Rmeas	0.101 (1.710)
Mean I/ σ (I)	10.7 (0.9)
CC _{1/2}	0.998 (0.365)
Average Mosaicity (°)	0.08
<i>Refinement</i>	
No. of amino acids	287
No. of water molecules	325
No. of glycerol molecules	1
No. of DMSO molecules	2
Identity of ligand bound	24
R-factor (%)	17.1
Rfree (%)	20.4
<i>Ramachandran plot</i>	
Favored (%)	99.62
Outliers (%)	0.38
RMSD bonds (Å)	0.01
RMSD angles (°)	1.08



*Top: Pymol image of pirin (light blue surface representation) in complex with bisamide **24** (cyan stick representation). 2 Fo-Fc map contoured at 1.0 σ (Blue mesh). Bottom: Pymol image of pirin (light blue surface representation) in complex with bisamide **26** (cyan stick representation).*

Figure S13. Pirin/CCT251236 crystallography images

Full Experimental Procedures

Biology Experimental

Cell line: The human ovarian carcinoma cell line (SK-OV-3) was obtained from an ICR collaborator in the 1990s. It was passaged in vivo in athymic mice to increase its tumorigenicity and reliability as a xenograft, and used within 10 passages of banked stocks. Prior to use, the cells were analyzed by short tandem repeat (STR) profiling. Polymorphic STR loci were amplified using a polymerase chain reaction (PCR) primer set. The PCR product (each locus being labelled with a different fluorophore) was analyzed simultaneously with size standards using automated fluorescent detection. The number of repeats at 10 different loci (as recommended by the American Type Culture Collection, ATCC) was used to define the STR profile and this was cross-referenced with online databases to confirm authenticity. Using this method, the in vivo subline showed an acceptable 85.71 % identity with the ATCC reference line (LGC Promochem, UK). The cells were free of mycoplasma contamination as determined by a sensitive nested PCR protocol (Venor GeM kit, Minerva Biolabs, Germany). Cells were grown in DMEM/10 % FCS, 2 mM glutamine and nonessential amino acids in 5 % CO₂.

Cell-based ELISA (Cellisa) for HSP72 expression

Cells were maintained in an incubator at 37 °C, 5% CO₂/95% air. Cells were grown in:

DMEM (Sigma, D5671)

10% FCS (PAA laboratories)

2 mM glutamine (Thermo Fisher Scientific, 25030-123)

Nonessential amino acids in 5% CO₂ (Thermo Fisher Scientific, 11140-068)

Final DMSO concentration was 0.1%

SK-OV-3 cells were free of Mycoplasma contamination (Lonza, MycoAlert™ PLUS Mycoplasma Detection Kit).

To follow HSP72 protein expression, a product of HSF1 transcriptional activity, the Cellisa assay was developed. Cells ($\sim 5\text{--}8 \times 10^4$ cells/mL) were seeded into 96-well plates and incubated at 37 °C for 48 h. Compounds were then added at a range of concentrations and incubated for 1 h before addition of 17-AAG (250 nM). Cells were then incubated for 18 h. The medium was removed and cells were fixed with fixing solution (4 % paraformaldehyde, 0.3 % TritonX-100 in PBS buffer) for 30 min at 4 °C. The plates were then washed with 0.1 % Tween-20/deionized water, before blocking with 5 % milk for 30 min at 37 °C. After washing the plates, HSP72 antibody (SPA-810, Enzo Life) was added for 1.5 h at 37 °C. Following 4x washes, the plates were incubated with europium-labelled anti-mouse antibody (0.6 µg/mL) in Delfia assay buffer (Perkin Elmer) for 1 h at 37 °C. After washing the plates, Delfia enhancement solution was added, shaken for 10 min before reading in the Envision plate reader (Perkin-Elmer) with excitation at 340 nm and emission at 615 nm. The plates were washed again before total protein determination using the Pierce BCA assay (Thermo Scientific) following the manufacturers standard protocol. The europium counts were normalized for the amount of protein in each well. The 50 % inhibitory concentration (IC_{50}) of the compound was determined by fitting the data to a dose-response curve without limits using non-linear regression. Each concentration was tested once.

Day 1

1. Split the cell line into 96 well plate at 8×10^4 cells/mL at 160 µL/well. Leave for 2 days at 37 °C for cell attachment.

Day 3 (late pm)

2. Treat cells with compounds at a range of concentrations. Make up 10x concentrated. Add 20µL/well. Leave for 1 h.

3. Treat with 250 nM 17-AAG. Make up 10x concentrated (2.5 μ M). Add 20 μ L/well. Leave for 12 h (overnight).

NOTE: Total wells contained cells and medium only plus 17-AAG. Blank wells contained cells and medium only.

Day 4 (am)

4. Flick media + drug off the plate by inverting onto white paper. Wash wells with PBS (2x by hand).

5. Add 100 μ L/well of fixing solution (4% paraformaldehyde in PBS) and place on ice (or fridge) for 30min.

6. Wash 2x with PBS (by hand).

7. Block with 5% milk in PBS (100 μ L/well) for 30 min at 37 °C.

8. Wash 2x with PBS (by hand).

9. Add primary antibody (HSP72, Stressgen SPA-810; 1:2000 dilution in PBS) at 50 μ L/well for 1.5 h at 37 °C.

10. Wash plate 4x with water + 0.1% Tween 20 (with plate washer machine).

11. Add secondary antibody (Eu- α Mouse, Delfia Europium-N1 labelled α Mouse AD0124, conc 50 μ g/mL, diluted 1:250 in Delfia assay buffer (1244-111) at 50 μ L/well for 1 h at 37 °C. Now using AD0207 (conc 909 μ g/mL) diluted 1:1600.

(If using rabbit for other antibodies, use Rabbit AD0105, 258 μ g/mL stock and dilute to 0.3 μ g/mL. Always check stock conc).

12. Wash as in 10.

13. Add 50 μ L/well of Delfia enhancement solution (Perkin Ekmer, 1244-105). Shake for 10 min at RT.

14. Read on Envision spectrophotometer.

15. Wash as in 10.

16. Normalised results with protein estimation using BCA protein reagents (Pierce, Reagent A 23223, Reagent B 23224). Add 200 μ L/well of BCA protein solution (mix A and B at 1 in 50 dilution). Incubate at 37 °C for 0.5h.

17. Read on spectrometer (540 nm).

18. The europium counts were normalised for the amount of protein in each well. The 50% inhibitory concentration value of the compound was then calculated.

In vitro cell viability assay

The CellTiter Blue viability (CTB) (Promega) assay provides a homogenous, fluorometric method for estimating the number of viable cells. It uses the dark blue indicator dye resazurin to measure the metabolic capacity of cells which is an indicator of cell viability. Viable cells are able to reduce resazurin into resorufin (pink), which is highly fluorescent. Briefly, cells ($\sim 6 \times 10^3$ cells/mL) were seeded into 384-well plates and were incubated for 24 h. Compounds (at a range of concentrations) were added using the ECHO 550 liquid handler (Labcyte, USA) and then left at 37 °C for 96 h. Titre blue reagent was added to each well and left at 37 °C for 3-4 h. Fluorescence was measured using the Envision machine (Perkin Elmer, UK). The 50 % growth inhibitory concentration (GI₅₀) was determined by fitting the data to a dose-response curve without limits using non-linear regression. Each concentration was tested twice.

In vivo Studies

Experimental work was done in accordance with Home Office regulations under the Animals (Scientific Procedures) Act 1986, ICR ethical review processes and according to the UK National Cancer Research CRI Guidelines with local Ethical Committee approval.⁹

Mouse Pharmacokinetics

Female BALB/c and Ncr-Foxn1^{nu} mice were obtained from Charles River (Margate, UK). Animals were adapted to laboratory conditions for at least 1 week prior to dosing and were

allowed food and water *ad libitum*. Compounds were administered iv or po (0.1 mL/10g) in either 10 % DMSO, 5 % Tween 20 in saline (BALB/c PK) or 10 % DMSO in 25 % w/v hydroxypropyl beta cyclodextrin in 50 mM sodium citrate buffer (Ncr-Foxn1^{nu} PK). Blood samples were collected from the tail vein (20 µL) at 8 time points over 24 h post dosing and spotted onto Whatman FTA-DMPK B cards (VWR) together with a calibration curve and quality controls spiked in control blood. Cards were allowed to dry at room temperature for at least 2 h. 6 mm discs were punched from the cards and extracted with 200 µL methanol containing 500 nM olomoucine as an internal standard. Following centrifugation, extracts were analyzed by multiple reaction monitoring of precursor and product ions by LC-ESI-MS/MS on a QTRAP 4000 (Sciex, Warrington, UK) using a short gradient consisting of 0.1 % formic acid and methanol on a Phenomenex (Macclesfield, UK) KinetexTM C18, 5 cm x 2.6 µm, 2.1 mm i.d UHPLC column. Pharmacokinetic parameters were derived from non-compartmental analysis using Phoenix (model 200 and 201) Pharsight WinNonlin® version 6.1/6.3.

Protein Binding

Protein binding was measured using Rapid Equilibrium Dialysis (RED, Thermo Fisher Scientific, Loughborough, UK). Plasma was obtained from female BALB/c and Ncr-Foxn1^{nu} mice (Charles River, Margate, UK) and stored at -20°C. Cell culture media was DMEM (Sigma Aldrich, Dorset, UK) supplemented with 10 % FCS (Invitrogen), 2 mmol/L of L-glutamine, and 1 x non-essential amino acids. The RED plate, buffer, plasma and media solutions were heated to 37 °C before dialysis. Test compound in DMSO was spiked into either diluted plasma (10-fold dilution in 100 mM phosphate buffer) or cell culture media as appropriate resulting in a concentration of 5 µM for dialysis, containing 1 % DMSO. 300 µL of spiked diluted plasma or media was added to the donor side of the RED plate and 500 µL of 100 mM phosphate buffer was added to the receiver well. The plate was sealed with a gas-

permeable lid and dialysis was performed by shaking for 4 h at 37 °C. After dialysis, samples were transferred from the RED plate and donor and receiver samples were matrix matched followed by protein precipitation with methanol containing internal standard. Samples were mixed, centrifuged and supernatant was taken for analysis by ESI-LCMS/MS on a QTRAP 4000 (Sciex, Warrington, UK) using a short gradient consisting of 0.1 % formic acid and methanol on a Phenomenex (Macclesfield, UK) Kinetex™ C18, 5 cm x 2.6 µm, 2.1 mm i.d UHPLC column. The fraction unbound (f_u) was calculated as follows:

$$f_u = \frac{PAR_{receiver}}{PAR_{donor}} \text{ where } PAR = \text{Peak Area Ratio of Analyte/Internal Standard.}$$

$f_u = 1/(1 + (\frac{1}{f_{u'}} - 1) * \text{dilution factor})$ where dilution factor = 10 for plasma, 1 for media.

Blood to Plasma Ratio

Fresh blood was obtained from female BALB/c and Ncr-Foxn1^{nu} mice (Charles River, Margate, UK) and an aliquot centrifuged to obtain plasma. Blood and plasma was pre-warmed to 37 °C. Test compound was spiked into blood and plasma to final concentrations of 1 and 10 µM containing 1 % of methanol:water and ≤0.1 % DMSO. Spiked samples were incubated for 30 min at 37 °C. Blood was then centrifuged to obtain plasma. Equal volumes of plasma from centrifuged blood and from original spiked plasma samples were protein precipitated with 10-fold methanol containing internal standard, mixed and centrifuged. Supernatant was taken for analysis by ESI-LCMS/MS on a QTRAP 4000 (Sciex, Warrington, UK) using a short gradient consisting of 0.1 % formic acid and methanol on a Phenomenex (Macclesfield, UK) Kinetex™ C18, 5 cm x 2.6 µm, 2.1 mm i.d UHPLC column. The blood to plasma ratio was calculated as

$$\frac{PAR \text{ in Spiked Plasma}}{PAR \text{ in Plasma from Spiked Blood}} \quad \text{where } PAR = \text{Peak Area Ratio of Analyte/Internal}$$

Standard.

Mouse Tolerability Study

Sterile Solvent Preparation

The formulation (10 % DMSO, 90 % of a 25 % (2-hydroxypropyl)- β -cyclodextrin in 50 mM citrate buffer pH 5) was prepared by dissolving of citric acid monohydrate (10.5 g) and trisodium citrate dehydrate (14.8 g) in sterile water (500 mL, respectively). The citric acid solution (87.5 mL) was then added to the sodium citrate dehydrate solution (163 mL) to generate the pH 5 citrate buffer. (2-hydroxypropyl)- β -cyclodextrin (50 g, average MW~1460) was then added to the pH 5 citrate buffer (150 mL) and the pH measured to be 5.07. Bisamide **26** (CCT251236) was dissolved in DMSO (20.6 mL) and then added to the 25 % (2-hydroxypropyl)- β -cyclodextrin in 50 mM citrate buffer pH 5 (185 mL). The mixture was then sonicated to give a clear solution. Unused formulation was stored for up to 1 week at 5 °C.

Bisamide **26** was dissolved in 10 % DMSO and diluted in 90 % sterile solvent (25 % w/v hydroxypropyl β -cyclodextrin in 50 mM sodium citrate buffer pH 5) such that mice received the dose required in 0.1 mL of final solution per 10 g body weight. Controls received an equal volume of vehicle only.

For multi-dose tolerability studies, female NCr athymic mice (n=2) were administered 30 mg/kg of bisamide **26** orally by gavage every day for five days. Animals were monitored for adverse effects and body weights were measured daily until full recovery was observed.

Mouse Efficacy Study

For efficacy studies, SK-OV-3 cells (5 million per site) were injected s.c. in the flanks of 6- to 8-week-old female NCr athymic mice (n=16). Dosing commenced when tumors were well established (~5-6 mm diameter). Tumors were measured with Vernier calipers across two perpendicular diameters and volumes were calculated as previously described.¹⁰ On study termination, heparinized blood samples were collected, and plasma was separated and stored

at -80 °C. Tumors were excised, weighed and snap frozen at -80 °C for subsequent PK and PD analyses.¹¹ Data was processed using Graphpad Prism 6 (Version 6.07).

Physicochemical Properties Experimental

Reagents: HPLC grade solvents, formic acid, or alternative eluent modifiers were purchased from Sigma Aldrich (Poole, UK) unless otherwise stated.

LogD_{7.4} Determination

Log D_{7.4} values were determined via an in-house RP-HPLC method based on previous work by Kerns and Di.¹² Calibration was achieved by comparing the retention time of eight commercially available drugs with a range of Log D_{7.4} values between -1.38 and 5.5, and correlating these retention times against literature Log D_{7.4} values of the compounds. The calibration was validated by comparing HPLC-determined Log D_{7.4} values of two other commercially-available drugs with literature Log D_{7.4} values. The HPLC Log D_{7.4} values of in-house compounds were determined by substituting the compounds' retention times into the equation obtained from the linear part of the calibration curve. Calibration, validation and in-house compounds were prepared at 1 mM in 10 % DMSO/90 % Trizma solution (100 mM Trizma in 75/25 methanol/water).

Two sets of 3 µL standard injections (with needle wash) of all calibration, validation and in-house samples were made onto a Phenomenex Luna C8 column (3 µm, 100 mm x 4.6 mm, 100A, Phenomenex, Torrance, USA). Chromatographic separation at 30 °C was carried out using a 1200 Series HPLC (Agilent, Santa Clara, USA) over a 5 minute gradient elution from 95:5 to 0:100 aqueous (20 mM Trizma in octanol-saturated water) and organic (acetonitrile + 0.25 % v/v octanol) at a flow rate of 2 mL/min. The gradient was held at 0:100 water:organic for 0.8 minutes, then returned to the starting conditions of 95:5 water:organic for 0.2 minutes. The column was re-equilibrated for 5 minutes at the starting conditions prior to the next injection. UV-Vis spectra were acquired at 254 nm, 280 nm and 220 nm on a 1200 Series

diode array detector (Agilent, Santa Clara, USA). Raw data was processed using Agilent Chemstation Rev.C.01.04.

Kinetic Solubility Determination

Kinetic Solubility values were determined via an in-house RP-HPLC method. Calibration standards were prepared at a concentration of 100 μ M in 100 % DMSO. Calibration was achieved by injecting 0.5, 2.5 and 5 μ L of the 100 μ M standard. Kinetic solubility samples were prepared at a concentration of 100 μ M in 1 % DMSO/99 % PBS (pH 7.4). The samples were shaken for 120 min at room temperature and then centrifuged for 15 min at 14,000 rpm. The supernatant was removed and a small volume of DMSO was added to ensure the compound remained in solution. Kinetic solubility values were determined by substituting the AUC of the kinetic solubility samples into the equation obtained from the linear part of the calibration curve.

Injections (with needle wash) of the calibration and kinetic solubility samples were made onto a Phenomenex Kinetex C18 column (5 μ m, 50 mm x 4.6 mm, 100A, Phenomenex, Torrance, USA). Chromatographic separation at 30 °C was carried out using a 1260 Series HPLC (Agilent, Santa Clara, USA) over a 5 minute gradient elution from 90:10 to 10:90 water:methanol (both modified with 0.1 % formic acid) at a flow rate of 1.5 mL/min. UV-Vis spectra were acquired at 254 nm on a 1260 Series diode array detector (Agilent, Santa Clara, USA). Raw data was processed using Agilent Chemstation Rev.C.01.05.8. The data was then reprocessed on ChemStation C.01.04 to generate the calibration curve and solubility value.

Pirin Surface Plasmon Resonance (SPR)

All surface plasmon resonance (SPR) experiments were carried out on a Biacore T100 enhanced to T200 sensitivity (GE Life Sciences, Amersham Place, UK). Amine coupling chemistry was used to immobilize the pirin protein on a research grade CM5 sensor chip. The running buffer used in the immobilization step consisted of 1 x phosphate buffered saline (10

mM NaHPO₄/NaH₂PO₄, pH 7.4, 2.7 mM KCl, 137 mM NaCl) and the chip's surface was activated for 10 min using a 1:1 mixture of 100 mM *N*-hydroxysuccinimide and 400 mM 1-ethyl-3-(3-dimethylaminopropyl)-carbodiimide. Pirin was injected at a concentration of ~5 µg/mL in a 10 mM acetate buffer pH 5.5 with 5 µM triphenyl compound A (Sigma-Aldrich Cat.No. T6205) added to provide protection for the active site lysines. The reaction was monitored in real time and stopped when a target immobilization level of ~5000RU was obtained. Finally, the surface was blocked via an injection of 1 M ethanolamine at pH 8.5 for 7 min. The flow rate was maintained at 10 µL/min for all the above procedures. Flow cell one was left unmodified and used as the reference surface.

Following protein immobilization, the running buffer was changed to 1 x phosphate buffered saline containing 0.05 % (v/v) Tween 20 and 5 % (v/v) DMSO in order to reduce the non-specific binding and solubility of the compounds. All liquid handling was carried out using an ECHO 550 acoustic liquid dispenser (Labcyte, Dublin, Ireland) and compounds were added to 384-well polypropylene V-bottomed plates (Greiner, Stonehouse, UK), which became the sample plates for the SPR. For each compound, an eight-point dose response experiment was carried out, using a concentration range suitable for the estimated pK_D, in a buffer mix compatible with the Biacore running buffer. The experiments were performed at a flow rate of 30 µL/min, a sample injection time of 90 seconds and a dissociation time of 200 seconds. The CM5 surface was not regenerated between sample injections.

The response units for the equilibrium analysis were measured 4 seconds prior to the end of the injection time. pK_D values were determined from analysis of the background normalized binding curve generated from the sensorgrams, under equilibrium conditions where possible, using the one-site specific binding model in Graphpad Prism 6 (Version 6.07). All results are reported as the geometric mean±standard error of the mean (SEM) from three independent measurements. The ratio of experimental to theoretical R_{max} was ~0.40.

Crystallography Experimental

Full-length His₆-tag pirin was produced in *E.coli* and purified as previously described.¹³ Purified full-length His₆-tag pirin produced in *E.coli* was crystallized using the hanging drop vapour diffusion method at 4 °C using 50 mg/mL of pirin and a reservoir solution of 0.1 M HEPES (pH 7.5), 8 % ethylene glycol, 20 % (w/v) PEG 8,000. Crystallization drops were formed using 1 µL each of pirin and reservoir solution placed over 200 µL of reservoir solution in a 15 well screw-top plate. Growth time for apo-crystals was 2 weeks. For pirin ligand complex formation apo crystals were soaked for 48 h in 25 mM of ligand in matching reservoir condition, and 20 % (v/v) DMSO. Soaked protein crystals were then briefly transferred to cryoprotectant solution of 0.1 M HEPES (pH 7.5), 8 % ethylene glycol, 22 % (w/v) PEG 8,000, 20 % Glycerol and cryocooled to 100 K in liquid nitrogen prior to data collection. X-ray data were collected at the European Synchrotron Radiation Facility (ESRF) using the automated data-collection facility on the beam-line ID30A-1/MASSIF-1. Crystals belonged to the space group P2₁2₁2₁ and diffracted to resolution of 1.73 Å.

Migration Assay Experimental

The WM266.4 cells were maintained in DMEM (Thermo-Fisher) supplemented with 10% Foetal Bovine Serum (SeraPlus (PanBioTech) and 1% non-essential amino acids (Thermo-Fisher) in a humidified incubator at 5% CO₂ and 37°C. The day before the experiment, WM266.4 cells were seeded at 3x10⁵ cells per mL into an ImageLock 96 well plate (Essen Biosciences) and left overnight to adhere. Compound dilutions of CCT251236 **26** and CCT273166 **28** were performed to give intermediate concentrations of 100, 10, 1, 0.1, 0.01 µM in 100% DMSO. The compound was then further diluted into complete growth media to final concentrations of 1000, 100, 10, 1 and 0.1nM (1% DMSO final). DMSO (1%) was used as a vehicle control. The scratch-wound was made using the WoundMaker™ tool (Essen

Biosciences). This was found to make highly reproducible wounds across a whole 96 well plate. Briefly, the plates were removed from the incubator and the wound made. The media was removed from the wells to remove the debris and 100 μ L of fresh media containing the diluted compounds was then added back into each well, with care to remove all bubbles. The plate was then placed into the IncuCyte ZOOM®(Essen Biosciences) and allowed to equilibrate for 5 minutes at 37°C/5% CO₂.

Images were then collected using a 10 x objective (Nikon) on wide mode, every 2 hours for 48 hours. The images acquired were analysed using the IncuCyte ZOOM® analysis software. The cells were segmented at all time points using the following criteria: minimum area of 700 μ m² and a background setting of 0.8. This allowed the wound density (%) to be calculated for each compound and this was compared to the vehicle (DMSO) control. All numerical data was exported and plotted in GraphPad Prism.

References

- ¹ Kabsch, W. Xds. *Acta Crystallogr., Sect. D* **2010**, *66*, 125–132.
- ² Evans, P. Scaling and assessment of data quality. *Acta Crystallogr., Sect. D* **2006**, *62*, 72–82.
- ³ (a) Winn, M. D.; Ballard, C. C.; Cowtan, K. D.; Dodson, E. J.; Emsley, P.; Evans, P. R.; Keegan, R. M.; Krissinel, E. B.; Leslie, A. G.; McCoy, A.; McNicholas, S. J.; Murshudov, G. N.; Pannu, N. S.; Potterton, E. A.; Powell, H. R.; Read, R. J.; Vagin, A.; Wilson, K. S. Overview of the CCP4 suite and current developments. *Acta Crystallogr., Sect. D* **2011**, *67*, 235–242. (b) McCoy, A. J.; Grosse-Kunstleve, R. W.; Adams, P. D.; Winn, M. D.; Storoni, L. C.; Read, R. J. Phaser crystallographic software. *J. Appl. Crystallogr.* **2007**, *40*, 58–674.
- ⁴ Liu, F.; Rehmani, I.; Esaki, S.; Fu, R.; Chen, L.; de Serrano, V.; Liu, A. Pirin is an iron-dependent redox regulator of NF-kappa B. *Proc. Natl. Acad. Sci. USA* **2013**, *110*, 9722–9727.
- ⁵ Emsley, P.; Cowtan, K. Coot: Model-building tools for molecular graphics. *Acta Crystallogr., Sect. D* **2004**, *60*, 2126–2132.
- ⁶ Bricogne, G.; Blanc, E.; Brandl, M.; Flensburg, C.; Keller, P.; Paciorek, W.; Roversi, P.; Sharff, A.; Smart, O. S.; Vonrhein, C.; Womack, T. O. *BUSTER*, version 2.11.4; Global Phasing Ltd.: Cambridge, United Kingdom, 2012.
- ⁷ Smart, O. S.; Womack, T. O.; Sharff, A.; Flensburg, C.; Keller, P.; Paciorek, W.; Vonrhein, C.; Bricogne, G. *Grade*, version 1.2.1; Global Phasing Ltd.: Cambridge, United Kingdom, 2012.
- ⁸ Davis, I. W.; Leaver-Fay, A.; Chen, V. B.; Block, J. N.; Kapral, G. J.; Wang, X.; Murray, L. W.; Arendall, W. B., 3rd; Snoeyink, J.; Richardson, J. S.; Richardson, D. C. MolProbity: All-atom contacts and structure validation for proteins and nucleic acids. *Nucleic Acids Res.* **2007**, *35*, W375–W383.
- ⁹ Workman, P.; Aboagye, E. O.; Balkwill, F.; Balmain, A.; Bruder, G.; Chaplin, D. J.; Double, J. A.; Everitt, J.; Farningham, D.; Glennie, M. J.; Kelland, L. R.; Robinson, V.; Stratford, I. J.; Tozer, G. M.; Watson, S.; Wedge, S. R.; Eccles, S. A. Guidelines for the welfare and use of animals in cancer research. *Br. J. Cancer* **2010**, *102*, 1555–1577.
- ¹⁰ Eccles, S. A.; Court, W. J.; Box, G. A.; Dean, C. J.; Melton, R. G.; Springer, C. J. Regression of established breast carcinoma xenografts with antibody-directed enzyme prodrug therapy against C-erbB2 p185. *Cancer Res.* **1994**, *54*, 5171–5177.
- ¹¹ Sugar, E.; Pascoe, A. J.; Azad, N. Reporting of Preclinical Tumor-Graft Cancer Therapeutic Studies. *Cancer Biol. Ther.* **2012**, *13*, 1262–1268.
- ¹² Kerns, E. H.; Li Di, L.; Petuskya, S.; Kleintop, T.; Huryn, D.; McConnell, O.; Carter, G. Pharmaceutical profiling method for lipophilicity and integrity using liquid chromatography-mass spectrometry. *J. Chromatogr. B: Anal. Technol. Biomed. Life Sci.* **2003**, *791*, 371–388.
- ¹³ Zeng, Q.; Li, X.; Bartlam, M.; Wang, G.; Pang, H.; Rao, Z. Purification, crystallization and preliminary x-ray analysis of human pirin. *Acta Crystallogr., Sect. D: Struct. Biol.* **2003**, *59*, 1496–1498.